DEPARTMENT OF CHEMISTRY

NOVA SCHOOL OF SCIENCE & TECHNOLOGY

ANDRÉ FILIPE DA SILVA SOUSA

BSc in Biochemistry

New biotreatments against saline rising on Ribatejo (Portugal) farmlands using Iberian Peninsula salt flats-isolated, halophile strains

MASTER IN BIOTECHNOLOGY

NOVA University Lisbon
September, 2024

NOVA SCHOOL OF SCIENCE & TECHNOLOGY

DEPARTMENT OF CHEMISTRY

New biotreatments against saline rising on Ribatejo (Portugal) farmlands using Iberian Peninsula salt flats-isolated, halophile strains

ANDRÉ FILIPE DA SILVA SOUSA

BSc in Biochemistry

Adviser: Juan Ignacio Vílchez
Auxiliar Researcher, PI at iPlantMicro Lab, ITQB-NOVA

Examination Committee:

Chair: Sérgio Joaquim Raposo Filipe,
Full Professor, FCT-NOVA

Rapporteurs: Isabel Videira e Castro,
Principal Investigator, INIAV

Adviser: Juan Ignacio Vílchez,
Principal Investigator, ITQB-NOVA

MASTER IN BIOTECHNOLOGY

NOVA University Lisbon
September, 2024

New biotreatments against saline rising on Ribatejo (Portugal) farmlands using Iberian Peninsula salt flats-isolated, halophile strains

ACKNOWLEDGMENTS

I would like to express my deepest gratitude to my advisor, Nacho, for his unwavering support, guidance, and encouragement throughout my master's project. I am especially thankful for the opportunity to work on such an amazing project. His expertise and insights were invaluable in shaping this thesis.

I am also grateful to my lab partners at iPlantMicro, with a special thank you to Tatiana, for their assistance and for fostering a positive environment in the lab, which greatly enriched this experience.

Special thanks to FCT-NOVA for the opportunity to participate in an exceptional Biotechnology master's program. I also want to thank ITQB-NOVA for providing the resources and support necessary for my research. Additionally, I would like to acknowledge the financial support from GREEN-IT, which made this research possible.

I want to express my gratitude to IIT Biotech GmbH and the Proteome and Metabolome Research group at CeBiTec for their valuable collaboration in this research. I would also like to thank Pé Da Planta and Anpromis for kindly providing the seeds used in this study.

On a personal note, I would like to thank my family and friends for their unwavering support and encouragement. Especially to my parents, Fernando and Mónica, and to my girlfriend, Ana Rita, your companionship and understanding have been a constant source of strength throughout this journey.

ABSTRACT

Soil salinity poses a significant challenge to various crops worldwide. Approximately 20% of irrigated land, which produces one-third of global food, is affected by underlying soil salinity, with Mediterranean countries in the EU being the most impacted. Besides, the accumulation of excess ions in the soil leads to salinization, hindering plant growth and function by disrupting nutrient and water absorption. This issue is particularly acute in crucial agricultural areas such as Lezíria Grande, where climatic conditions and estuarine tides exacerbate soil salinity. Moreover, the productivity of major Portuguese crops, including tomato (*Solanum lycopersicum*) and maize (*Zea mays*), has been reduced due to salinity stress, jeopardizing agricultural output and food security. However, in environments characterized by stress and unique biodiversity, a microbiome has evolved to withstand salt-stress, potentially aiding plants in coping with these conditions. Therefore, the development of a novel bioformulation utilizing adapted microbiota could transform agriculture, enabling plants to thrive in stressful environments. Thus, this research aims to formulate a halophile bacteria-based solution to enhance plant growth and salt tolerance in saline conditions. Various strains were identified with the potential to help maize and/or tomato plants thrive under salt-stress conditions. However, *Vreelandella* sp. DE and *Idiomarina loihiensis* EA were demonstrated to be the most promising strains, as they enhanced both plants' overall growth under saline stress in long-term greenhouse assays. Additionally, genes associated with plant growth-promoting traits were found in *Vreelandella* sp. DE, as well as its ability to modulate the genetic expression of maize plants, resulting in enhanced growth and improved tolerance to salinity. These effects were mediated through mechanisms including increased production of osmoprotectants, elevated antioxidant enzymes activity and enhanced hormonal regulation. Nevertheless, important metabolites for plant improvement and salt tolerance were found to be secreted by the candidate strains. These findings indicate the potential of this approach to enhance crop resilience and growth in saline environments, which could revolutionize agriculture, particularly in regions affected by soil salinity.

Keywords: Salt-stress, Tomato, Maize, Halophile bacteria, Biotreatment

RESUMO

A salinidade do solo constitui um desafio significativo para várias plantações em todo o mundo. Cerca de 20% das terras irrigadas, que produzem um terço dos alimentos a nível mundial, são afetadas pela salinidade subjacente do solo, sendo os países mediterrânicos da UE os mais afetados. Além disso, a acumulação de iões em excesso no solo conduz à salinização, prejudicando o crescimento e o funcionamento das plantas ao perturbar a absorção de nutrientes e de água. Este problema é particularmente grave em zonas agrícolas cruciais como a Lezíria Grande, onde as condições climáticas e as marés estuarinas agravam a salinidade do solo. Além disso, a produtividade das principais culturas portuguesas, incluindo o tomate (*Solanum lycopersicum*) e o milho (*Zea mays*), tem sido reduzida devido ao stress salino, pondo em risco a produção agrícola e a segurança alimentar. No entanto, em ambientes caracterizados pelo stress e por uma biodiversidade única, um microbioma evoluiu para resistir ao stress salino, ajudando potencialmente as plantas a lidar com estas condições adversas. Por conseguinte, o desenvolvimento de uma nova bioformulação que utilize a microbiota adaptada pode transformar a agricultura, permitindo que as plantas prosperem em ambientes de stress. Assim, esta investigação tem como objetivo formular uma solução à base de bactérias halófilas para melhorar o crescimento das plantas e a tolerância ao sal em condições salinas. Foram identificadas várias estirpes com potencial para ajudar as plantas de milho e/ou tomate a prosperar em condições de stress salino. No entanto, *Vreelandella* sp. DE e *Idiomarina loihiensis* EA demonstraram ser as estirpes mais promissoras, uma vez que melhoraram o crescimento geral de ambas as plantas sob stress salino em ensaios de estufa a longo prazo. Adicionalmente, foram encontrados na *Vreelandella* sp. DE genes relacionados com caraterísticas promotoras do crescimento das plantas, bem como a sua capacidade de modular a expressão genética das plantas de milho, resultando num maior crescimento e numa melhor tolerância à salinidade. Estes efeitos foram mediados por mecanismos que incluem o aumento da produção de osmoprotetores, o aumento da atividade das enzimas antioxidantes e o aumento da regulação hormonal. No entanto, verificou-se que as estirpes candidatas secretam metabolitos importantes para o melhoramento das plantas e para a tolerância ao sal. Estes resultados indicam o potencial desta abordagem para aumentar a resistência e o crescimento das plantações em ambientes salinos, o que poderá revolucionar a agricultura, particularmente em regiões afetadas pela salinidade do solo.

Palavras chave: Stress salino, Tomate, Milho, Bactérias halófilas, Biotratamento

CONTENTS

LIST OF FIGURES

LIST OF TABLES

LIST OF EQUATIONS

GLOSSARY

Acclimation	The process by which an organism adjusts to changes in its environment over time.
Antioxidants	Molecules that prevent oxidative damage by neutralizing free radicals.
Auxins	A class of plant hormones that regulate growth.
Biofertilization	The use of natural organisms to improve soil fertility.
Biofilm	A structured community of microorganisms embedded in a self-produced matrix.
Bioformulation	A mixture of beneficial microorganisms used in agriculture to enhance plant growth or control diseases.
Biocontrol	The use of living organisms to reduce the population of pest organisms.
Biomass	The total mass of living matter in a given area.
Bioinoculant	Microorganisms added to soil or plants to improve their growth or resistance to stress.
Biotreatment	The use of biological processes, often involving microorganisms, to treat contaminated environments.
Calvin Cyle	A series of biochemical reactions in plants that occur during photosynthesis, converting carbon dioxide into glucose.
Chemotaxis	The movement of an organism or cell in response to a chemical stimulus.
Colony-Forming Units	A measure of viable bacterial or fungal cells in a sample.
Contigs	Overlapping DNA segments that together represent a consensus region of DNA.
Crop Wild Relatives	Wild plant species genetically related to domesticated crops.
Cytokinins	Plant hormones involved in cell division, shoot formation and delaying leaf senescence.
Dicotyledons	A group of flowering plants with two embryonic leaves (cotyledons).
DNA replication	The process by which a cell duplicates its DNA before cell division.
DNA shearing	The process of breaking DNA into smaller fragments for sequencing.
Electrical conductivity	A measure of soil's ability to conduct electrical current, often used to assess salinity levels.
Evenness	A measure of how equally species are represented in a community.
Evapotranspiration	The sum of evaporation and plant transpiration, contributing to water loss from the soil and plants.

Exopolysaccharides	Polysaccharides secreted by microorganisms that help form biofilms and protect against stress.
Exudates	Substances secreted by plants, roots or microorganisms, often involved in nutrient exchange or defence.
Gibberellins	Plant hormones that regulate growth, seed germination and flowering.
Genome assembly	The process of piecing together DNA sequences to reconstruct the genome of an organism.
Genomics	The study of an organism's entire genetic material (genome).
Glycolysis	A metabolic pathway that converts glucose into pyruvate, producing energy.
Gypsic soils	Soils rich in gypsum, typically found in arid or semi-arid regions.
Halophile	Organisms that thrive in high-salinity environments.
Halophytes	Salt-tolerant plants that can grow in saline soils.
Halotolerant	Organisms that can survive in saline conditions but do not necessarily thrive there.
Homeostasis	The ability of an organism to maintain internal stability despite external changes.
Hygroscopic	The ability of a substance to absorb moisture from the air.
Ion antiporter	A membrane protein that exchanges one type of ion for another, helping cells maintain ionic balance.
Induced Systemic Resistance	A plant defence mechanism triggered by beneficial microorganisms to protect against pathogens.
Leaf senescence	The aging process of leaves, leading to their eventual death.
Lyophilization	A freeze-drying process used to preserve biological samples.
Metabolomics	The study of the complete set of metabolites within a biological system.
Microbial consortium	A community of different microorganisms that live together and interact for mutual benefit
Microbiota	The community of microorganisms living in a particular environment.
Molecular marker	A biomarker used to identify specific genes or physiological responses.
Monocotyledons	A group of flowering plants that have one embryonic leaf (cotyledon).
Motility	The ability of an organism or cell to move independently, often using flagella or other structures.
N50	A statistic used to assess the quality of a genome assembly, representing the length at which 50% of the genome is contained in contigs of that length or longer.
Nitrogen fixation	The conversion of atmospheric nitrogen into a form that plants can use.
Nutrient solubilization	The process by which microorganisms convert insoluble nutrients into forms accessible to plants.
Optical density	A measure of how much light is absorbed by a sample, commonly used to estimate bacterial growth.
Orthologs	Genes in different species that originated from a common ancestor and retain similar functions.
Osmolytes	Small molecules that help cells maintain osmotic balance.

Osmotic agent	A substance that regulates water movement in cells to maintain osmotic pressure.
Plant growth-promoting bacteria	Beneficial bacteria that enhance plant growth and stress resilience.
Phenotype	The observable characteristics of an organism.
Phytohormone	Plant hormones.
Phylogenetic tree	A diagram showing the evolutionary relationships among different species based on their genetic similarities.
Photosystem II	A complex of proteins and pigments in plants that plays a key role in photosynthesis by absorbing light energy.
Putative functions	Predicted functions of genes or proteins based on sequence similarity to known genes or proteins.
Respiration	The process by which organisms break down organic molecules to produce energy.
Ribosome	A cellular structure that synthesizes proteins by translating mRNA.
Richness	A measure of the number of different species present in a community.
Root colonization	The process by which microorganisms establish themselves on or within plant roots.
Salinity threshold	The maximum salt concentration a plant can tolerate before its growth is adversely affected.
Seedlings	Young plants that have recently germinated from seeds.
Siderophores	Molecules produced by microorganisms to bind and transport iron, improving nutrient availability to plants.
Synergy	The interaction between two or more factors or organisms that results in a greater combined effect than the sum of their individual effects.
Taxonomy	The science of classifying organisms based on their characteristics and evolutionary relationships.
Transcriptomics	The study of the complete set of RNA transcripts produced by the genome under specific conditions.
Vermiculite	A mineral used in horticulture as a soil conditioner, improving water retention and aeration.
Xylem	Plant tissue that transports water and nutrients from the roots to other parts of the plant.

ABBREVIATIONS

ABA	Abscisic Acid.
ACC	1-Aminocyclopropane-1-Carboxylic Acid.
ACCd	1-Aminocyclopropane-1-Carboxylate Deaminase.
BLAST	Basic Local Alignment Search Tool.
BTB	Bromothymol Blue.
BUSCO	Benchmarking Universal Single-Copy Orthologs.
CAS	Chrome Azurol Sulfonate.
CaSB	Calcium Solubilizing Bacteria.
CAT	Catalase.
CDS	Coding Sequences.
CFU	Colony-Forming Units.
CI	Confidence Interval.
CWR	Crop Wild Relative.
DAT	Days After Treatment.
dDDH	Digital DNA-DNA Hybridization.
ddH_2O	Double Distilled Water.
DEG	Differentially Expressed Gene.
Dicots	Dicotyledons.
DW	Dry Weight.
EC	Electrical Conductivity.
EDTA	Ethylenediaminetetraacetic Acid.
EPS	Exopolysaccharides.
FPKM	Fragments Per Kilobase of transcript sequence per Millions base pairs sequenced.
GABA	4-Aminobutyric Acid.
GC-MS/MS	Gas Chromatography-Tandem Mass Spectrometry.
GBDP	Genome BLAST Distance Phylogeny.
GRF	Growth-Regulating Factor.

GSEA	Gene Set Enrichment Analysis.
GST	Glutathione S-Transferases.
HDTMA	Hexadecyl Trimethyl Ammonium Bromide.
HSP	High-scoring Segment Pair.
IAA	Indole-3-acetic Acid.
ISR	Induced Systemic Resistance.
ITS	Internal Transcribed Spacer.
KEGG	Kyoto Encyclopedia of Genes and Genomes.
MAMSL	Meters Above Mean Sea Level.
MDA	Malondialdehyde.
Monocots	Monocotyledons.
MSTFA	N-Metil-N-(trimetilsilil)trifluoroacetamide.
NBRIP	National Botanical Research Institute's Phosphate.
OD	Optical Density.
OG	Optimal Growth.
PCA	Principal Component Analysis.
PCR	Polymerase Chain Reaction.
PEP	Phosphoenolpyruvate.
PIPES	Piperazine-N,N′-bis (2-Ethanesulfonic acid).
PGPB	Plant Growth Promoting Bacteria.
PGPT	Plant Growth Promoting Traits.
PSII	Photosystem II.
PSU	Percentage Siderophore Unit.
QY	Photosystem II Quantum Yield.
RL	Root Length.
ROS	Reactive Oxygen Species.
SI	Solubilization Index.
SL	Shoot Length.
SnRK1	Sucrose non-fermenting 1-Related protein Kinase1.
SOD	Superoxide Dismutase.
T6P	Trehalose-6-Phosphate.
tmRNA	Transfer-Message RNA.
TSM	Thiosulfate Mineral.
TYGS	Type (Strain) Genome Server.

SYMBOLS

1-D	Simpson’s Diversity Index.
1/D	Simpson’s Reciprocal Index.
bp	Base Pairs.
D	Simpson’s Similarity Index.
dS/m	Decisiemens per Meter.
H	Shannon Diversity Index.
m/z	Mass-to-charge Ratio.

1

INTRODUCTION

Plants encounter various stressful conditions throughout their lifespan. These stressors are typically categorized into two groups: biotic and abiotic [1]. Biotic stresses are caused by living organisms, while abiotic stresses are inflicted on plants by environmental factors. Abiotic stresses can be further divided into physical and chemical stresses [2], which include salinity, chilling/freezing, heat shock, drought, nutrient imbalance, waterlogging, xenobiotic and heavy metals stress. Furthermore, the combined effect of these abiotic stresses leads to a 50% reduction in plant productivity [3]. One of the main abiotic stresses that limit crop production, particularly in arid and semi-arid areas, is salt-stress [4]. Salt-stress occurs when excessive accumulation of ions disrupts the plant's physiological balance, leading to primary unbalances such as osmotic stress, reduced nutrient uptake and growth [5], [6]. Additionally, salt-stress can result in secondary unbalances, such as the generation of reactive oxygen species (ROS) such as hydroxyl radical (OH^-), singlet oxygen ($^1O_2$), hydrogen peroxide (H_2O_2) and superoxide (O_2^-) [6], which can damage nucleic acids, proteins, carbohydrates and membrane lipids [7], [8], [9].

Salt-stress affects roughly 20% of global agricultural land [10], [11], [12], [13], leading to a decrease in agricultural productivity by 20-40%. It is estimated that, globally, almost half of the agricultural land will be affected by salt-stress by 2030 [14]. Soil salinization can be categorized into two types: natural and anthropogenic. Natural (primary) salinization is mainly caused by groundwater tables of marine origin, seepage, deposition of sea salts carried by wind, tidal effects and ascending capillary flow due to evapotranspiration in regions with low precipitation [15]. Climate change is expected to exacerbate salinization due to rising sea levels, evaporation and heat events [16]. Anthropogenic (secondary) salinization, on the other hand, results from human activities, which involves the use of unsuitable soils for irrigation, irrigation with high-soluble salt water, excessive use of fertilizers or soil amendments, poor irrigation practices, such as inadequate irrigation depths and uneven water distribution, which can lead to rising groundwater tables and the use of wastewater or saline industrial by-products can also contribute to salinization. [15]. The regions most affected by saline soils, generally recognized by an electrical conductivity (EC) above 4 dS/m [17], across the globe are Southern, East and North Africa, Western and Central China, Central Asia, the Middle East, Western United States, Australia and Argentina [18], [19], with the Mediterranean coastline being the most affected area in Europe [19]. In the Iberian Peninsula, the Algarve, Alentejo, North Meseta, Ebro basin and Tagus basin are the most affected regions. Both countries have significant areas with high salt content, which serve as repositories for valuable salt resources, including salt flats and saltpans [20]. Lezíria Grande, an important agricultural area near Vila Franca de Xira, suffers from high soil salinity, particularly in the southern part as depicted in Figure 1.1, due to its location surrounded by the Tagus River and Sorraia River [21], both of which are subject to tidal movement. The shallow saline groundwater arising from estuarine tides contributes to the salinity of the region [22]. The main crops produced in this area are maize (*Zea Mays* L.), tomato (*Solanum Lycopersicum* L.) and rice (*Oryza Sativa* L.) [21], [23], with the first two being saline-sensitive crops with corresponding salinity thresholds of 1.7 dS/m for maize and 2.5 dS/m for tomato [24], thus both are adversely affected by soil salinization [25].

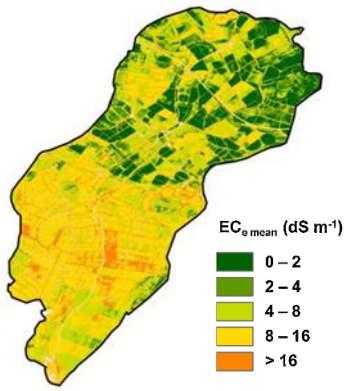

Figure 1.1 – Lezíria Grande soil salinity. This model calculated from Sentinel-2 multispectral imagery represents the soil salinity levels in the Lezíria Grande area. The dark green sectors stand for non-saline soils (EC between 0 and 2 dS/m), green sectors stand for slightly saline soils (EC between 2 and 4 dS/m), light green sectors stand for saline soils (EC between 4 and 8 dS/m), yellow sectors stand for highly saline soils (EC between 8 and 16 dS/m) and orange sectors stand for extremely saline soils (EC above 16 dS/m). Figure adapted from [21].

There are two categories of plants according to their ability to withstand salt levels: halophytes, which are plants that can flourish in saline environments due to their adaptation to high salt levels (>200 mM) [26], [27] and glycophytes, which are adversely affected by soil salinization, leading to hindered growth and development in the presence of 100-200 mM of salt [28], [29]. The majority of crops fall under the glycophyte category, making them susceptible to salinization, which can significantly limit their productivity, posing a serious threat to food security [10]. High salinity levels have a profound impact on plants, affecting various physiological and biochemical processes. Nutrient absorption is disrupted, as essential minerals become less accessible [30]. Cell membrane stability is compromised, leading to increased permeability and potential cell damage [30], [31]. Additionally, transport pathways within the plant are hindered, impeding the movement of nutrients and water [30]. Cellular damage and oxidative stress are caused by elevated ROS levels as mentioned before [31], [32]. Furthermore, root development is adversely affected, leading to stunted growth and reduced water absorption [33], [34]. Seed germination rates decline, impacting plant establishment [34]. Moreover, photosynthesis efficiency is reduced, limiting energy production, while plant transpiration rates are altered, affecting water regulation [33], [35]. Furthermore, salinity influences the levels of sugars such as sucrose, fructose and those involved in glycolysis, disrupting metabolic processes [36]. In order to survive and maintain productivity in saline environments, plants employ various strategies. They regulate ion transport and homeostasis to maintain cellular ion balance and mitigate toxicity [10], [28], [37]. Furthermore, ion detoxification processes are activated to manage excess salts [10], [37]. Crucial non-enzymatic and enzymatic antioxidant systems oppose oxidative stress induced by salinity [38], [39]. Additionally, plants regulate water channels to optimize water uptake and transport [28]. The synthesis of osmolytes helps maintain cellular osmotic balance of plants under saline conditions, as it modulates these processes in a crucial manner [39]. The interplay of these mechanisms enables plants to acclimate and prosper in environments with high salinity levels. However, the process of domestication has led to the loss of salt tolerance in numerous plant species as a result of selective breeding for a limited number of desirable traits, which in turn has reduced genetic variability and created an evolutionary bottleneck [40]. This phenomenon is evident in crops such as maize and tomato, where the crop wild relatives (CWRs), such as eastern gamagrass (*Tripsacum dactyloides*) and *Solanum pimpinellifolium*, exhibit greater salinity tolerance compared to their modern counterparts, *Zea mays* and *Solanum lycopersicum*, respectively [41], [42], showing the impacts of domestication over stress-dealing of current crops. Given that salt-stress severely impairs plant growth and productivity, it is imperative to develop effective coping mechanisms to enhance plant resilience, ensure food security and promote sustainable agriculture.

Efforts to improve crop salt tolerance through genetic engineering, plant breeding and management practices have demonstrated limited success due to the complex genetic and physiological characteristics associated with salt tolerance [43], [44]. An environmentally friendly, sustainable, economical and effective solution involves the utilization of beneficial bacteria [45], [46], [47]. Previous research has reported that plant growth-promoting bacteria (PGPB) have enhanced crop plant growth, resilience and productivity under stressful conditions [48], [49], like the bacteria *Rossellomorea aquimaris* improving maize seedlings' salt tolerance, *Peribacillus castrilensis* increasing tomato dry weight (DW) in salt-stress

conditions and *Planococcus rifietoensis* promoting the growth and productivity of wheat on saline soils [50], [51], [52]. Moreover, previous research has indicated that the impact of PGPB on plants is highly dependent of the specific interactions between bacterial strains and plant genotypes [53], [54]. Additionally, the nutritional status of the plant and abiotic stresses, including salinity, can also influence the interaction mechanisms between PGPB and their host plants [55], [56]. PGPBs provide several mechanisms to aid plants in thriving under saline environments. One such mechanism is by regulating the 1-aminocyclopropane-1-carboxylic acid (ACC) through the ACC deaminase (ACCd), which catalyses the reaction of cleaving ACC into ammonia and α-ketobutyrate. ACC is a precursor of ethylene, which functions as a stress hormone regulating many of the plant's developmental and physiological processes, such as leaf senescence, root elongation, stress signalling and seed germination under abiotic stress conditions. Protecting the plant from deleterious effects, ethylene is beneficial when stress is mild. Conversely, when stress becomes harsher, ethylene is produced in higher amounts, exceeding the acceptable threshold, inhibiting shoot and root proliferation and promoting leaf senescence, thereby disrupting plant growth and development [57], [58]. In addition to ACCd activity, PGPBs possess the capacity to produce auxins, which are a crucial group of phytohormones that significantly influence plant growth and development, either independently or in conjunction with other plant hormones. Among these, indole-3-acetic acid (IAA) is the most well-known and physiologically active natural auxin in plants, recognized as the key auxin in most species. IAA plays a central role in root development and elongation by stimulating the excessive production of capillary root hairs and lateral roots, as well as promoting cell division and elongation. Additionally, microbial auxin production can enhance ACCd activity, as auxin stimulates the biosynthesis of the ACC synthase enzyme in plants, leading to increased ACC expression. Thus, the interaction between IAA and ACC results in the facilitation of plant growth by IAA through the reduction of plant ethylene levels by ACCd [59]. On the other hand, biofilms produced by PGPBs act as a protective shield around the root, preventing direct interaction with ions [60]. These biofilms protect plants from pathogens by producing antimicrobials, stimulating induced systemic resistance (ISR), competing with pathogens and inhibiting their colonization [61]. Furthermore, beneficial biofilms on plant roots facilitate nutrient cycling and supply vital macronutrients and micronutrients, improve root colonization and produce substances with growth-promoting capabilities, including auxins, gibberellins and cytokinins [61]. The enhanced formation of exopolysaccharides (EPS) supports biofilms and improves resilience to abiotic stresses [62]. Notably, some PGPBs form EPS capable of binding cations such as Na^+, indicating a role in mitigating salt-stress by lowering Na^+ availability, enhancing K^+ absorption and boosting water uptake. This process helps maintain ion homeostasis and ionic balance to ensure plant growth [61], [63]. EPS constitutes most of the biofilm's composition, while microbes comprise only 5%–25% of it [64]. Additionally, PGPBs also play a crucial role in mitigating salt-stress in plants by providing and regulating antioxidants, which help manage the ROS induced during salt-stress, counteracting their adverse effects and enhancing the plant’s resilience [65], [66]. Additionally, other mechanisms provided by PGPBs include the production of protective osmolytes, such as proline, which ranks among the most extensively researched solutes [67]. Proline prevents the accumulation of toxic ions, such as Na^+, in plant shoots by excluding ions, preventing ion uptake and restricting their transport [68]. Moreover, proline accumulates under abiotic stress conditions, such as salt-stress, functioning as an antioxidant and osmolyte to assist plants in maintaining cell turgor [67]. It also regulates the expression of numerous genes associated to antioxidant enzymes in saline stress conditions [69]. The increase in free proline in plants growing under salt-stress serves as an adaptive mechanism, providing a source of nitrogen, carbon and reduction equivalents [70]. Furthermore, PGPBs also produce siderophores, which function as iron-binding agents sequestering iron from their surroundings, providing it as a nutrient for plants and hindering the growth of pathogenic microorganisms competing for the iron available. Additionally, siderophores trigger the ISR in plants [71], [72]. Finally, PGPBs are beneficial to plants as them provides essential nutrients that are lacking under salt-stress conditions through fixation, solubilization, oxidation, reduction and mineralization. Nitrogen (N) is the most critical nutrient and is highly susceptible to loss, influenced by factors such as precipitation, nitrogen source, tillage, crop rotation and soil type [73]. It is necessary for photosynthesis, growth, productivity and the production of storage proteins that are critical for technological quality [74]. Plants accumulates nitrate in vacuoles and can endure high ion concentrations, using nitrate as an osmotic agent [75]. Additionally, nitrate is involved in several processes, such as xylem transport, vacuole storage, absorption, reduction and incorporation into organic forms [76]. Phosphorus (P) is the second most limiting nutrient for crop growth behind nitrogen [77]. Some bacteria enhance phosphorus availability by solubilizing insoluble inorganic phosphate compounds or liberating organic phosphates [74]. This enhancement stimulates shoot and root growth, improves shoot and root length and increases dry and fresh shoot weights [77]. Phosphorus is vital for

energy transfer and storage, photosynthesis, respiration, cell membrane formation, glycolysis and enzyme activities. It also increases root development, strengthens stems, improves seed formation, accelerates crop maturity and enhances nitrogen fixation [78]. Potassium (K) is the third most crucial nutrient after nitrogen and phosphorus, plays a fundamental role in plant metabolism, charge balance, osmotic regulation and enzyme activation [79]. Moreover, bacteria can solubilize insoluble phosphorus and potassium in the soil using the same mechanism, increasing their availability and uptake by plants [80]. In addition, sulfur (S), deemed the fourth most relevant plant nutrient [81], is essential for growth and metabolism, known for its role in protein synthesis and synergistic relationships with nitrogen, phosphorus, potassium, manganese, iron and magnesium, thus improving their availability [82]. Likewise, calcium (Ca^{2+}) serves as a vital micronutrient and regulatory element in plant growth and development, which is solubilized by beneficial bacteria and plays an important role in various aspects of plant development [83]. Calcium is essential for maintaining cell membranes' integrity and regulating ion transport. Indeed, elevated levels of calcium have been shown to alleviate the harmful effects of NaCl by inhibiting sodium (Na^+) uptake [84]. Similarly, manganese (Mn) functions as an essential micronutrient, with bacteria being capable of reducing it to a form accessible to plants. Mn serves several essential functions in plant physiology, mainly in electron transport within photosystem II (PSII), the architecture of chloroplast and nitrogen metabolism [85]. Furthermore, it also functions as an activator and cofactor for several metalloenzymes, catalyzing enzymatic reactions, such as phosphorylation, decarboxylation, redox reactions and hydrolysis [86].

Some PGPB are either halotolerant, meaning they can grow in the presence of NaCl or halophiles, which require NaCl for growth [87]. These bacteria have evolved mechanisms to thrive in saline environments, such as alterations in plasmatic membrane and cell wall to block salt entry, such as antiporter channels and Na^+ and K^+ pumps, the accumulation of osmoprotectants such as organic molecules with low molecular weight that balance osmotic pressure in cells (e.g. proline, trehalose, betaines), modifications to proteins and enzymes to maintain activity under high levels of NaCl, the secretion of exopolysaccharides to support biofilm formation and DNA modifications (e.g. increased cytosine and guanine content) [88]. Therefore, utilizing adapted microbiota that evolved to cope with highly saline environments as a bioinoculant is becoming a highly promising strategy to potentially help crops tackle the escalating issue of salinization in agricultural lands [89], [90], [91], such as the Lezíria Grande, which is severely affected due to climatic conditions and estuarine tides.

The incorporation of omics approaches, which encompass genomics, transcriptomics and metabolomics, has significantly advanced our comprehension of the complex molecular plant-microbe interactions, especially under salt-stress conditions [92], [93], [94]. These advanced techniques enable an extensive analysis of the genes, transcripts and metabolites connected with the stress response pathways, providing valuable insights into how plants and their associated microbial communities adapt to high salinity environments. The genomics and metabolomics application to plant-associated bacteria enables the identification and functional characterization of microbial genes and metabolic pathways that contribute to plant stress resilience [95], [96]. For instance, the identification of genes associated with plant growth promotion and salt-stress mitigation in the genome of *Stenotrophomonas rhizophila* IS26 has resulted in improved tomato plant growth and salt resilience [97]. Additionally, the *Pseudomonas* sp. has been reported to increase the amount of ROS-scavenging compounds and antioxidants, enhancing tomato biomass under salt-stress conditions [98]. Transcriptomics, when applied to plants, showed to be a powerful tool providing a detailed perspective on the gene expression patterns that are responsive to stress, revealing how plants modulate their transcriptome to alleviate the consequences of salinity and how microbial interactions affect these gene networks [96], [99]. Research has shown that *Azospirillum brasilense* enhances rice growth under saline conditions by modulating the expression of crucial genes in rice plant related to defence and stress responses, jasmonic acid and abscisic acid (ABA) signalling pathways, as well as ion and nutrient transport [100]. By utilizing these omics strategies, we can deepen our understanding of the signalling mechanisms underlying plant-microbe interactions under salt-stress, ultimately contributing to the identification of biomarkers that can be used for the rapid screening and selection of crop varieties with improved stress resilience and bacteria with the capacity to improve crop performance under stressing conditions [95].

With all this, the development of a new bioformulation with the adapted microbiota could be a game-changer, enabling plants to thrive in salt-stress environments. The primary objective of this study is to develop a bioformulation that comprises halophile/halotolerant bacteria sourced from the Iberian Peninsula saltpans and salt flats, with the intention of improving crop growth and salt tolerance in saline environments. Additionally, this research seeks to better understand the plant-microbe interactions in these stressful conditions. The application of bioinoculants may improve the resilience and productivity

of crop plants, such as maize and tomato, which are of great significance in Portuguese agriculturally important regions, such as Lezíria Grande, which are affected by soil salinization and have the potential to revolutionize the agriculture as we know it.

2

MATERIALS AND METHODS

2.1 Sampling

The soil samples were obtained from a survey conducted by Gil and collaborators [20]. Sampling locations were selected based on their significant salinity and high gypsum content (≥15% gypsum accumulated under wet conditions), with no prior agricultural use and, in some instances, solely utilized for mineral extraction. Climatically, apart from Alcochete, which experiences a moderate Mediterranean climate, all locations were classified as Mediterranean, either mid-mountain or coastal. Three samples, each weighing between 30–50 g, were collected from regions without vegetation at a depth of 0–10 cm using a column collector from 14 distinct locations (Figure 2.1 and Table 2.1). These samples were mixed to form a single composite sample per location, with any visible saline or gypsum crusts removed. The samples gathered in 2022 and 2023, were kept at 4°C until further processing. The pH of the soil samples was determined using the method outlined by Mclean [101], salinity measured as electrical conductivity (EC) utilizing the YIERYI EC-8801 device (Shenzhen, China) and water content percentage was calculated by measuring the weight difference after incubating the sample for 7 days at 60°C, following the method described by Li and Wang [102].

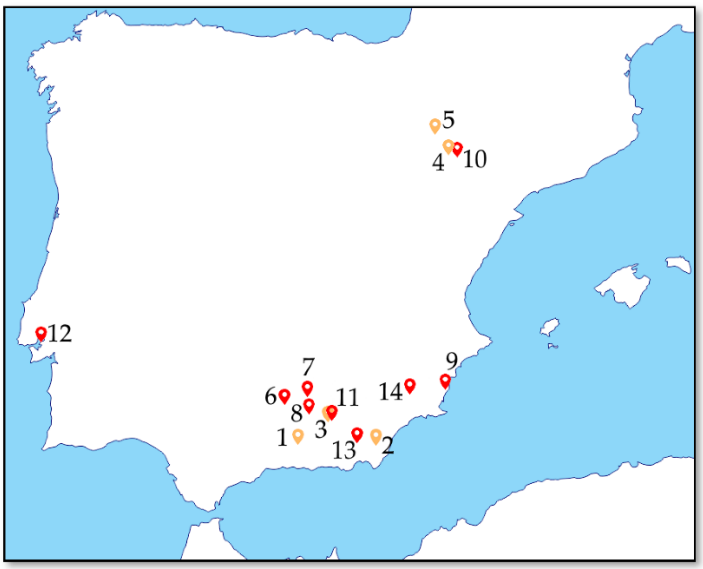

Figure 2.1 – Sampling locations. The map illustrates the chosen sampling locations across the Iberian Peninsula with each number matching a location listed in Table 2.1. Red pins indicate samples collected in saline soils, while yellow pins represent samples collected in gypsic soils. Figure retrieved from [20].

Table 2.1 – Sampling locations. Samples were gathered from multiple locations on the Iberian Peninsula, as shown by the numbered sites on the map (Figure 2.1) and their respective names. These sites were located in Portugal (PT) and Spain (SP). Samples were taken from gypsic and saline soils at a depth of 0–15 cm. The altitudes in mamsl (meters above mean sea level) and GPS coordinates (World Geodetic System 1984, WGS84) are approximate. The soil type, soil variables (pH and electrical conductivity) and geological context were assessed as factors influencing the microbiota. Table adapted from [20].

No.	Type	Name	Location	GPS coordinates	Altitude (mamsl)	Main Basal Lithology	Type of soil	pH	EC
1	Gypsum	Arroyo Salado	La Malaha, Granada (SP)	37°06'25.3"N 3°43'14.7"W	726	Dolomites and marbles	Cambic Calcisol	8.02	0.31
2	Gypsum	Rambla de la Mojonera	Sorbas, Almería (SP)	37°05'59.5"N 2°08'08.7"W	726	Sands and gravels	Cambic Calcisol	9.79	0.06
3	Gypsum	Hoya de Baza	Baza, Granada (SP)	37°30'50.4"N 2°45'34.5"W	792	Clays with pebbles	Calcaric Fluvisol	8.52	0.4
4	Gypsum	Quinto	Quinto, Zaragoza (SP)	41°26'51.8"N 0°32'15.5"W	195	Gypsum, marlstones, limestones	Haplic Calcisol	8.46	0.52
5	Gypsum	Zuera	Zuera, Zaragoza (SP)	41°52'56.7"N 0°47'21.6"W	335	Gypsum and clays	Haplic Gypsisol	8.56	0.18
6	Salt	Salina de San José	Torredonjimeno, Jaén (SP)	37°45'26.8"N 4°00'12.1"W	451	Marlstones and marly siltstones	Cambic Calcisol	8.66	2.08
7	Salt	Salinas de las Escuelas	Baeza, Jaén (SP)	37°52'15.9"N 3°31'18.1"W	479	Dolomites	Cambic Calcisol	9.58	2.16
8	Salt	Salinas de Las Cañadas	Montejícar, Jaén (SP)	37°36'31.9"N 3°30'19.9"W	1028	Conglomerates, sandstones, clays	Cambic Calcisol	8.64	2.18
9	Salt	Laguna Roja	Torrevieja, Alicante (SP)	37°59'46.8"N 0°42'11.8"W	-2	Siltstones	Calcaric Leptosol	9.24	2.68
10	Salt	Saladas de Bujaraloz	Bujaraloz, Zaragoza (SP)	41°25'15.6"N 0°11'39.6"W	322	Clays and siltstones	Calcaric Fluvisol	8.22	2.42
11	Salt	Saladar del Balco	El Baico, Granada (SP)	37°32'28.5"N 2°43'57.1"W	711	Marls, conglomerates, limestones, sandstones	Cambic Calcisol	8.97	5.37
12	Salt	Salinas do Samouco	Alcochete, Setúbal (PT)	38°44'11.6"N 9°00'01.7"W	0	Sandstones and conglomerates	Eutric Regosol	6.88	2.23
13	Salt	Barranco de las Salinas	Gador, Almería (SP)	37°01'01.9"N 2°26'51.7"W	263	Marls, sandstones, siltstones	Cambic Calcisol	9.38	1.94
14	Salt	Rambla de Librilla	Librilla, Murcia (SP)	37°54'23.7"N 1°22'15.8"W	205	Conglomerates and sandstones	Cambic Calcisol	9.21	3.78

2.2 Isolation, identification and analysis of culturable bacteria populations from saline soils

Firstly, soil samples weighing 0.25 g were processed and subjected to serial dilution in a sterile solution containing 0.45% NaCl in order to culture bacteria on LB plates with 2 M of NaCl (per litre: 116.9 g of NaCl, 5 g of yeast extract, 10 g of tryptone and 15 g of agar) in triplicates. Colony-forming units (CFUs) were counted for each sampling point and standardized to the dry weight of the original soil sample (in mg). Subsequently, for each sampling point, colonies exhibiting morphological differences, as per the guidelines of the PathElective [98], were selected, isolated and purified. These pure cultures

were then preserved at -80 ºC in 40% glycerol. The isolates were identified by amplifying either the hypervariable V5-V8 region (~700 bp) or the full region (~1500 bp) of the bacterial 16S rRNA gene. This was achieved using pairs of universal primers: 799F (5′-AACMGGATTAGATACCCKG-3′) and 1392R (5′-GGTTACCTTGTTACGACTT-3′) or 27F (5′-AGAGTTTGATCCTGGCTCAG-3′) and 1492R (5′-CTACGGCTACCTTGTTACGA-3′). DNA templates were extracted from individual colonies using the heat shock method [99], which involved suspending a well-grown colony in 100 µL of sterile double distilled water (ddH_2O), incubating at 95 ºC for 10 minutes and centrifuging at 14000 x g for 5 minutes, retaining only the supernatant. DNA quality was assessed using a NanoDrop™ One (Thermo Scientific™, Waltham, MA, USA). Polymerase chain reaction (PCR) was performed using the NZYTaq II 2x Master Mix by Nzytech (Lisbon, Portugal), under the following conditions: initial denaturation phase at 95 °C for 2 minutes, followed by 40 cycles of denaturation at 95 ºC for 3 seconds, annealing at 45 ºC for 30 seconds, elongation at 72 ºC for 2 minutes and a final extension phase at 72 ºC for 7 minutes. Then, amplicon bands were assessed utilizing a 1% agarose gel electrophoresis with a Mupid®-exU System (Tokyo, Japan) at 135 V for 15 min and visualized with a transilluminator (UVIvue™, UVITEC Company, Cambridge, UK). Subsequently, the sequences were then sent to GENEWIZ (Leipzig, Germany) for Sanger sequencing. The resulting sequences were compared to the National Library of Medicine BLAST database and strains were identified with a similarity threshold of >97%. Strains that were labelled as 'Unidentified' could not be identified due to insufficient DNA quality or the inability to amplify despite multiple attempts.

Furthermore, the Shannon and Simpson biodiversity indexes, similarity index, reciprocal index, richness and evenness were calculated using the Omni Calculator website (Omni Calculator, Kraków, Poland) to gain a deeper understanding of the diversity and distribution within each sample.

2.3 Plant Growth Promoting and Salt-Stress Relieving Traits Performance and Strains Growth under High Salinity Levels

To ensure comparability and enable statistical analysis, all bacterial characterization tests were conducted in triplicate and quantitative tests were initially inoculated to an optical density (OD) of 0.05.

2.3.1 Strains Growth under High Salinity Levels

To test if the strains performed well under high salinity concentrations was carried out a growth assay in a 96-well plate with LB liquid medium at 0.25, 0.5, 0.75, 1 and 2 M of NaCl for 48 hours under continuous shaking (160 rpm) at 28 ºC. All the strains were initially inoculated at an OD of 0.05. The bacterial growth was measured periodically (2, 4, 24, 26, 28 and 48 hours) using a microplate reader at 600 nm.

2.3.2 Production of 1-Aminocyclopropane-1-Carboxylate Deaminase (ACCd)

The production of 1-aminocyclopropane-1-carboxylate deaminase (ACCd) was evaluated by following the methodology adapted by Niza-Costa and collaborators [103]. In summary, the strains were cultivated in a 96-well plate using M9 medium (Merck) supplemented with 3 mM of ACC as the sole carbon and nitrogen source and 2 M of NaCl. After 72 hours at 28 ºC and 160 rpm, the culture's growth was assessed at 600 nm. This measurement indirectly confirmed the ACCd production by each strain.

2.3.3 Auxins Production

Regarding auxin production, the procedure outlined by Ambrosini and Passaglia was utilized [104]. Thus, 200 µL of LB medium with 0.5 g/L of tryptophan and 2 M of NaCl were inoculated with each strain and incubated at 28 ºC and 160 rpm for 48 hours. Following centrifugation at 3800 rpm for 50 minutes, 100 µL of the supernatant was combined with 100 µL of Salkowski reagent (35% $HClO_4$ and

0.5 M of $FeCl_3$). Lastly, after a 30-minute incubation at room temperature in the dark, absorbance was measured at 530 nm. The results were expressed as indole-3-acetic acid (IAA) equivalents using a calibration curve.

2.3.4 Biofilm Formation

Biofilm formation was assessed following the method by Coffey and Anderson [105], with minor adjustments. In brief, strains were cultured in LB medium with 2 M of NaCl in a 96-well plate at 28 ºC and 160 rpm for 24 hours. Planktonic structures were then washed with ddH_2O and only biofilm structures were stained with 200 µL of 0.5% crystal violet solution (0.5% crystal violet and 25% CH_3OH). After a 10-minute incubation in the dark at room temperature, the excess stain was washed and structures were solubilized with 30% glacial acetic acid solution for 10 minutes. Lastly, a 1:4 dilution was prepared and the solution was measured at 550 nm.

2.3.5 Exopolysaccharides (EPS) Production

The exopolysaccharides production was evaluated as Mu'minah and collaborators [106] described with slight modification. The strains were grown in LB plates for 2 days at 28 ºC and the strains that produced exopolysaccharides formed a thick slime (mucoid texture) around the bacterial colonies.

2.3.6 Antioxidants Production

The antioxidants production was evaluated following the thiocyanate method, as depicted by Takao and collaborators [107]. Basically, 200 µL of supernatant from 2-day cultured strain in LB medium amended with 2 M of NaCl centrifuged at 4000 rpm for 7 minutes was mixed with 200 µL linoleic acid solution (25 mg/mL in pure ethanol), 400 µL of phosphate buffer (per litre: 3.394 g of $NaH_2PO_4 \cdot H_2O$, 20.214 g of $Na_2HPO_4 \cdot 7H_2O$; pH 7.0) and 200 µL of ddH_2O. The samples were incubated at 40 ºC for 10 minutes in the dark. Then, 100 µL were mixed with 3 mL of 70% ethanol, 100 µL of NH_4SCN solution (0.3 g/mL in ddH_2O) and 100 µL of ferrous chloride reagent (2.45 mg/mL of $FeCl_2$ in 3.5% hydrochloric acid). Lastly, after a 3-minutes incubation at room temperature, 20 µL were diluted in 280 µL ddH_2O and the absorbance was measured at 500 nm. The results were expressed as antioxidant equivalents using a calibration curve.

2.3.7 Proline Secretion

The extracellular proline production was measured by its reaction with ninhydrin, as depicted by Goswami and collaborators [108] with some adjustments. Basically, 1 mL of supernatant from 2-day cultured strain in LB medium amended with 2 M of NaCl centrifuged at 4000 rpm for 10 minutes at 4 ºC was mixed with 600 µL of sulfosalicylic acid solution (3% aqueous solution), then was centrifuged at 13000 rpm for 10 minutes at 4 ºC and 1 mL of the supernatant was mixed with 1 mL of 30% glacial acetic acid solution and 1 mL of ninhydrin solution (2% acetone solution). The samples were incubated at 90 ºC for 60 minutes and then cooled in an ice bath. Subsequently, were added 2 mL of toluene and mixed vigorously for 10 seconds. Finally, was mixed 20 µL of the organic phase (top) with 180 µL of toluene and the absorbance was measured at 520 nm. A proline standard curve was prepared utilizing proline stock solutions.

2.3.8 Siderophores Production

Siderophore production was evaluated according to the guidelines of Arora and Verma, with slight adjustments. [109]. A LB with 2 M of NaCl culture of each strain was centrifuged at 4000 rpm for 10 minutes and 100 µL of the supernatant was mixed with 100 µL of chrome azurol sulfonate (CAS) reagent (for 100 mL: 7.5 mL of 2 mM CAS dye, 1.5 mL of 1 mM $FeCl_3$-HCl solution, 6 mL of 10 mM HDTMA, 20 mL of 2.5 mM PIPES, 65 mL of ddH_2O) in a 96-well plate. Following a 20-minutes incubation at room temperature, absorbance was measured at 630 nm. Siderophore production was determined as the percentage siderophore unit (psu), where A_c is the absorbance of control (uninoculated broth +

CAS reagent) and A_s is the absorbance of sample (inoculated broth + CAS reagent) (Equation 2.1) [109]:

Equation 2.1 – Calculation of siderophore production as the psu.

$$psu = \frac{(A_c - A_s) \times 100}{A_c}$$

2.3.9 Nitrogen Fixation

The nitrogen-fixing activity was evaluated according to the guidelines of Sulistiyani and Meliah, using Bromothymol Blue (BTB) at a concentration of 100 mg/L as the indicator [110]. In this assay, strains were grown in Jensen's medium amended with 2 M of NaCl and BTB (per litre: 20 g of sucrose, 2 g of $CaCO_3$, 0.005 g of $Na_2MoO_4 \cdot 2H_2O$, 0.1 g of Fe_2S0_4, 0.5 g of $MgSO_4$, 1 g of K_2HPO_4, 116.9 g of NaCl; pH 7.2) for 3 days (160 rpm, 28 ºC). For quantification, the absorbance was assessed at 640 nm. The nitrogen-equivalent standard curve was constructed with NH_3.

2.3.10 Phosphate Solubilization

To measure the phosphate-solubilizing performance was followed Zheng and collaborators protocol with some amendments [111]. Each strain was incubated in National Botanical Research Institute's Phosphate (NBRIP) liquid medium with 2 M of NaCl (per litre: 10 g of glucose, 0.1 g of $(NH_4)_2SO_4$, 0.2 g of KCl, 0.25 g of $MgSO_4 \cdot 7H_2O$, 5 g of $MgCl_2 \cdot 6H_2O$, 5 g of $Ca_3(PO_4)_2$ and 116.9 g of NaCl) for 3 days (160 rpm, 28 ºC). After, the plates were centrifuged at 4000 rpm for 10 minutes, and the supernatant was combined with vanadate-molybdate reagent in a 3.5:1 ratio (v:v). Following a 10-minute incubation in the dark, the absorbance was recorded at 420 nm. A phosphate standard curve was prepared utilizing anhydrous KH_2PO_4.

2.3.11 Potassium Solubilization

Regarding potassium solubilization, each strain was incubated in Aleksandrov liquid medium with 2 M of NaCl (per litre: 5.0 g of glucose, 0.1 g of $CaCO_3$, 0.5 g of $MgSO_4 \cdot 7H_2O$, 0.006 g of $FeCl_3$, 1.5 g of KH_2PO_4, 1.5 g of K_2HPO_4, 3 g of potassium aluminium silicate (mica) and 116.9 g of NaCl; pH 7.2), amended with BTB (100 mg/mL), according to Rajawat and collaborators [112] for 3 days (160 rpm, 28 ºC). Following the initial growth incubation, samples were measured at 430 nm. The standard curve was constructed using the Rajawat formula [112].

2.3.12 Sulfur Oxidation

The sulfur-oxidizing activity test was prepared as described per Hidayat, Saud and Samsudin, with slight alterations [113]. A 10 µL drop of each cultured strain was placed on thiosulfate mineral medium (TSM) with 2 M of NaCl added (per litre: 10 g of $Na_2S_2O_3 \cdot 5H_2O$, 0.1 g of $CaCl_2 \cdot 2H_2O$, 0.8 g of $MgCl_2 \cdot 6H_2O$, 0.4 g of NH_4Cl, 1.5 g of KH_2PO_4, 1.5 g of K_2HPO_4, 116.9 g of NaCl and 15 g of agar; pH 7.5), with the addition of 0.01 g of bromocresol purple and incubated for 14 days at 28 ºC. Following the measurement of the yellow halos diameter and the colony diameter the relative activity index was calculated utilizing the Equation 2.2.

Equation 2.2 – Calculation of the relative activity index.

$$\text{Relative activity Index} = \frac{\text{Halo diameter} - \text{Bacterial colony diameter}}{\text{Bacterial colony diameter}}$$

2.3.13 Calcium Solubilization

The calcium solubilization test was assessed following the indications of Tamilselvi, Chitdeshwari and Uthandi with slight modifications [114]. A 10 µL drop of each cultured strain was placed on Calcium Solubilizing Bacteria (CaSB) differentiating medium amended with 2 M of NaCl (per litre: 5 g of glucose, 0.4 g of K_2HPO_4, 0.01 g of $MgSO_4$, 1 g of peptone, 5 g of $CaCO_3$, 0.05 g of $(NH_4)_2SO_4$, 116.9 g of NaCl and 15 g of agar; pH 7.5) and incubated for 7 days at 28 ºC. Following the measurement of the discolouration halos diameter and the colony diameter the solubilization index was calculated using the Equation 2.3 [85].

Equation 2.3 – Calculation of the solubilization index.

$$\text{Solubilization Index} = \frac{\text{Halo diameter} - \text{Bacterial colony diameter}}{\text{Bacterial colony diameter}}$$

2.3.14 Manganese Solubilization

The manganese solubilization test was assessed following the indications of Ijaz and collaborators [85]. A 10 µL drop of each cultured strain was placed on LB agar medium amended with 2 M of NaCl and MnO_2 (4.34 g/L) and incubated for 3 days at 28 ºC. Following the measurement of the discolouration halos diameter and the colony diameter the solubilization index was calculated using the Equation 2.3.

2.4 Plant Material: Tomato and Maize

To execute plant tests of the candidate strains were used tomato (*Solanum lycopersicum* L.) and maize seeds (*Zea mays L.*), were used as model crops. The selected tomato variety was the H1015 F1, a hybrid variety developed by Heinz and was kindly provided by Pé Da Planta-Produção E Comercialização De Produtos Agrícolas, Lda. (Lourinhã, Portugal) and SY Carioca and Clipser were the maize varieties from Syngenta Crop Protection - Soluções Para A Agricultura, Lda. (Lisbon, Portugal) and kindly provided by Associação Nacional de Produtores de Milho e Sorgo (Anpromis). All varieties have a high productivity and are widely used on the Iberian Peninsula [115], but specially representative of the crops used in Ribatejo region. The maize seeds were thoroughly washed in order to remove the antifungal coating they were treated with.

2.5 *In Vitro* Colonization Tests under Salinity Stress

The *in vitro* colonization tests were carried out according to the guidelines provided by Vilchez and collaborators, with certain adjustments to accommodate the specific plant type and stress conditions applied [116]. Initially, maize seeds were surface-sterilized by standing them in 20% bleach for 5 minutes under agitation, followed by 5 minutes of agitation in 70% ethanol. The seeds were then washed three times with sterile ddH_2O and incubated in water, overnight to favour the germination. After incubation, the seeds were placed in plastic containers with wet filter paper. For tomato seeds, after same surface-sterilization process described for maize, they were put in square petri dishes with soaked filter paper and stored in the dark. After 5 days of incubation, the roots of the germinated seedlings of both plants were disinfected by standing them in 70% ethanol for 1 minute under agitation and then washed three times with sterile ddH_2O. The surface-sterilized roots were placed in 1.5 mL sterile tubes with a bacterial solution (10^8 CFUs/mL), with 0.5 M of NaCl added to a set of the samples to work as salt-stress condition. The samples were then incubated overnight with agitation (150 rpm) at 28 °C. Thereafter, the roots were surface sterilized in 70% ethanol and washed three times with sterile ddH_2O before being ground and serially diluted. The dilutions were spread on LB plates containing 2 M NaCl and incubated at 28 °C for 48 hours. Subsequently, CFUs were counted and normalized to the root dry weight of the initial sample (in mg). The differential colonization rates between treatments with and without salt stress were documented for each bacterial treatment. Each treatment was conducted in triplicate.

2.6 Evaluation of Plant Salt-Tolerance Enhancement

To perform the early-stage tests, maize seeds were first sterilized as described in Section 2.5. Following sterilization, the seeds were placed in plastic containers with wet filter paper and incubated at room temperature for 7 days. After germinating, the seedlings were transferred to 0.5 L pots containing a mixture of turf and vermiculite (3:1, v:v) and were grown in a greenhouse for 5 days more. The seedlings were then inoculated with 40 mL per pot of the selected candidate strain (10^8 CFUs/mL), prepared in either 0.45% NaCl for non-saline conditions or 0.5 M NaCl to simulate high salt-stress. In the case of tomatoes, three seeds were directly planted in each 0.5 L pot filled with the turf:vermiculite mixture (3:1, v:v) and maintained under greenhouse conditions. Prior to inoculation, the seedlings were thinned or transferred to ensure only one seedling per pot. The pots were then inoculated with 40 mL of the selected candidate strain (10^8 CFUs/mL) in either 0.45% NaCl for non-saline conditions or 0.25 M NaCl to ensure a high salt-stress. Control set (mock) treatments involved inoculating the seedlings with 40 mL of 0.45% NaCl for non-saline conditions or 0.5 M (maize) or 0.25 (tomato) NaCl for high salt-stress. Salinity levels were monitored and maintained through the irrigation water throughout the experiment, when required. The test was concluded at 7 days after treatment (DAT) for maize and 14 DAT for tomato, when the phenotypes were evident. All treatment and condition combinations were performed in triplicate.

On the other hand, long-term pot tests were conducted under the same conditions as the early-stage tests, with the following modifications: 2 L pots were used, the maize salt-stress was reduced to 0.35 M NaCl, all treatment and condition combinations were performed in six replicas and the test durations were extended to 44 DAT for maize and 48 DAT for tomato. Although the experiment was initially intended to continue until fruit production, it had to be terminated prematurely due to the death of uninoculated plants under salt-stress conditions.

Phenotypic data were collected by measuring shoot and root lengths, total dry weight (DW) and photosystem II quantum yield (QY) recurring to the FluorPen FP 110 (Photon Systems Instruments, Drásov, Czech Republic). Measurements were standardized and analyzed using ImageJ software (v1.54f) [117].

2.7 Full Genome Sequencing and Genomic Analysis of Halophilic Bacteria

The DE strain genomic DNA was extracted with the PromoCell's Bacteria DNA Extraction Kit from PromoKine (Heidelberg, Germany), following manufacturer indications. Bacterial cells were grown in LB with 0.75 M of NaCl for 2 days at 28 °C. Following this, 1 mL of the bacterial culture was transferred into a 1.5 mL sterile tube and subjected to centrifugation at 15000 x g for 1 minute, to separate the cells from the liquid medium. The supernatant was discarded and the cell pellet was resuspended in 300 µL of a cell resuspension solution. Here, 2 µL of lysozyme solution (100 mg/mL) was added and the mixture was gently inverted. The tube was then incubated at 37 °C for 20 minutes with occasional inversion. After incubation, the cells were once again subjected to centrifugation at 15000 x g for 1 minute and the supernatant was discarded. The resulting cell pellet was resuspended in 300 µL of a cell lysis solution, followed by the addition of 1.5 µL of RNase A solution (4 mg/mL) and gentle inversion. The sample was then incubated at 37 °C for 15 minutes and subsequently cooled on ice for 1 minute. Then, 100 µL of a protein precipitation solution were added to the lysate and the mixture was vigorously vortexed for 10 seconds. The sample was then centrifuged at 15000 x g for 5 minutes and the supernatant, containing the DNA, was transferred to a clean 1.5 mL tube preloaded with 300 µL of 99% isopropanol. The sample was allowed to incubate for an hour, followed by two centrifugations at 15000 x g for 1 minute. After centrifugation, the supernatant was discarded and the tube was drained on clean absorbent paper. The DNA pellet was then washed by adding 500 µL of a washing buffer, inverting the tube several times and centrifuging at 15000 x g for 1 minute. The supernatant was discarded with the help of a micropipette, and the DNA pellet was air-dried at room temperature for 15 minutes. Finally, the dried DNA pellet was resuspended in 50 µL of ddH_2O. The DNA was hydrated after being incubated at 60 °C for 20 minutes. The DNA quality was evaluated using a NanoDrop™ One (Thermo Scientific™, Waltham, MA, USA).

The whole genome was sequenced at IIT Biotech GmbH (Bielefeld, Germany) utilizing Oxford Nanopore Technologies. Both long and short DNA reads were produced using Nanopore. For library preparation, the SQK-LSK112 sequencing kit (Oxford Nanopore Technologies) was employed without

prior DNA shearing. Short reads were generated through a 2×300-nucleotide run using the MiSeq reagent kit v3 (600 cycles). Long reads were produced on a GridION platform with an R10.4 flow cell. Base calling and demultiplexing were conducted using Guppy (v.6.2.11) with the super accurate base-calling model. Assemblies were performed using Flye (v.2.9) [118] for the Nanopore long read data. The Flye-based assembly was subsequently polished using Medaka (v.1.6.1), Pilon (v.1.22) [119] and Bowtie2 [120] for mapping.

Quality assessment of the genome assembly was performed using three complementary tools. QUAST (v.5.2.0) [121] was employed to evaluate the overall assembly statistics. CheckM (v.1.0.13) [122] was utilized to assess the completeness and contamination of the assembled genome. Finally, BUSCO (v.5.7.1) [123] was used to evaluate the presence of single copy orthologs, providing an indication of the assembly's completeness and accuracy in terms of gene content.

PROKKA (v.1.14.6) [124] was utilized for rapid prokaryotic genome annotation, which included the identification and annotation of genes, coding sequences (CDS), rRNA, tRNA and other genomic features.

The 16S rRNA sequences were extracted from the genome assembly using the search_pcr2 function of USEARCH (v.11.0.667). These sequences were then subjected to BLAST searches against both the NR (Non-Redundant) and RefSeq 16S rRNA databases for further taxonomic identification and comparison. Additionally, the genome sequence data were analyzed using the Type (Strain) Genome Server (TYGS) [125], a free bioinformatics platform available at https://tygs.dsmz.de, to perform a whole genome-based taxonomic analysis.

Bacterial plant growth-promoting traits were identified through DIAMOND (v.2.1.9) [126] BLAST searches against the PLaBAse database (v.Aug2021) [127].

2.8 Identifying Bacterial Metabolites Improving Plant Growth and Salt Resilience

To identify which compounds are being produced and/or secreted by the selected bacterial candidates under high salt levels firstly the bacteria were grown in LB with 0.5 M of NaCl for 2 days at 28 ºC, then were centrifuged at 4000 rpm for 10 min and saved both supernatant and bacterial pellet into different tubes. The supernatant and pellet were then lyophilized at -80 ºC for 2 days in a FreeZone Plus 4.5 Litre Cascade Benchtop Freeze Dry Systems (Labconco, Kansas City, MO, USA). The lyophilized samples were sent to analyze to the Proteome and Metabolome Research group at CeBiTec (Bielefeld, Germany) in triplicates. Metabolites were extracted from 5 mg of lyophilized material using 1 mL of 80% methanol, which included 10 µM of ribitol as an internal standard, in a Precellys24 Instrument (Peqlab, Erlangen, Germany) with 1 mm zirconia beads (Roth, Karlsruhe, Germany). The extracts were treated three times at 6.5 m/s for 45 seconds. Following this, the extracts were centrifuged at 15000 x g and 750 µL of the clear supernatant was transferred to 1 mL glass vials (Supelco, Bellfonte, California) and evaporated under a nitrogen stream. Metabolites were derivatized with 75 µL of methoxylamine hydrochloride in pyridine (20 mg/mL) for 90 minutes at 37 ºC, followed by 75 µL of N-Methyl-N-(trimethylsilyl)trifluoroacetamide (MSTFA) for 30 minutes at 37 ºC. All chemicals and standard compounds were sourced from Sigma-Aldrich-Fluka (Taufkirchen, Germany), Merck (Darmstadt, Germany) or Macherey-Nagel (Düren, Germany).

Samples of 1 µL were analyzed using a TSQ 9000 Triple Quadrupole GC-MS/MS (Thermo Electron, Dreieich, Germany). Derivatized metabolites were vaporized at 280 ºC in splitless mode and separated on a 30 m x 0.25 mm OPTIMA-5MS capillary column with a 0.25 µm coating. Helium was used as the carrier gas at a flow rate of 1 mL/min. The interface temperature was set to 250 ºC and the ion source temperature was 280 ºC. The oven temperature was maintained at 80 ºC for 3 minutes, then increased to 320 ºC at a rate of 5 ºC/min and held at 320 ºC for 2 minutes. The system was equilibrated at 80 ºC for 2 minutes after each analysis. Mass spectra were recorded at a rate of 1 scan per second, with a scanning range of 50-750 m/z. A total of 120 metabolites were identified and analyzed by comparison with purified standards, with additional identification support from the Golm Metabolome Database (v.2022) [128]. Relative levels of selected metabolites were automatically quantified by integrating the peak areas of selective ions using the processing setup in Xcalibur 4.5 software (Thermo Electron, Dreieich, Germany) [129]. Relative response ratios were calculated by normalizing the respective peak areas to the internal standard’s peak area and dividing the result by the weight of the extracted sample.

2.9 Transcriptomic Analysis of Plants Treated with Bacteria under Saline Stress

For time reason and clearer phenotypes, transcriptomic analysis was focused on maize model plant. These studies commenced with the cultivation of maize plants, as detailed in early-stage tests (Section 2.6). The first batch of triplicate samples for each treatment and condition combination was collected at 3 DAT and a second batch of triplicate samples was collected at 5 DAT. The first batch of plants were instantaneously frozen in liquid nitrogen. Following this, the frozen shoots of the plants were thoroughly ground using a mortar and pestle. To prevent the sample from thawing during the grinding process, liquid nitrogen was repeatedly mixed. The RNA extraction was performed using TRIzol method as described by Afifah and collaborators with slight modifications [130]. 70-100 mg of frozen sample was added to a 1.5 mL tube, followed by the addition of 1 mL of TRIzol reagent (ABP Biosciences, Rockville, MD, USA) and subsequent homogenization. After a 10-minute incubation at room temperature, the mixture was centrifuged at 12200 x g for 10 minutes at 4 ºC. The supernatant was then transferred into a new tube, where 200 µL of chloroform was added, homogenized by inverting for 15 seconds and incubated for 3 minutes. The homogenate was then centrifuged at 12200 x g for 15 minutes at 4 ºC. The aqueous phase (top) was transferred into a new tube and 200 µL of chloroform extraction was added to repeat the chloroform extraction. The new aqueous phase was then transferred to a new tube containing 300 µL of 99% cold isopropanol. The mixture was allowed to stand overnight at -20 ºC, then was centrifuged at 12200 x g for 15 minutes at 4 ºC. The supernatant was discarded and the RNA pellet was washed through the addition of 1 mL of 70% ethanol (dissolved in 0.1 mM EDTA solution) and then centrifuged at 4600 x g for 5 minutes at 4 ºC. The supernatant was removed with the help of a micropipette and the washing steps were repeated two more times. Finally, the RNA pellet was dried for 30 minutes at room temperature, then dissolved in 20 µL of RNase-free water and incubated at 60 ºC for 10 minutes. The quality of the RNA was evaluated by using the NanoDrop™ One (Thermo Scientific™, Waltham, MA, USA).

A second batch of plants was collected and phenotyped as mentioned in Section 2.6 to ensure that differentially expressed genes detected in this analysis were actually leading to previously described and evident phenotypes.

Furthermore, the RNA-seq analysis was conducted by Novogene. Initially, RNA integrity was assessed utilizing the Bioanalyzer 2100 system (Agilent Technologies, CA, USA). Additionally, mRNA was purified from total RNA utilizing poly-T oligo-attached magnetic beads. After fragmentation, the first strand cDNA was synthesized with random hexamer primers, followed by the synthesis of the second strand cDNA. The library preparation included end repair, A-tailing, adapter ligation, size selection, amplification and purification. The library was assessed using Qubit and real-time PCR for quantification and bioanalyzer for size distribution detection. For the strand-specific library, the process was analogous, however, the second strand cDNA was synthesized utilizing dUTP as a replacement for dTTP to maintain directionality. This directional library was also evaluated with Qubit, real-time PCR and a bioanalyzer for size distribution. After quality control, libraries were pooled based on effective concentration and targeted data amount, then sequenced using Illumina technology. Moreover, raw data (raw reads) in fastq format were processed with fastp software to obtain clean data (clean reads) by removing adapter-containing reads, reads with poly-N and low-quality reads. Simultaneously, Q20, Q30 and GC content of the clean data were determined. All subsequent analyses were based on high-quality clean data. Besides, reference genome and gene model annotation files were downloaded from the genome website. The reference genome index was built using Hisat2 (v.2.0.5) and paired-end clean reads were aligned to the reference genome using Hisat2, which was chosen for its ability to generate a splice junction database based on the gene model annotation file, providing superior mapping results. In addition, mapped reads of each sample were assembled by StringTie (v.1.3.3b) [131] in a reference-based approach. StringTie employs a novel network flow algorithm as well as an optional *de novo* assembly step to assemble and quantitate full-length transcripts representing multiple splice variants for each gene locus. Additionally, featureCounts (v.1.5.0-p3) was utilized to count reads mapped to each gene. Subsequently, the expected number of Fragments Per Kilobase of transcript sequence per Millions base pairs sequenced (FPKM) for each gene was determined based on the length and read count. Moreover, differential expression analysis for two conditions/groups was performed utilizing the DESeq2 R package (v.1.20.0) for biological replicates and the edgeR R package (v.3.22.5) for samples without biological replicates. DESeq2 uses statistical models based on negative binomial distribution to determine differential expression in digital gene expression data. For edgeR, read counts were normalized to

eliminate differences in sequencing depth between samples before differential gene expression analysis. In both cases, the resulting *p*-value was adjusted using Benjamini and Hochberg's methods to control the false discovery rate. A corrected *p*-value ≤ 0.05 and $|\log_2(\text{foldchange})| \geq 1$ was set as the threshold of significant differential expression. Furthermore, the clusterProfiler R package was utilized to test the statistical enrichment of differential expression genes in Kyoto Encyclopedia of Genes and Genomes (KEGG) pathways. Besides, genes were ranked by their degree of differential expression in the two samples. The predefined gene set was subsequently tested to determine if it was enriched at the top or bottom of the list. Gene set enrichment analysis (GSEA) was used to detect subtle expression changes, with the local version of the GSEA analysis tool employed [132]. In addition, alternative splicing is a crucial mechanism for regulating gene expression and protein diversity. The rMATS (v.3.2.5) software was employed to analyze alternative splicing events, which primarily include five types: skipped exons, retained introns, mutually exclusive exons, 5' alternative splice sites and 3' alternative splice sites. Lastly, GATK (v.4.1.1.0) software was utilized for single nucleotide polymorphism (SNP) calling and SnpEff (v.4.3.1q) software was employed to annotate the variant sites.

2.10 Statistical Analysis

Statistical analyses were conducted using Prism software (v10.3.0, GraphPad Software, Boston, MA, USA). Student's t-test or two- or one-way ANOVA were applied, with Šidák and Tukey's tests used for post-hoc comparisons. Principal component analysis (PCA) and heatmap generation were performed using an R script in RStudio (v.2023.06.2+561, Posit Software, Boston, MA, USA).

3

RESULTS

3.1 Populational Analysis of Culturable Halophile/Halotolerant Bacteria

From a total of 14 different soil locations, 54 strains were isolated that were capable of surviving at a concentration of 2 M of NaCl, which were identified by their morphology and listed in Table 7.1. Out of the 54 isolated strains, 42 strains were identified as 30 different species (Figure 3.1). In terms of the location where the strains were isolated, 24 species were unique to saline soils (80%), 3 species were only identified in gypsic soils (10%), the *Bacillus atrophaeus*, *B. halotolerans* and *Rossellomorea aquimaris* and the *Halobacillus faecis*, *Halomonas elongata* and *Oceanobacillus picturae* were identified in both types of soils (10%).

The *Bacillaceae* family was the most predominant within the collection accounting for almost half of the strains (43%) and was also the most prevalent family in 9 out of 14 soils, engulfing both saline and gypsic soils as seen in Figure 3.2. The genus with the most represented strains was Halobacillus, with a total of 8 strains, of which 5 were Halobacillus faecis, the species with the most strains and the rest were *H. trueperi* (2) and *H. sediminis*. Oceanobacillus was the second most prevalent genus, with 5 strains, of which 4 were *Oceanobacillus picturae* and there was also the *O. kimchi.* The genus *Bacillus* had 3 strains from the species *Bacillus atrophaeus*, *B. halotolerans* and *B. swezeyi* and were mostly found in gypsic soils. The genera *Rossellomorea* and *Virgibacillus* had 2 strains each, with *Rossellomorea aquimaris*, *Rossellomorea vietnamensis* and 2 *Virgibacillus salarius*. Furthermore, there was one strain identified as *Alkalicoccobacillus gibsonii, Paraliobacillus sediminis, Priestia megaterium* and *Pseudalkalibacillus hwajinpoensis* belonging to the *Bacillaceae* family.

The *Halomonadaceae* family had the second highest number of strains (6) slightly above 10% of the collection, with four belonging to the genus *Halomonas*, including two strains of *Halomonas elongata,* a *H. glaciei* and a *H. taeanensis*. *Kushneria marisflavi* from the genus *Kushneria* also belonging to this family and finally, a novel species of the genus *Vreelandella*. The *Idiomarinaceae* family had two strains of *Idiomarina abyssalis* and one of *I. loihiensis.* Other families with strains isolated from the soil include *Planococcaceae* (*Planococcus citreus* and *P. rifietoensis)*, *Carnobacteriaceae* (*Alkalibacterium putridalgicola*), *Marinobacteraceae* (*Marinobacter persicus*) and *Vibrionaceae* (*Salinivibrio costicola*).

However, strains identification may be subjected to changes in the future after more precise analyses.

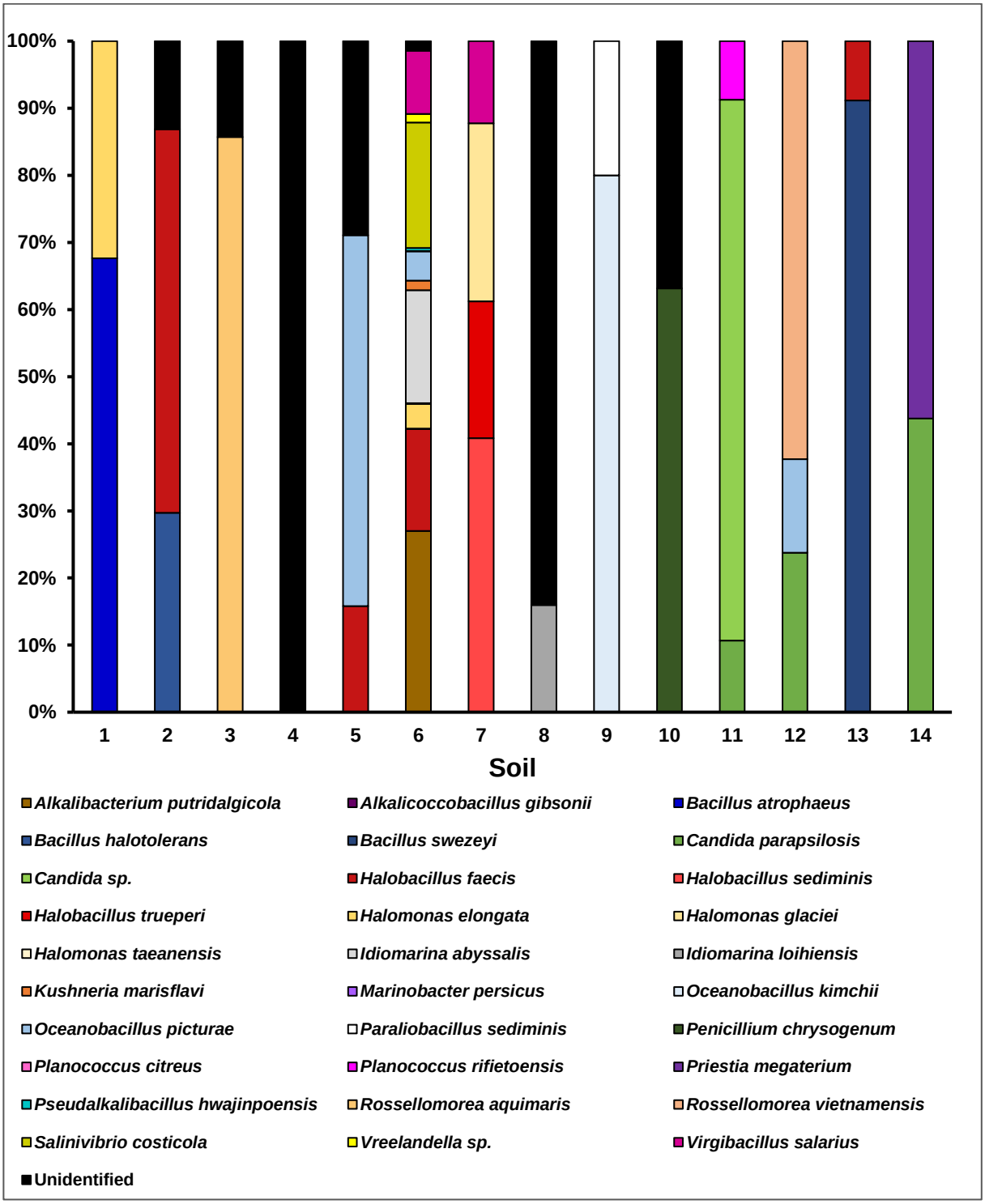

Figure 3.1 – Population distribution at species level. The columns represent the distribution of populations (relative abundance) at each sample site (referenced in Table 2.1) in gypsic (1-5) and saline (6-14) soils. The species names were determined through the comparison of 16S or internal transcribed spacer (ITS) rRNA sequences, for bacteria and yeasts, respectively, using the BLAST database. Hues of the same colour were chosen to represent different species inside the same genus. The unidentified strains are represented by black-coloured sectors, while the identified yeasts are denoted by green hues.

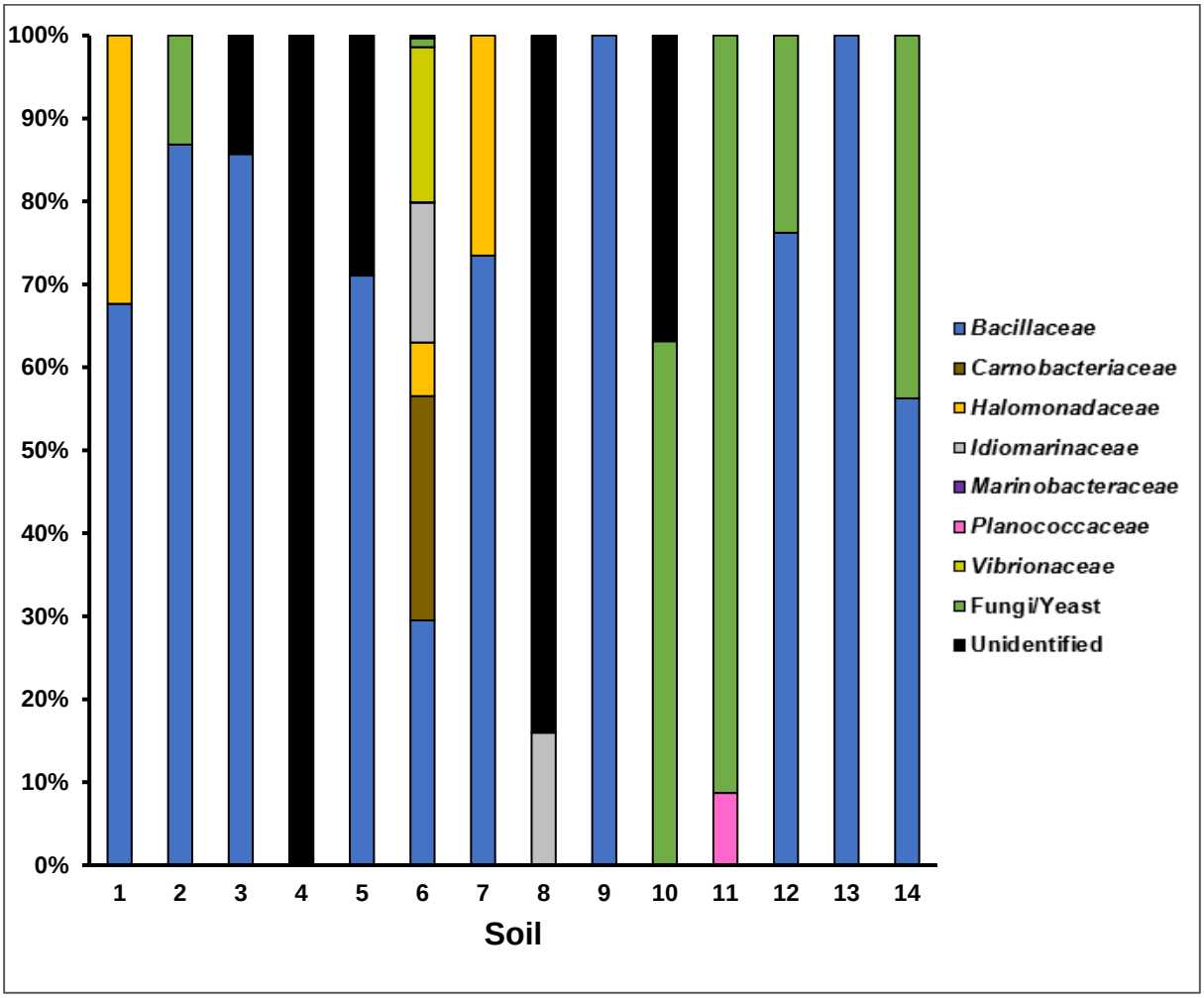

Figure 3.2 – Population distribution at family level. The columns represent the distribution of populations (relative abundance) at each sample site (referenced in Table 2.1) in gypsic (1-5) and saline (6-14) soils. The family names were sourced from the National Library of Medicine Taxonomy database. The colours chosen for each family were inspired by the hues of a genus from within each family. The blue colour of *Bacillaceae* originated from *Bacillus*, the brown colour of *Carnobacteriaceae* from *Alkalibacterium*, the yellow colour of *Halomonadaceae* from *Halomonas*, the grey colour of *Idiomarinaceae* from *Idiomarina*, the purple colour of *Marinobacteraceae* from *Marinobacter*, the pink colour of *Planococcaceae* from *Planococcus* and the greenish yellow colour of *Vibrionaceae* from *Salinvibrio*. Unidentified strains are represented by black-coloured sectors, while yeasts (identified the families *Debaryomycetaceae* and *Aspergillaceae*) or fungi are denoted by green.

The biodiversity of the soils from the 14 locations was assessed through the calculation of Shannon and Simpson's biodiversity indexes as well as other parameters such as species evenness and richness. The results presented in Table 3.1 indicate that soil 6 had the highest species diversity among all the samples, as evidenced by a Shannon Diversity Index (H) of 1.96. The Simpson's Diversiy (1-D) and Reciprocal Indexes (1/D) for this sample were also the highest, with a value of 0.82 and 5.53, respectively, further confirming the high level of biodiversity. Logically, soil 6 also had the highest richness, with 17 different species. Despite this high richness, the evenness of the sample was relatively low (0.69), suggesting that the species present are not evenly distributed, with certain species dominating the sample as seen in Figure 3.1 and the inverse relationship between species richness and evenness. Soils with higher species richness, such as soils 6 and 8, tended to have lower evenness, suggesting that as the number of species increases, the relative abundance among species becomes more unbalanced. In contrast, soil 14 had the highest evenness (0.99), reflecting a more balanced distribution of species, despite containing only two species. It is worth noting that soil 4 had no diversity, with Shannon and Simpson's Diversity Indexes both registering values of 0, thus indicating the presence of a

single species in this soil sample. The biodiversity indexes values revealed no significant differences between gypsic and saline soils.

Table 3.1 – Population diversity. This table presents the biodiversity at each sampling point (referenced in Table 2.1) in gypsic (1-5) and saline (6-14) soils through Shannon and Simpson's biodiversity indexes that evaluate the species diversity within each soil sample, Simpson's Similarity index that indicates the probability that two individuals randomly selected from a sample will belong to the same species, the evenness that reflects how evenly the individuals are distributed across the different species and finally, the richness that is the number of species present in each soil sample.

Soil No.	Shannon Diversity Index (H)	Simpson's Diversity Index (1-D)	Simpson's Similarity Index (D)	Simpson's Reciprocal Index (1/D)	Evenness	Richness
1	0,63	0,44	0,56	1,80	0,91	2
2	0,95	0,59	0,41	2,43	0,86	3
3	0,41	0,29	0,71	1,40	0,59	2
4	0	0	1	1	-	1
5	0,98	0,60	0,40	2,51	0,89	3
6	1,96	0,82	0,18	5,53	0,69	17
7	1,30	0,72	0,28	3,59	0,94	4
8	1,11	0,63	0,37	2,67	0,57	7
9	0,50	0,40	0,60	1,67	0,72	2
10	0,66	0,47	0,53	1,90	0,95	2
11	0,63	0,33	0,67	1,50	0,57	3
12	0,91	0,54	0,46	2,16	0,83	3
13	0,30	0,16	0,84	1,19	0,43	2
14	0,69	0,53	0,47	2,11	0,99	2

The abundance of culturable bacteria in the soils was measured in terms of CFUs per milligram of soil (dry weight). The results, shown in Figure 3.3, indicate that saline soils generally have a higher biomass when grown in LB plates with 2 M of NaCl added than gypsic soils. Soil 11 had the highest biomass, with an average of 1599 CFUs/mg, followed by soil 12 with 474 CFUs/mg and soil 8 with 161 CFUs/mg. All of these soils had statistically higher biomass than any of the gypsic soils, which were all below 25 CFUs/mg. The soil with the lowest biomass was soil 9.

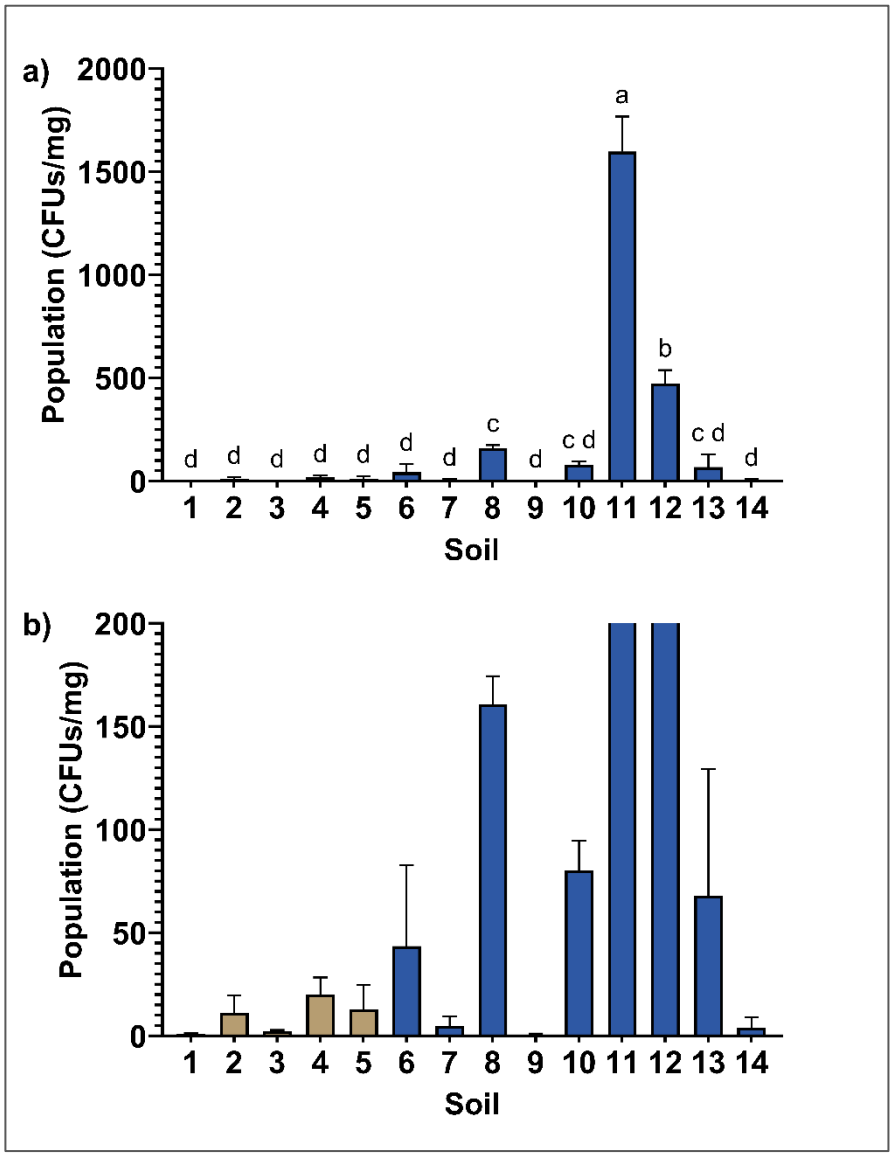

Figure 3.3 – Culturable bacteria abundance. a) The columns represent the abundance of culturable bacteria in LB with 2 M of NaCl added, measured in terms of CFUs per milligram of soil (dry weight), at each sampling point (referenced in Table 2.1) in gypsic (1-5, light brown) and saline (6-14, blue) soils. **b)** Ampliation of Figure 3.3a with the population (y-axis) ranging from 0-200 CFUs/mg. The data sets (n = 3) were analyzed recurring to a one-way ANOVA, with letters denoting identical significance levels (*p*-value < 0.05). Error bars indicate standard deviation.

3.2 Characterization and Selection of Bacterial Candidates

From the previous mentioned collection, a total of 32 strains were tested, excluding those that were unable to refresh after several attempts. Thus, the remaining 32 bacterial strains were assessed to determine their performance in various plant growth-promoting and salt-stress-relieving traits under high salinity levels (Figure 7.1 and Figure 7.2).

Hence, the production of ACCd was analyzed through an indirect measurement, where ACC served as the sole carbon and nitrogen source for the bacteria to grow. Results indicated that 90% of the strains were capable of growing using only ACC as a source of carbon and nitrogen as shown in Figure 3.4. Strains *I. abyssalis* HB and *H. faecis* 109 were particularly noteworthy for their growth above 0.8. Regarding auxins production, 72% of the strains were found to produce these phytohormones (Figure 3.4). *I. loihiensis* EA was particularly noteworthy for producing IAA equivalents at a concentration of 98 µg/mL. Additionally, almost half of the strains produced more than 25 µg/mL. In terms of biofilm

production, 69% of the strains were able to do it (Figure 3.4), with *Vreelandella* sp. DE achieving an $OD_{550\ nm}$ of 1.86 and with four additional strains above the $OD_{550\ nm}$ of 0.54, including *P. citreus* ID, *H. faecis* 103, *H. faecis* 109 and *P. hwajinpoensis* IC with 0.59, 0.59, 0.57 and 0.54 respectively. The only strain presenting a mucoid texture more similar to the exopolysaccharides (EPS) production was *B. swezeyi* 119. Moreover, 3/4 of the strains were found able to produce antioxidants (Figure 3.4), with *K. marisflavi* AA producing antioxidants equivalents at a concentration of 44 mM and *A. gibsonii* 111, *Vreelandella* sp. DE, *I. loihiensis* EA and *O. picturae* 107 producing above 15 mM of antioxidants equivalents (18, 17, 16 and 16 mM, respectively). Proline was significantly secreted by 5 strains, namely *B. swezeyi* 119, *I. abyssalis* IA, *A. gibsonii* 111, *H. taeanensis* HC and *V. salarius* GC, at values of 63, 50, 38, 25 and 20 µg/mL of proline equivalents, respectively. A significant proportion of the strains (78%) produced siderophores (Figure 3.4), with ten strains surpassing 40 psu. *Vreelandella* sp. DE and *M. persicus* EE were both capable of fixing nitrogen at a 2 M NaCl concentration fixing 1.35 and 1.07 µg/mL of NH_3^+ equivalents, respectively. Out of these tested bacteria, 69% are phosphate-solubilizing bacteria (Figure 3.4), with *P. citreus* ID and *H. faecis* 109 showing the highest phosphate equivalents production (46 and 41 mg/L, respectively). About 30% of the strains were able to solubilize potassium (Figure 3.4), outstanding *O. picturae* 123 and *I. loihiensis* EA both with more than 2.5 mg of potassium equivalents per Kg of soil (3.9 and 2.7, respectively). Additionally, more than 20% of the tested strains were sulfur-oxidizing bacteria and 5 strains were characterized calcium-solubilizing bacteria, namely *I. loihiensis* EA, *H. taeanensis* HC, *I. abyssalis* IA, *R. aquimaris* 104 and *H. trueperi* FA. Lastly, 3 strains were found to be capable of solubilizing manganese, including *V. salarius* DD, *V. salarius* GC and *O. kimchi* 115.

The candidate strains to help plants thriving under saline environments were selected taking into account their performance on these biochemical tests carried out in high salinity levels, and supported by a PCA (Figure 3.5) as well as by a complementary heatmap (Figure 3.6). A literature review was also conducted as an extra selection criterion. The performance of the selected candidate strains is depicted in Figure 3.7 and Figure 3.8.

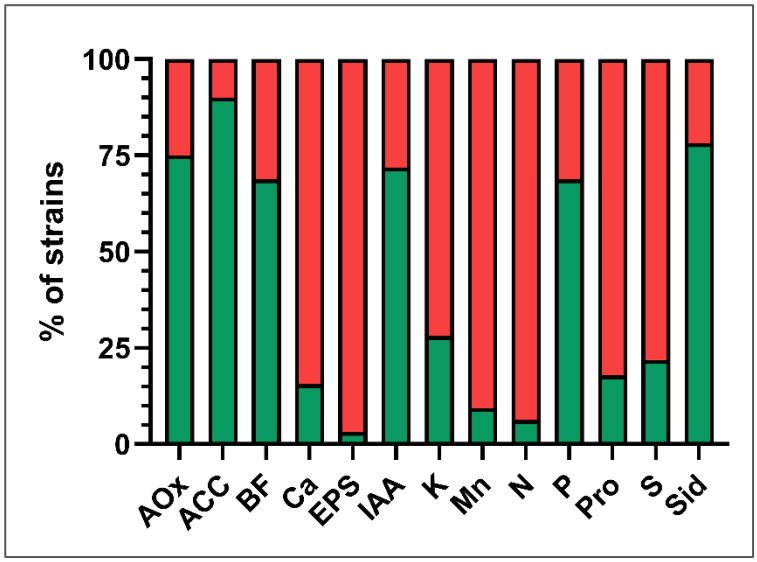

Figure 3.4 – Presence/absence of plant growth-promoting and salt-stress relieving traits. The column graph indicates the percentage of tested strains possessing (green sectors) and lacking (red sectors) different plant growth-promoting and salt-stress-relieving traits. “AOx” corresponds to antioxidants production, “ACC” to ACC deaminase production, “BF” to biofilm production, “Ca” to calcium solubilization, “EPS” to exopolysaccharides production, “IAA” to auxins production, “K” to potassium solubilization, “Mn” to manganese solubilization, “N” to nitrogen fixation, “P” to phosphate solubilization, “Pro” to proline secretion, “S” to sulfur oxidation and “Sid” to siderophores production.

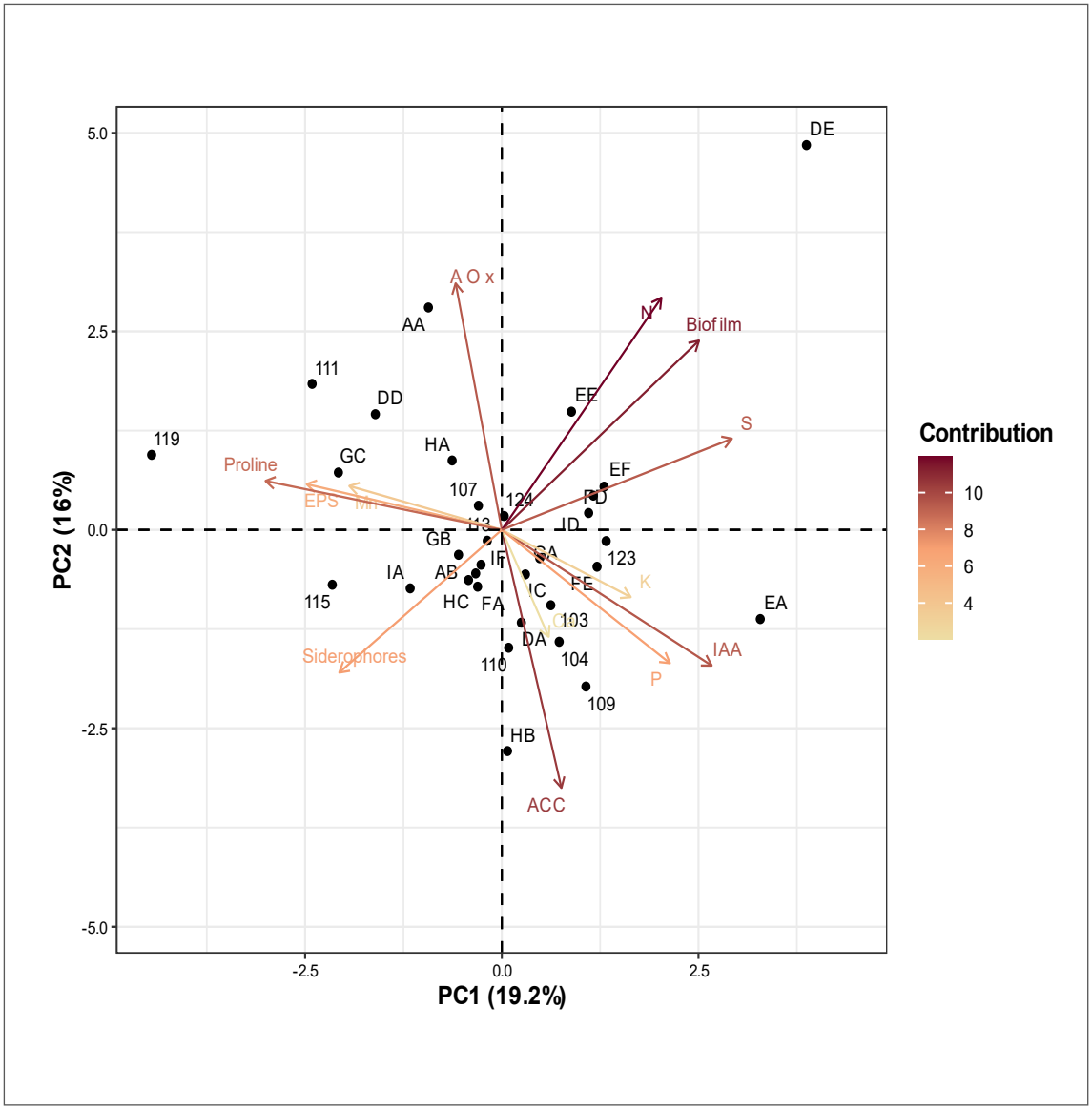

Figure 3.5 – Principal component analysis (PCA) of plant growth-promoting and salt-stress relieving traits. The first principal component (PC1, x-axis) elucidates 19.2% of the data's variance, while the second principal component (PC2, y-axis) enhances the cumulative explained variance to 16%. Each trait assessed is illustrated with a vector in either red or yellow on the graph, with the dark red vectors having a higher contribution to the sample position, while the light-yellow vectors contributed less to the sample position. "AOx" corresponds to anti-oxidants production, "ACC" to ACC deaminase production, "Biofilm" to biofilm production, "Ca" to calcium solubili-zation, "EPS" to exopolysaccharides production, "IAA" to auxins production, "K" to potassium solubilization, "Mn" to manganese solubilization, "N" to nitrogen fixation, "P" to phosphate solubilization, "Proline" to proline secretion, "S" to sulfur oxidation and "Siderophores" to siderophores production.

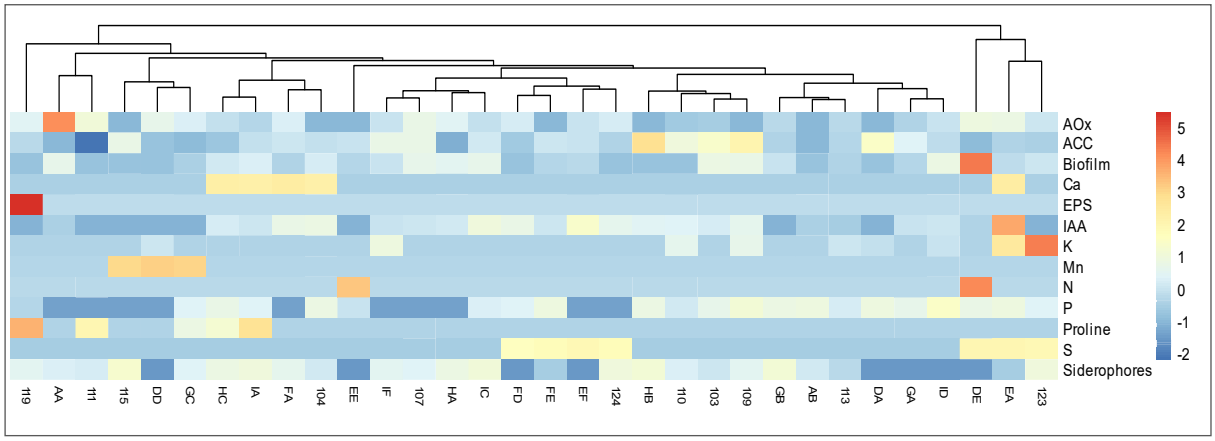

Figure 3.6 – Strains performance under high salinity levels. This heatmap shows the relative performance of all tested strains in the various biochemical tests at 2 M of NaCl and orders the strains by similarity of the results. “AOx” corresponds to antioxidants production, “ACC” to ACC deaminase production, “Biofilm” to biofilm production, “Ca” to calcium solubilization, “EPS” to exopolysaccharides production, “IAA” to auxins production, “K” to potassium solubilization, “Mn” to manganese solubilization, “N” to nitrogen fixation, “P” to phosphate solubilization, “Proline” to proline secretion, “S” to sulfur oxidation and “Siderophores” to siderophores production.

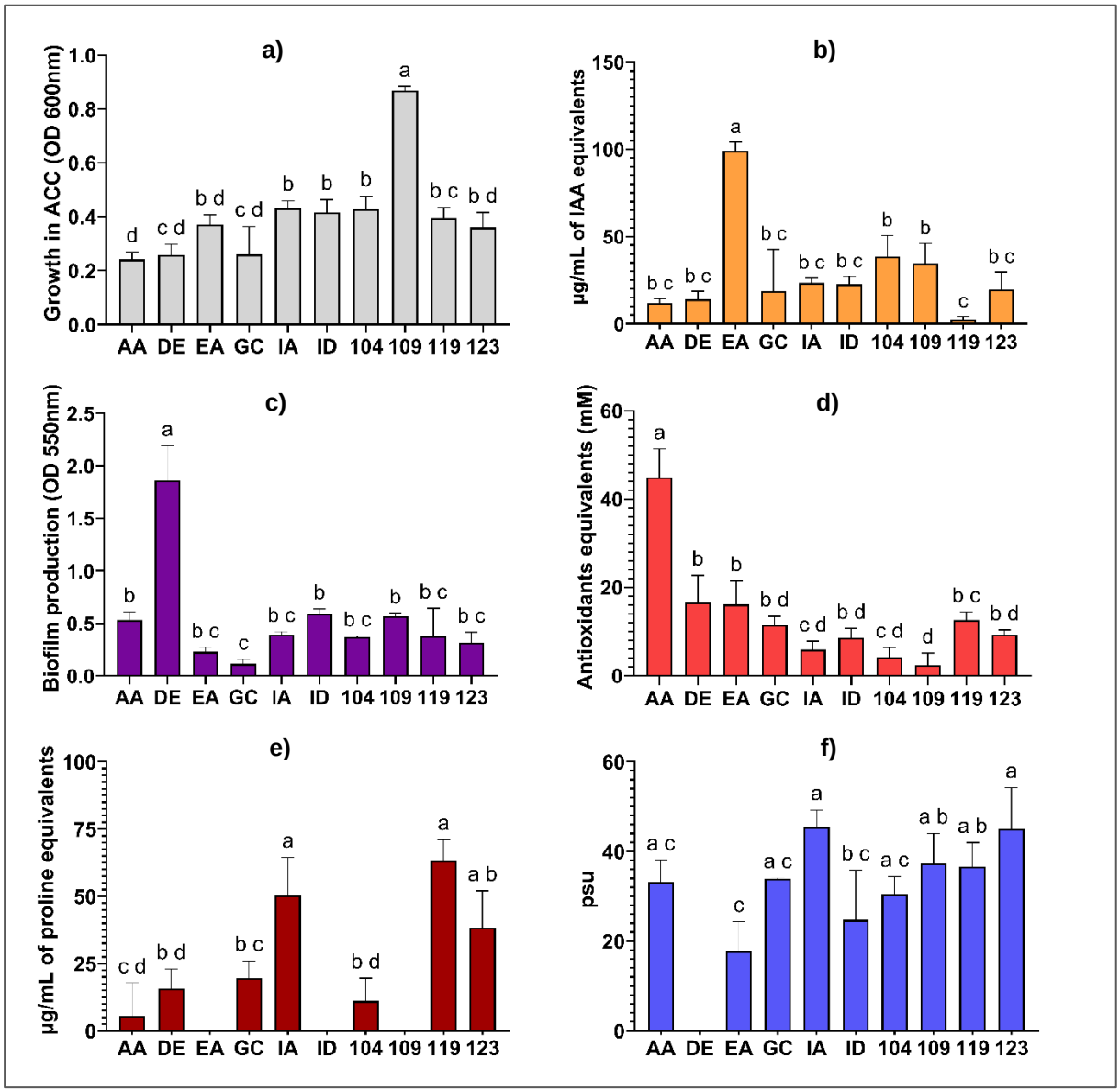

Figure 3.7 – Candidates characterization under high salinity levels. The column graphs represent the performance at a 2 M of NaCl concentration of each candidate strain. Strains were characterized for **a)** their growth in ACC medium (in OD at 600 nm) **b)** auxins production (in IAA equivalents) **c)** biofilm production (in OD at 550 nm) **d)** antioxidants equivalents production (in mM) **e)** proline equivalents secretion and **f)** siderophores production (in psu). The label "AA" stands for *K. marisflavi* AA, "DE" for *Vreelandella* sp. DE, "EA" for *I. loihiensis* EA, "GC" for *V. salarius* GC, "IA" for *I. abyssalis* IA, "ID" for *P. citreus* ID, "104" for *R. aquimaris* 104, "109" for *H. faecis* 109, "119" for *B. swezeyi* 119 and "123" for *O. picturae* 123. The data sets (n = 3) were analyzed recurring to a one-way ANOVA, with letters denoting identical significance levels (p-value < 0.05). Error bars indicate standard deviation.

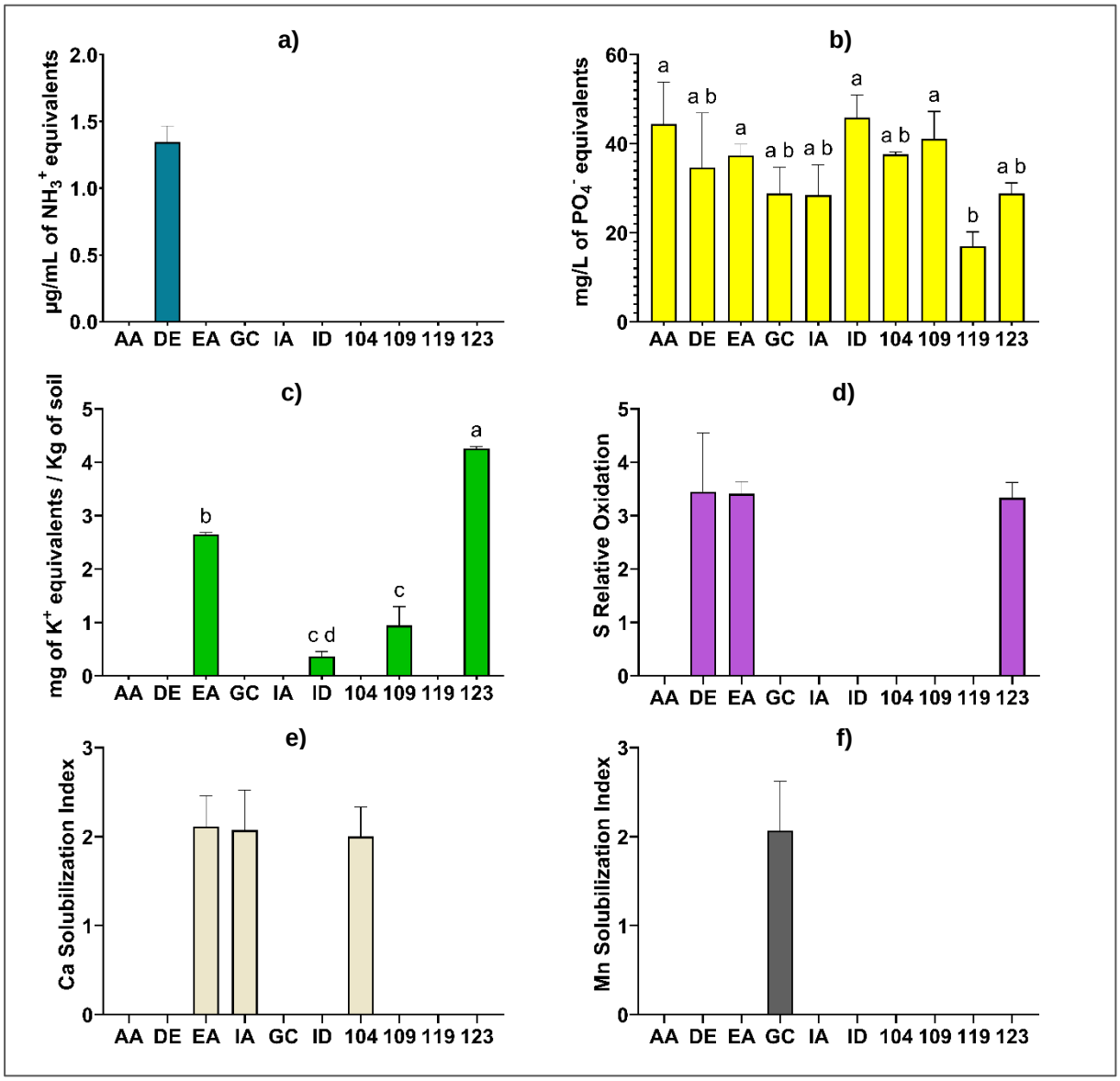

Figure 3.8 – Candidates nutrient characterization under high salinity levels. The column graphs represent the performance at a 2 M of NaCl concentration of each candidate strain in the nutrient disposability tests. Strains were characterized for **a)** nitrogen fixation (NH_3^+ equivalents) **b)** phosphate solubilization (in PO_4^{3-} equivalents) **c)** potassium solubilization (in K^+ equivalents) **d)** sulfur oxidation (in relative oxidation) **e)** calcium solubilization (in solubilization index, SI) and **f)** manganese solubilization (in SI). The label "AA" stands for *K. marisflavi* AA, "DE" for *Vreelandella* sp. DE, "EA" for *I. loihiensis* EA, "GC" for *V. salarius* GC, "IA" for *I. abyssalis* IA, "ID" for *P. citreus* ID, "104" for *R. aquimaris* 104, "109" for *H. faecis* 109, "119" for *B. swezeyi* 119 and "123" for *O. picturae* 123. The data sets (n = 3) were analyzed recurring to a one-way ANOVA, with letters denoting identical significance levels (*p*-value < 0.05). Error bars indicate standard deviation.

3.3 Selected Candidates and their Salt-Stress Resilience

The characterization of all candidates on the tested desirable traits is presented in Figure 3.7 and Figure 3.8. Furthermore, their growth capacity under different salinity levels was assessed, as illustrated in Figure 3.9. A rise in salinity levels led to an increase in growth for all candidate strains, with an upper limit observed starting from 1 M of NaCl. *K. marisflavi* AA and *O. picturae* 123 exhibited optimal growth (OG) at 1 M of NaCl, while *V. salarius* GC had its OG ranging between 0.75-1 M of NaCl. These three strains showed significant decreases at 2 M of NaCl. The OG for *I. abyssalis* IA, *P. citreus* ID, *R.*

aquimaris 104, *H. faecis* 109 and *B. swezeyi* 119 was at 0.75 M of NaCl, with a progressively decreased growth observed with the increase of salinity beyond 1 M of NaCl. *Vreelandella* sp. DE and *I. loihiensis* EA did not exhibit an upper limit within the range of values tested. *I. loihiensis* EA showed the highest growth capacity overall. Most of the strains did not attain a stationary state in two days of growth except for *I. loihiensis* EA, *R. aquimaris* 104, *B. swezeyi* 119 and *O. picturae* 123 which reached the stationary phase after one day of growth at the lower concentrations of NaCl. Finally, the appearance of all candidate strains is depicted in Figure 3.10.

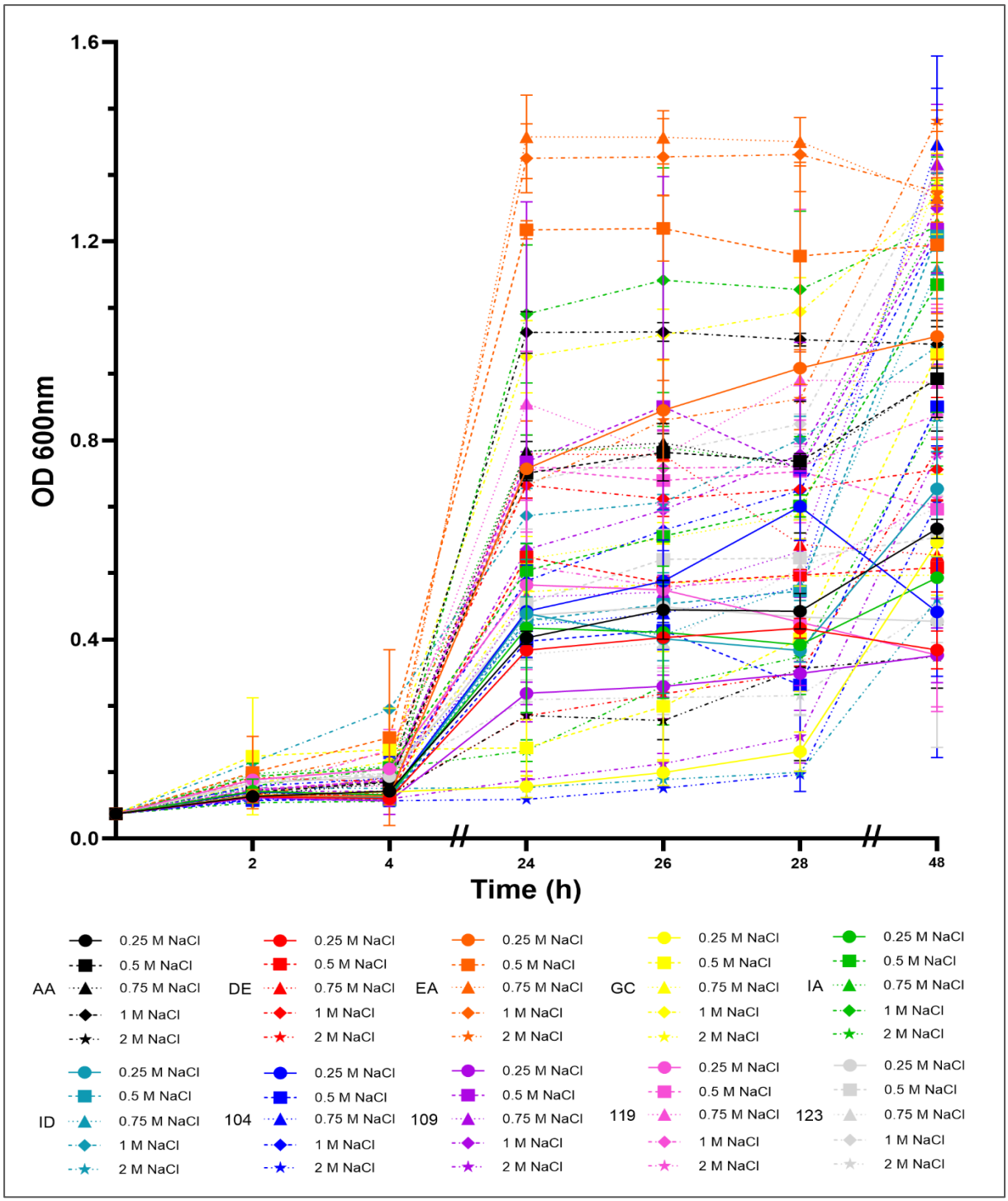

Figure 3.9 – Growth curves. The line graphs illustrate the growth patterns of the candidate strains in LB medium across various NaCl concentrations [0.25 (round shape), 0.5 (square shape), 0.75 (triangle shape), 1 (diamond shape) and 2 (star shape) M] and at different time points (2, 4, 24, 26, 28 and 48 hours). The label "AA" stands for

K. marisflavi AA represented in black, “DE” for *Vreelandella* sp. DE represented in red, “EA” for *I. loihiensis* EA represented in orange, “GC” for *V. salarius* GC represented in yellow, “IA” for *I. abyssalis* IA represented in green, “ID” for *P. citreus* ID represented in cyan, “104” for *R. aquimaris* 104 represented in blue, “109” for *H. faecis* 109 represented in purple, “119” for *B. swezeyi* 119 represented in pink and “123” for *O. picturae* 123 represented in grey. Error bars indicate standard deviation.

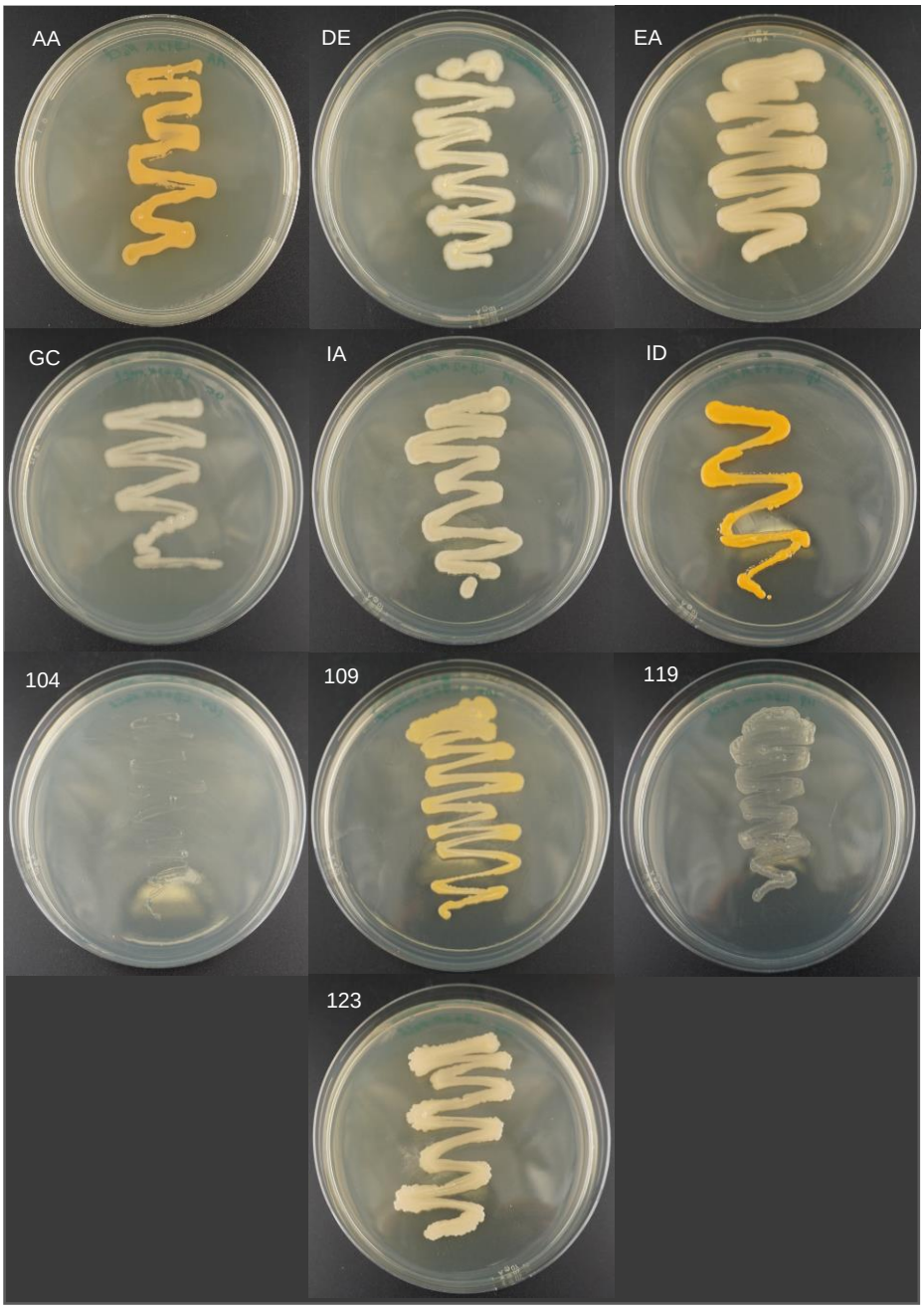

Figure 3.10 – Candidate strains. The figure shows representative images of the candidate bacterial strains grown in LB agar medium supplemented with 2 M of NaCl. The label “AA” stands for *K. marisflavi* AA, “DE” for *Vreelandella* sp. DE, “EA” for *I. loihiensis* EA, “GC” for *V. salarius* GC, “IA” for *I. abyssalis* IA, “ID” for *P. citreus* ID, “104” for *R. aquimaris* 104, “109” for *H. faecis* 109, “119” for *B. swezeyi* 119 and “123” for *O. picturae* 123.

3.4 Preliminary Biotreatment Tests in Crops under Salt-Stress

The candidate strains were applied as different treatment inocula and salt-stress was induced by adjusting the irrigation water to 0.5 M NaCl in maize plants and 0.25 M NaCl in tomato plants. These plants were chosen because they are important crops in salt-affected areas such as Ribatejo. The maize trials were divided into two batches due to the lack of available pots.

3.4.1 Early-Stage Biotreatment Test in Maize Plants (*Zea mays* L.)

The results of the first batch of treatments performed on maize plants are quantified in Figure 3.11 and depicted in Figure 3.12. Under salt-stress, shoot length (SL) decreased by half in the mock group (without bacterial treatment), while root length (RL) also showed a tendency to decrease, although not significantly. The dry weight (DW) results were not same considered for this test due to the significant influence of the seed weight on the results (detaching seed was damaging the plant). Moreover, the photosystem II quantum yield (QY) experienced a slight reduction under salt-stress. Interestingly, the treatment with *I. loihiensis* EA increased SL under control conditions compared to the mock and both *Vreelandella sp.* DE and *I. loihiensis* EA treatments improved SL under salt-stress by 85%. Additionally, *Vreelandella* sp. DE treatment did not show significant differences when comparing control with salt-stress conditions. For RL, *Vreelandella* sp. DE treatment increased root length by 54% under stress conditions. Regarding QY, treatment with *I. loihiensis* EA was capable of enhancing photosynthetic efficiency under stress and both *Vreelandella* sp. DE and *I. loihiensis* EA treatments maintained their QY levels under salt-stress.

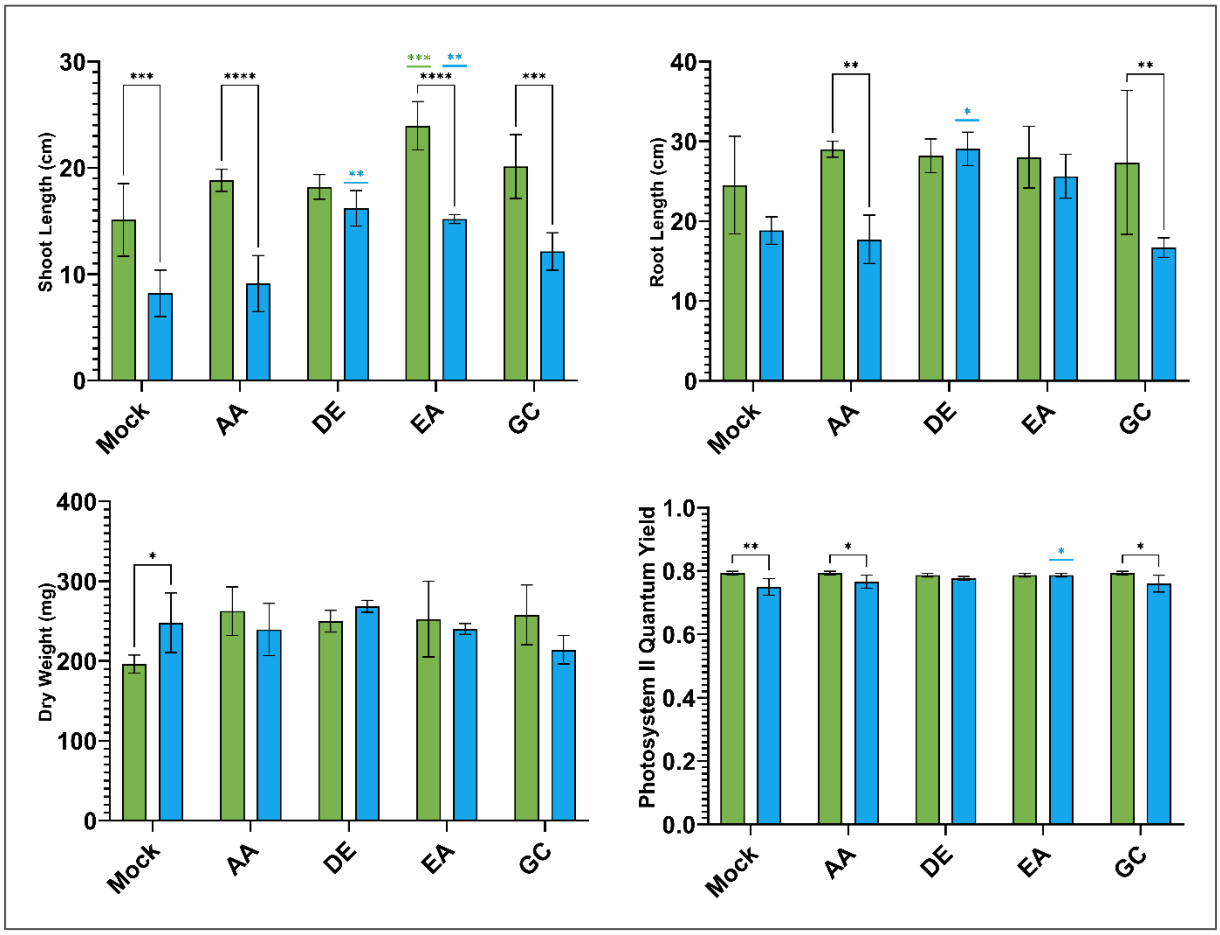

Figure 3.11 – Phenotypic quantification of the first batch of candidate treatments in maize seedlings. The column graphs represent the shoot length, root length, full-plant dry weight biomass and photosystem II quantum

yield recorded in maize in an early-stage development phase after treatment with the first set of candidate strains tested. The label “Mock” stands for mock treatment (without bacterial treatment), “AA” for treatment using the strain *K. marisflavi* AA, “DE” for treatment using the strain *Vreelandella* sp. DE, “EA” for treatment using the strain *I. loihiensis* EA and “GC” for treatment using the strain *V. salarius* GC. The green columns indicate the control conditions, while the blue bars depict the salt-stress conditions. The data sets (n = 3) were analyzed using a two-way ANOVA. Asterisks indicate statistically significant differences at the following levels: * for $p < 0.05$, ** for $p < 0.01$, *** for $p < 0.001$, and **** for $p < 0.0001$, with respect to the control and salt-stress conditions (black asterisks), the mock treatment in control conditions (green asterisks) and the mock treatment in salt-stress conditions (blue asterisks). If there is no statistical difference, there will be no representation. Error bars indicate standard deviation.

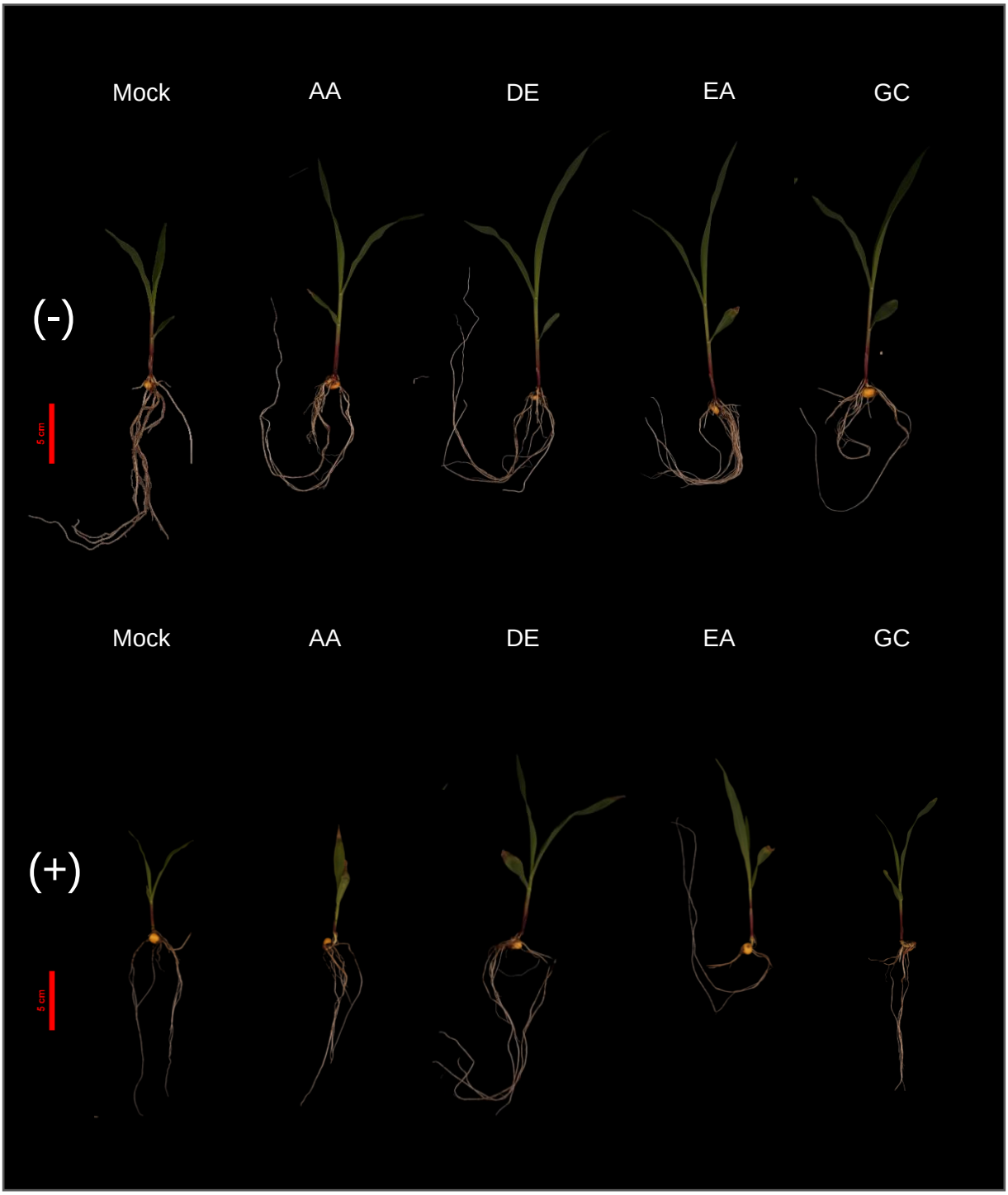

Figure 3.12 – Effects of the first batch of candidate treatments in maize seedlings. The complete plant images display the typical phenotype observed in maize plants during the early developmental stage following treatment with the first set of candidate strains. The label “Mock” stands for mock treatment (without bacterial treatment), “AA” for treatment using the strain *K. marisflavi* AA, “DE” for treatment using the strain *Vreelandella* sp. DE, “EA” for treatment using the strain *I. loihiensis* EA and “GC” for treatment using the strain *V. salarius* GC. Moreover, the label “-” indicates the control condition without salt-stress and “+” indicates the salt-stress condition.

In the second set of treatments applied to maize plants, the outcomes are quantified in Figure 3.13 and illustrated in Figure 3.14. The mock set indicated that the shoots and roots of the maize plants under stress were reduced by more than half (around 55%) of their length. Once again, the DW results

were again not same considered due to the reason mentioned earlier. It was recorded that there was a noticeable decrease in QY from 0.77 in control conditions to 0.67 in salt-stress conditions. Treatments with *R. aquimaris* 104 and *H. faecis* 109 significantly increased SL under stress in comparison to the mock (112 and 101%, respectively), with *R. aquimaris* 104 treatment was able to maintain its shoot length even under stress conditions. For RL, treatments using *P. citreus* ID and 103 showed notable improvements in control conditions. While treatments using *R. aquimaris* 104, *H. faecis* 109 and *B. swezeyi* 119 demonstrated increased RL in the order of 194, 126 and 168%, respectively, under salt-stress and were able to sustain their RL values regarding stress application. Several treatments including *P. citreus* ID, *H. faecis* 109, *B. swezeyi* 119 and *O. picturae* 123 successfully maintained their QY levels under stress conditions.

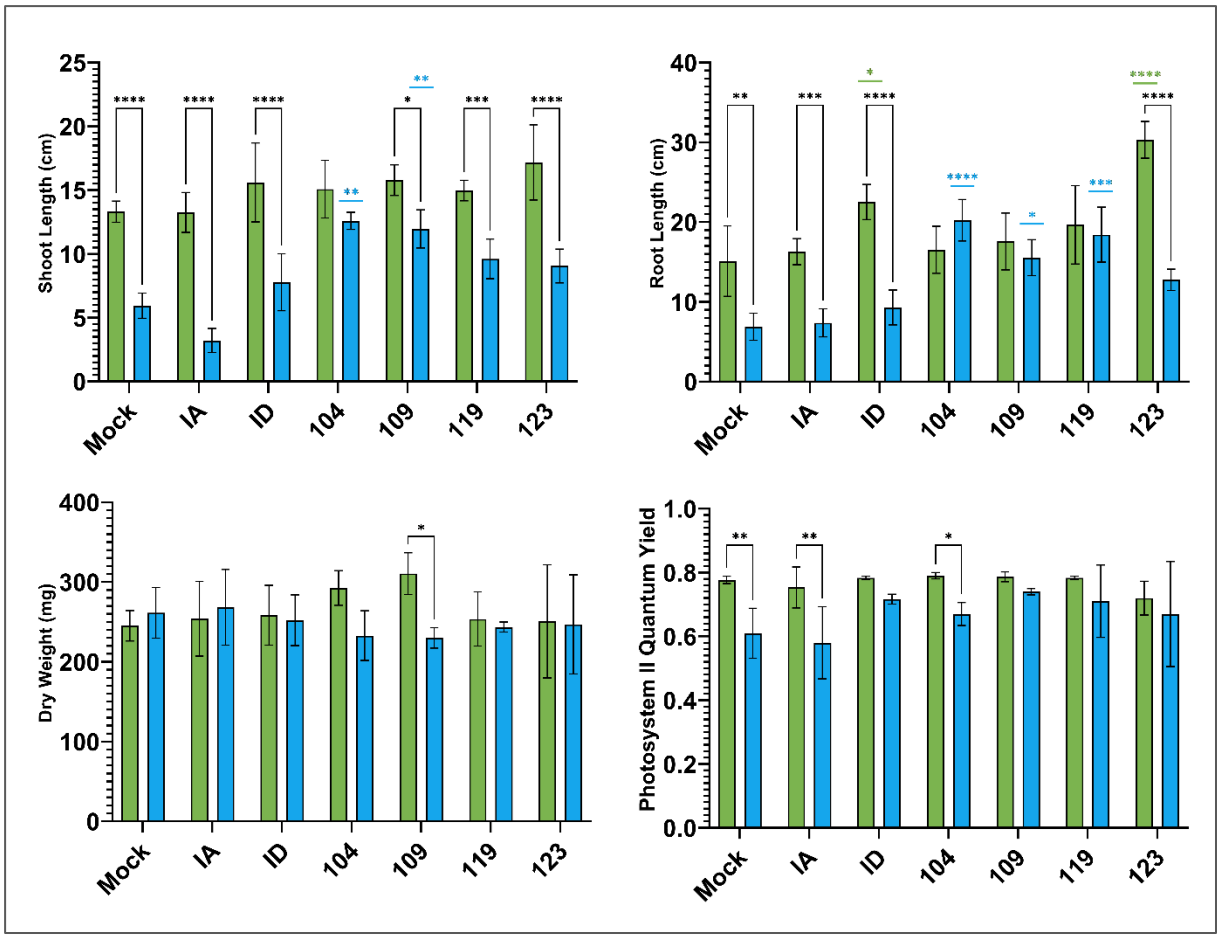

Figure 3.13 – Phenotypic quantification of the second batch of candidate treatments in maize seedlings. The column graphs represent the shoot length, root length, full-plant dry weight biomass and photosystem II quantum yield recorded in maize in an early-stage development phase after treatment with the second set of candidate strains tested. The label "Mock" stands for mock treatment (without bacterial treatment), "IA" for treatment using the strain *I. abyssalis* IA, "ID" for treatment using the strain *P. citreus* ID, "104" for treatment using the strain *R. aquimaris* 104, "109" for treatment using the strain *H. faecis* 109, "119" for treatment using the strain *B. swezeyi* 119 and "123" for treatment using the strain *O. picturae* 123. The green columns indicate the control conditions, while the blue bars depict the salt-stress conditions. The data sets (n = 3) were analyzed using a two-way ANOVA. Asterisks indicate statistically significant differences at the following levels: * for $p < 0.05$, ** for $p < 0.01$, *** for $p < 0.001$, and **** for $p < 0.0001$, with respect to the control and salt-stress conditions (black asterisks), the mock treatment in control conditions (green asterisks) and the mock treatment in salt-stress conditions (blue asterisks). If there is no statistical difference, there will be no representation. Error bars indicate standard deviation.

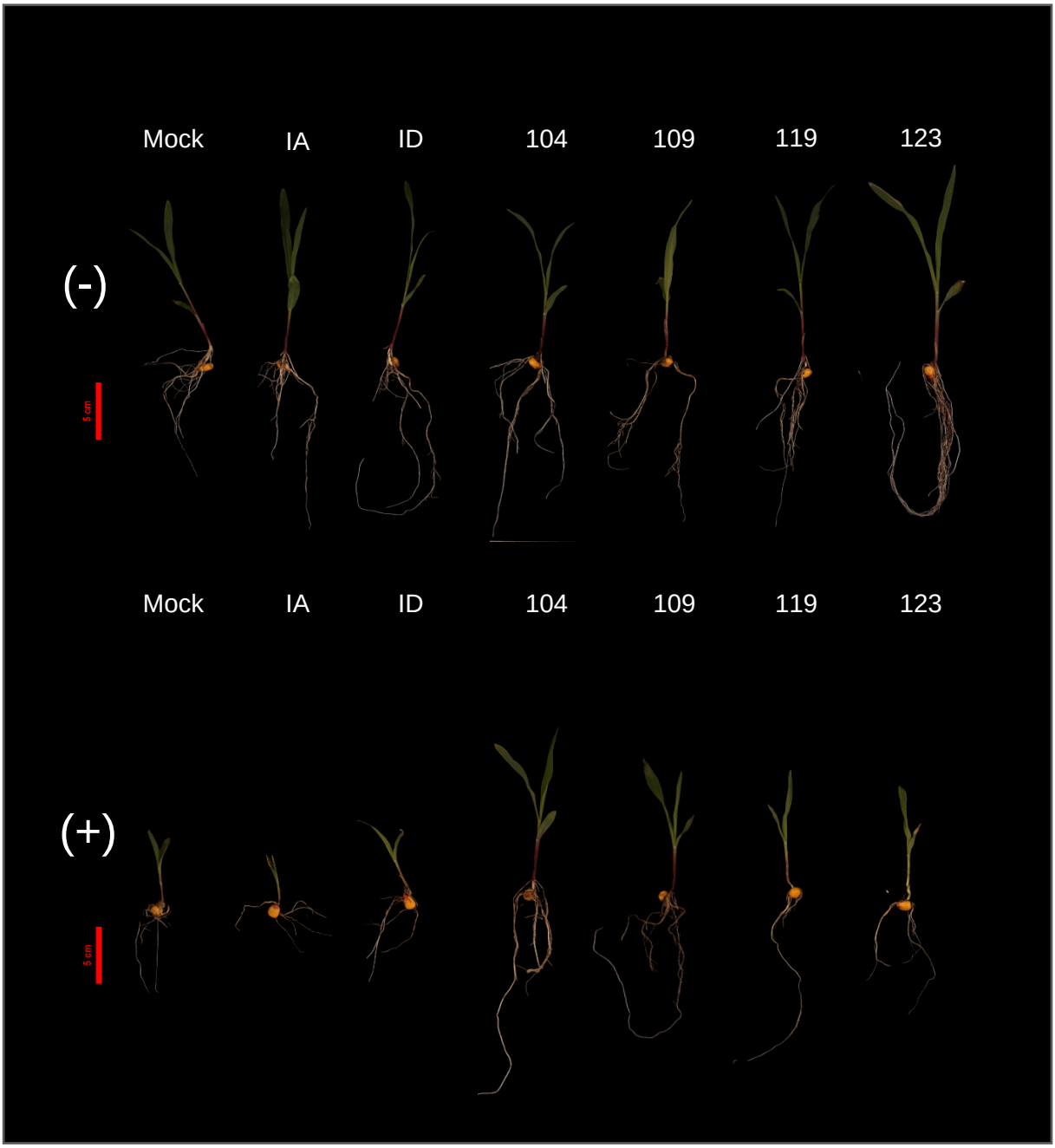

Figure 3.14 – Effects of the second batch of candidate treatments in maize seedlings. The complete plant images display the typical phenotype observed in maize plants during the early developmental stage following treatment with the second set of candidate strains. The label “Mock” stands for mock treatment (without bacterial treatment), “IA” for treatment using the strain *I. abyssalis* IA, “ID” for treatment using the strain *P. citreus* ID, “104” for treatment using the strain *R. aquimaris* 104, “109” for treatment using the strain *H. faecis* 109, “119” for treatment using the strain *B. swezeyi* 119 and “123” for treatment using the strain *O. picturae* 123. Moreover, the label “-” indicates the control condition without salt-stress and “+” indicates the salt-stress condition.

3.4.2 Early-Stage Biotreatment Test in Tomato Plants (*Solanum lycopersicum* L.)

The results of the treatments in tomato plants are quantified in Figure 3.15 and shown in Figure 3.16. The mock set revealed an increase in SL from 3.7 ± 0.7 to 5.5 ± 0.4 cm while changing the conditions from control to salt-stress. However, no significant differences were noted in RL or DW and QY had a decrease from 0.58 to 0.38. Additionally, tomato plants under salt-stress developed a third leaf, whereas those in control conditions retained only their initial two leaves. Under control conditions, treatments using *K. marisflavi* AA, *Vreelandella* sp. DE and *V. salarius* GC resulted in significant increases in SL compared to the mock. While under stress, treatments using *K. marisflavi* AA, *I. loihiensis* EA and *V. salarius* GC showed enhanced SL by 49, 78 and 67%, respectively. For RL, the treatment with *O. picturae* 123 demonstrated a substantial improvement of 4-fold under salt-stress. Additionally, treatments with *I. loihiensis* EA and *O. picturae* 123 resulted in longer roots under stress than under control conditions. In terms of DW, treatments with *K. marisflavi* AA, *Vreelandella* sp. DE and *V. salarius* GC led to increases under control conditions. Under salt-stress, DW was enhanced by treatments with *K. marisflavi* AA, *I. loihiensis* EA, *V. salarius* GC and *I. abyssalis* IA, showing increases of 3- and 4-fold, compared to the mock. QY under stress improved in 80% of the treatments relative to the mock, including *K. marisflavi* AA, *Vreelandella* sp. DE, *I. loihiensis* EA, *V. salarius* GC, *I. abyssalis* IA, *P. citreus* ID, *B. swezeyi* 119 and *O. picturae* 123. All these strains maintained their performance under stress. Furthermore, several treatments demonstrated accelerated development, as evidenced by increased leaf number and/or branching, such as in the cases of *K. marisflavi* AA, *Vreelandella* sp. DE, *I. loihiensis* EA, *V. salarius* GC and *B. swezeyi* 119 under control conditions and *K. marisflavi* AA, *Vreelandella* sp. DE, *I. loihiensis* EA, *V. salarius* GC, *I. abyssalis* IA, *B. swezeyi* 119 and *O. picturae* 123 under saline stress.

The strains with the highest SL in tomato plants under salt-stress conditions were chosen for further testing, which were *I. loihiensis* EA and *V. salarius* GC. From the strains that showed a significant improvement in leaf number in tomato plants (as seen in Figure 3.16), *Vreelandella* sp. DE showed the highest shoot length in maize plants under stress conditions, also advancing to further testing. Another criterion for selecting strains to proceed with testing would be colonization rate, although none of the candidate strains were able to colonize either maize or tomato plant roots in both control and stress conditions.

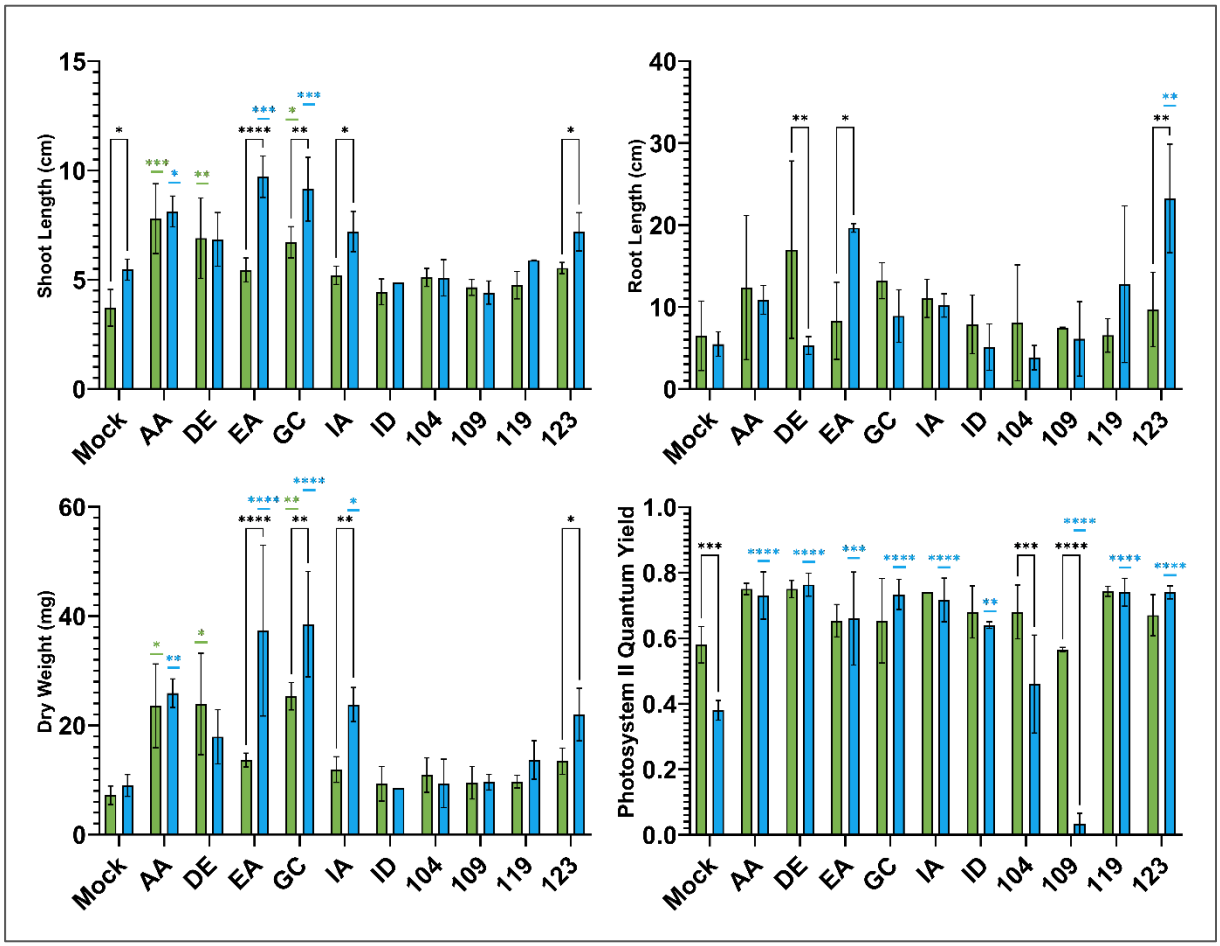

Figure 3.15 – Phenotypic quantification of candidate treatments in tomato seedlings. The column graphs represent the shoot length, root length, full-plant dry weight biomass and photosystem II quantum yield recorded in tomato in an early-stage development phase after treatment with the candidate strains. The label “Mock” stands for mock treatment (without bacterial treatment), “AA” for treatment using the strain *K. marisflavi* AA, “DE” for treatment using the strain *Vreelandella* sp. DE, “EA” for treatment using the strain *I. loihiensis* EA, “GC” for treatment using the strain *V. salarius* GC, “IA” for treatment using the strain *I. abyssalis* IA, “ID” for treatment using the strain *P. citreus* ID, “104” for treatment using the strain *R. aquimaris* 104, “109” for treatment using the strain *H. faecis* 109, “119” for treatment using the strain *B. swezeyi* 119 and “123” for treatment using the strain *O. picturae* 123. The green columns indicate the control conditions, while the blue bars depict the salt-stress conditions. The data sets (n = 3) were analyzed using a two-way ANOVA. Asterisks indicate statistically significant differences at the following levels: * for $p < 0.05$, ** for $p < 0.01$, *** for $p < 0.001$, and **** for $p < 0.0001$, with respect to the control and salt-stress conditions (black asterisks), the mock treatment in control conditions (green asterisks) and the mock treatment in salt-stress conditions (blue asterisks). If there is no statistical difference, there will be no representation. Error bars indicate standard deviation.

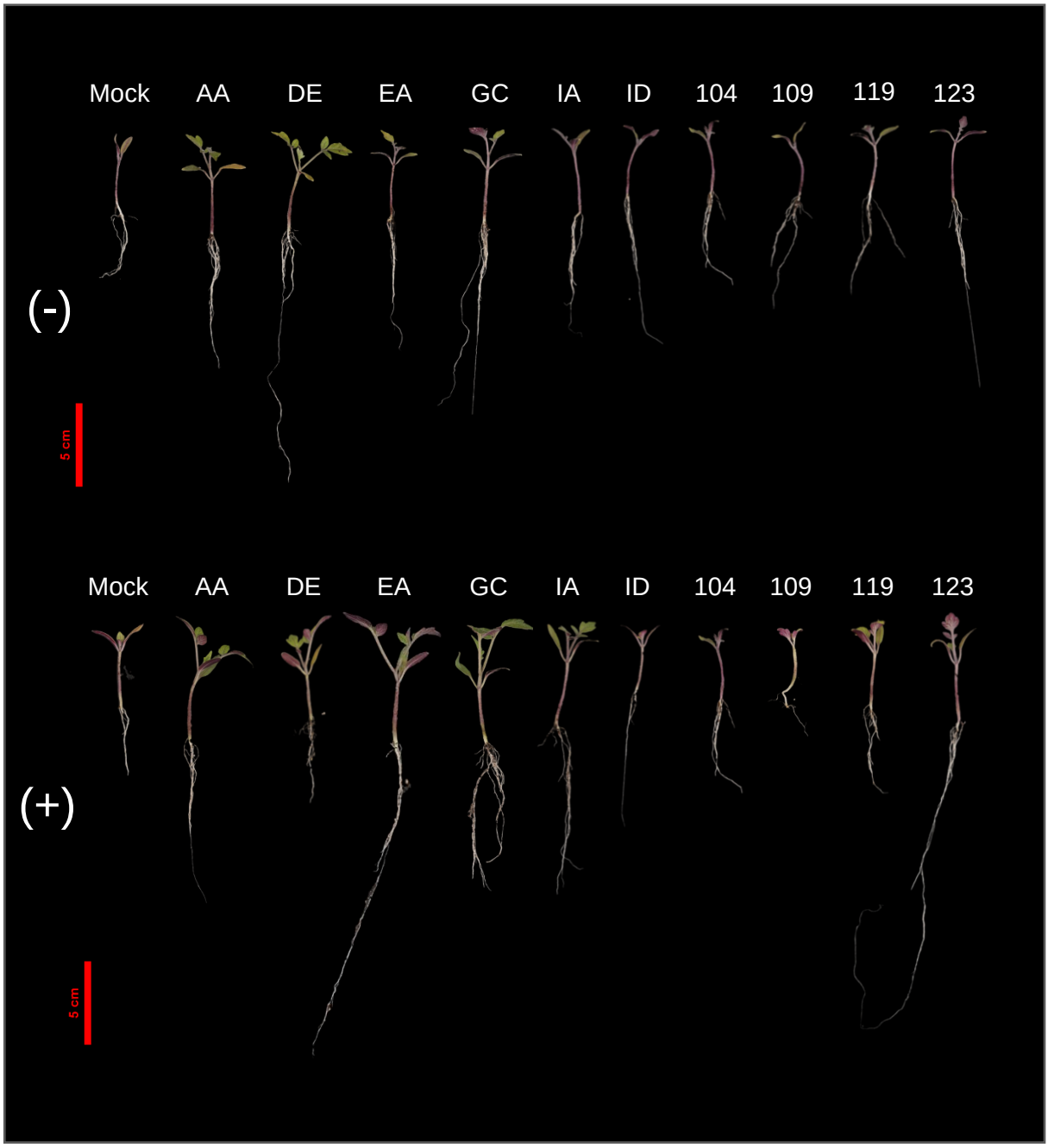

Figure 3.16 – Effects of candidate treatments in tomato seedlings. The complete plant images depict the typical phenotype observed in tomato plants during the early developmental stage following treatment with the candidate strains. The label "Mock" stands for mock treatment (without bacterial treatment), "AA" for treatment using the strain *K. marisflavi* AA, "DE" for treatment using the strain *Vreelandella* sp. DE, "EA" for treatment using the strain *I. loihiensis* EA, "GC" for treatment using the strain *V. salarius* GC, "IA" for treatment using the strain *I. abyssalis* IA, "ID" for treatment using the strain *P. citreus* ID, "104" for treatment using the strain *R. aquimaris* 104, "109" for treatment using the strain *H. faecis* 109, "119" for treatment using the strain *B. swezeyi* 119 and "123" for treatment using the strain *O. picturae* 123. Moreover, the label "-" indicates the control condition without salt-stress and "+" indicates the salt-stress condition.

3.5 Evaluation of Long-Term Biotreatment Tests in Crops under Salt-Stress

Again, the candidate strains were applied as distinct and promising treatment inocula and salt-stress was induced by adjusting the irrigation water to 0.35 M NaCl in maize plants and 0.25 M NaCl in tomato plants. The reduction in NaCl concentration was necessary by the extension of the assay duration to increase the likelihood of survival of the maize plants. This prolonged assay allowed the plants to grow more and subsequently provided a more comprehensive understanding of the candidate strains' potential to augment crop growth and resilience in saline environments.

3.5.1 Long-Term Biotreatment Test in Maize Plants (*Zea mays* L.)

The results of the treatments in the maize plants are quantified in Figure 3.17 and depicted in Figure 3.18. The mock set under salt-stress exhibited adverse effects; no significant differences were observed in SL, but RL demonstrated a significant decrease by one-third of its length. DW did not differ significantly. However, QY experienced a substantial decline from 0.74 to 0.15 and the maize plants exhibited reduced viability under salt-stress conditions. For SL, the treatments with *Vreelandella* sp. DE and *I. loihiensis* EA significantly improved SL under control conditions by 37% and 29%, respectively, while treatments with *Vreelandella* sp. DE (66 ± 3 cm), *I. loihiensis* EA (56 ± 8 cm) and *V. salarius* GC (59 ± 1 cm) enhanced SL under salt-stress, surpassing the mock treatment under control conditions (42 ± 2 cm). In terms of RL, no significant differences were observed in either control or stress conditions. In terms of DW, *Vreelandella* sp. DE and *V. salarius* GC treatments increased DW by 4-fold the weight of the mock treatment under stress conditions. While *I. loihiensis* EA treatment increased DW under stress by 2-fold. QY levels were maintained across all bacterial treatments, unlike the significant reduction observed in the mock. Notably, the maize plants in the mock group under salt-stress were the only ones dying, indicating severe stress. All other treatments not only improved plant growth but also kept the maize plants alive under stressful conditions.

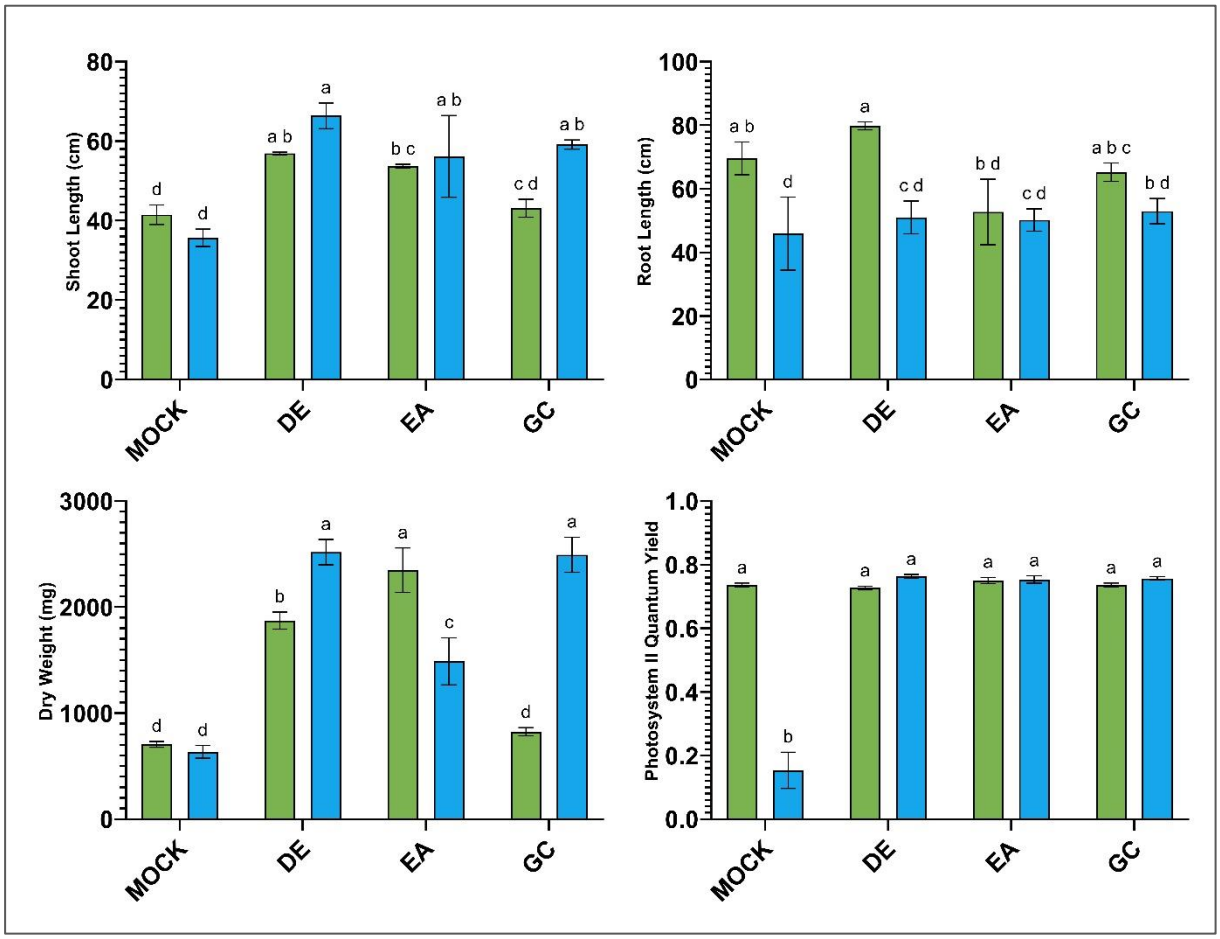

Figure 3.17 – Phenotypic quantification of candidate treatments in maize plants. The column graphs represent the shoot length, root length, full-plant dry weight biomass and photosystem II quantum yield recorded in maize after treatment with the candidate strains. The label “Mock” stands for mock treatment (without bacterial treatment), “DE” for treatment using the strain *Vreelandella* sp. DE, “EA” for treatment using the strain *I. loihiensis* EA and “GC” for treatment using the strain *V. salarius* GC. The green columns indicate the control conditions, while the blue bars depict the salt-stress conditions. The data sets (n = 3) were analyzed using a two-way ANOVA. Identical letters denote no statistically significant difference ($p < 0.05$). Error bars indicate standard deviation.

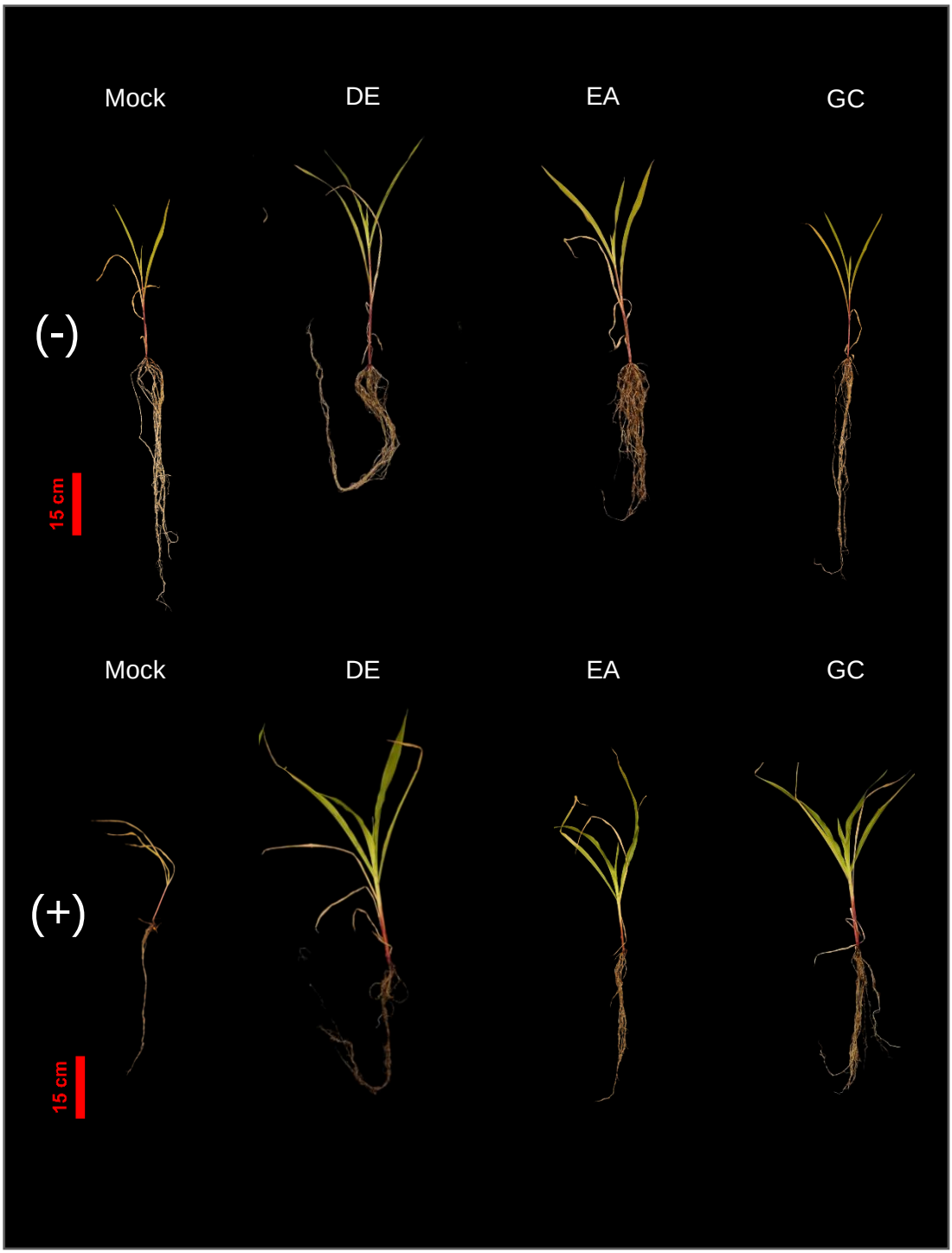

Figure 3.18 – Effects of candidate treatments in maize plants. The complete plant images display the typical phenotype observed in maize plants following treatment with the candidate strains. The label “Mock” stands for mock treatment (without bacterial treatment), “DE” for treatment using the strain *Vreelandella* sp. DE, “EA” for treatment using the strain *I. loihiensis* EA and “GC” for treatment using the strain *V. salarius* GC. Moreover, the label “-” indicates the control condition without salt-stress and “+” indicates the salt-stress condition.

3.5.2 Long-Term Biotreatment Test in Tomato Plants (*Solanum lycopersicum* L.)

Regarding tomato plants, the phenotype results are quantified in Figure 3.19 and shown in Figure 3.20. Under salt-stress conditions, the mock set showed no significant differences in SL, a tendency for RL to decrease as the average RL diminished from 12 ± 1 to 4 ± 0 cm under salt-stress, no significant differences in DW and a substantial reduction in QY from 0.71 to 0.03 in salt-stress conditions. The mock treatment was ineffective in maintaining plant viability under stress conditions. By contrast, treatments with *Vreelandella* sp. DE and *I. loihiensis* EA substantially increased both SL and RL under salt-stress stress conditions and enhanced the DW by 15- and 17-fold, respectively. Both treatments also improved their SL and DW under salt-stress conditions. *Vreelandella* sp. DE and *I. loihiensis* EA treatments also improved QY under salt-stress compared to the mock and were able to maintain their performance under stress at 0.73 and 0.79, respectively, unlike *V. salarius* GC treatment, which decreased to 0. In terms of survival, *Vreelandella* sp. DE and *I. loihiensis* EA treatments were not only successful in keeping the tomato plants alive under salt-stress but also significantly boosted overall vegetative growth compared to the mock, which failed to survive under salt-stress conditions.

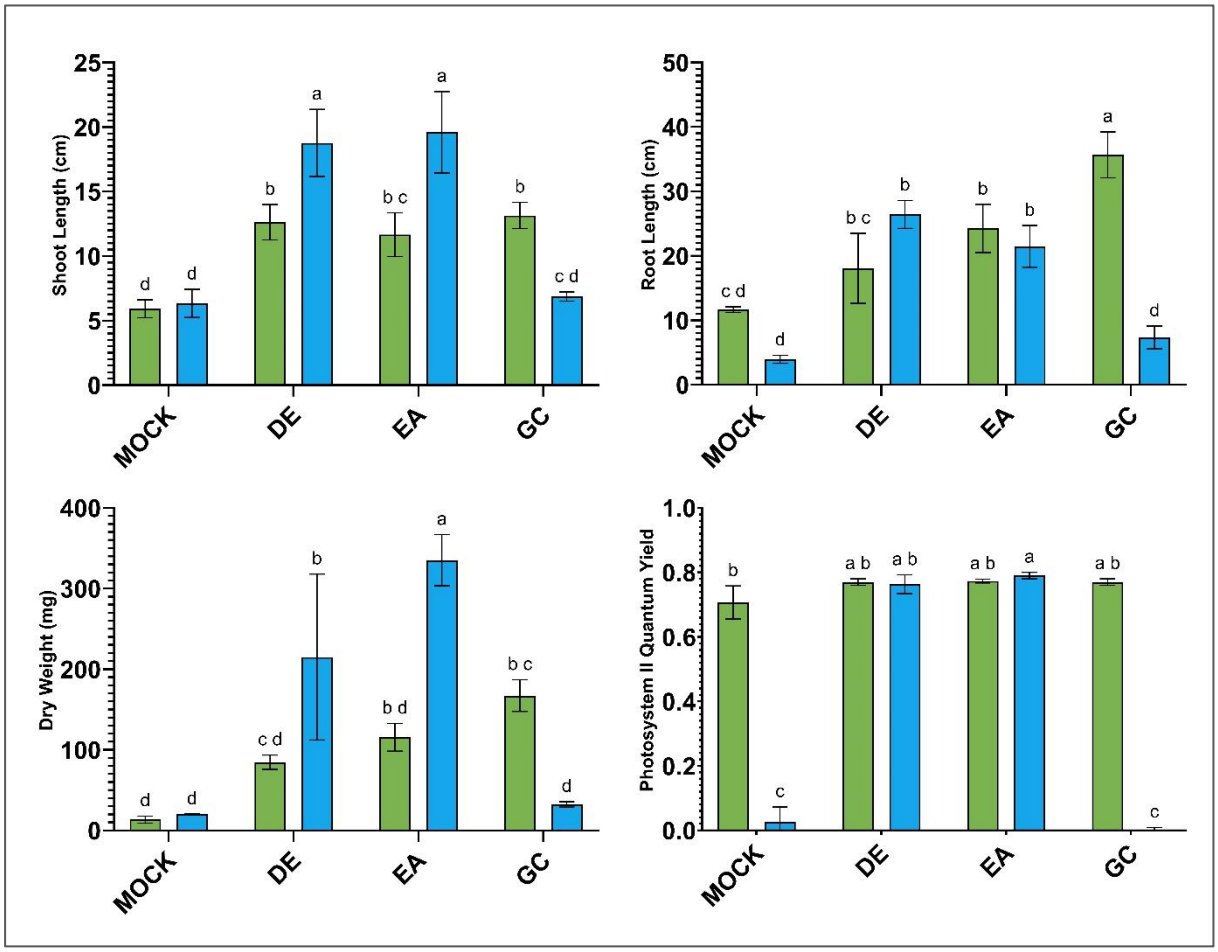

Figure 3.19 – Phenotypic quantification of candidate treatments in tomato plants. The column graphs represent the shoot length, root length, full-plant dry weight biomass and photosystem II quantum yield recorded in tomato after treatment with the candidate strains. The label “Mock” stands for mock treatment (without bacterial treatment), “DE” for treatment using the strain *Vreelandella* sp. DE, “EA” for treatment using the strain *I. loihiensis* EA and “GC” for treatment using the strain *V. salarius* GC. The green columns indicate the control conditions, while

the blue bars depict the salt-stress conditions. The data sets (n = 3) were analyzed using a two-way ANOVA. Identical letters denote no statistically significant difference ($p < 0.05$). Error bars indicate standard deviation.

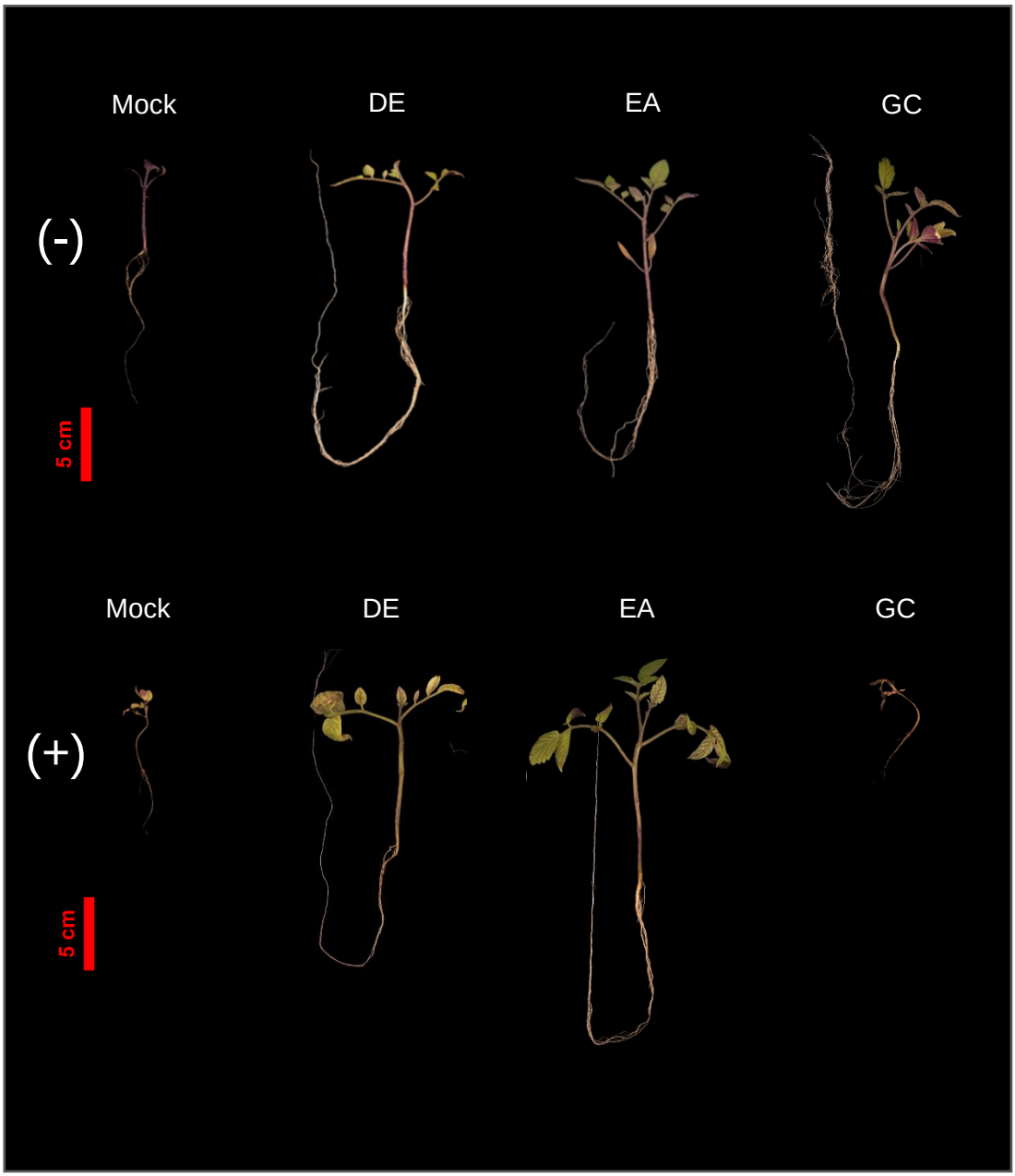

Figure 3.20 – Effects of candidate treatments in tomato plants. The complete plant images display the typical phenotype observed in tomato plants following treatment with the candidate strains. The label “Mock” stands for mock treatment (without bacterial treatment), “DE” for treatment using the strain *Vreelandella* sp. DE, “EA” for treatment using the strain *I. loihiensis* EA and “GC” for treatment using the strain *V. salarius* GC. Moreover, the label “-” indicates the control condition without salt-stress and “+” indicates the salt-stress condition.

3.6 Characterization of *Vreelandella* sp. DE Genome

To elucidate the potential mechanisms employed by halophile strains in enhancing salt resilience and plant growth, the genome of strain DE, which demonstrated overall growth improvement in both maize and tomato plants, was sequenced. The full genome sequencing (FGS) revealed that strain DE was a novel species from the genus *Vreelandella* rather than *Halomonas sulfidaeris*, as identified by

BLAST of the 16S rRNA region. The genome of *Vreelandella* sp. DE comprises four contigs, with a N50 of 3,227,286 bp and a total genome length of 4833136 bp with a GC content of 53.76% as seen in Table 3.2. The PROKKA analysis revealed that *Vreelandella* sp. DE genome contained 4570 genes, 4478 coding sequences (CDS), 13 misc RNA, 18 rRNA, 60 tRNA and 1 transfer-message RNA (tmRNA) as shown in Table 3.3. Analysis using CheckM revealed that the genome assembly exhibited a high level of completeness at 99.95%. The BUSCO analysis identified a total of 820 orthologs, of which 792 (97%) were complete, including two duplicated orthologs, six fragmented orthologs and 22 missing orthologs.

Table 3.2 – Basic genome assembly attributes. This table provides key statistics on the genome assembly of *Vreelandella* sp. DE obtained using QUAST, including total length, number of contigs, N50, GC content and other relevant metrics, offering an overview of the assembly's quality.

Statistics	DE genome
# of contigs	4
# of contigs (>= 1000 bp)	3
# of contigs (>= 5000 bp)	3
# of contigs (>= 50000 bp)	2
Total length	4833136
N50	3227286
GC (%)	53,76

Table 3.3 – PROKKA genome annotations. This table provides key statistics on genome features of *Vreelandella* sp. DE obtained using PROKKA, including number of genes, coding sequences (CDS), misc RNA, rRNA, tRNA and transfer-message RNA (tmRNA).

Statistics	DE genome
# of genes	4570
# of CDS	4478
# of misc RNA	13
# of rRNA	18
# of tRNA	60
# of tmRNA	1

3.6.1 Phylogenomic Comparison with Closest Type Strains

The genome BLAST distance phylogeny (GBDP) analysis of the *Vreelandella* sp. DE in comparison with the fourteen closest type strains is summarized in Table 3.4 and illustrated in Figure 3.21. The digital DNA-DNA hybridization (dDDH) values were determined with three distinct formulas d_0, d_4 and d_6. These formulas measure the ratio of high-scoring pairs (HSPs) length to total genome length, the proportion of identities in HSPs to overall HSP length and the ratio of identities in HSPs to total genome length, respectively. The dDDH values ranged from 14.8% to 58.7%, with *Vreelandella sulfidaeris* DSM 15722 (synonym of *Halomonas sulfidaeris*) exhibiting the highest similarity (58.2% in d_4) to the *Vreelandella* sp. DE. Regarding G+C content difference, *Vreelandella sulfidaeris* DSM 15722 demonstrated the greatest similarity to *Vreelandella* sp. DE with a minimal difference of 0.01%, whilst some of the other type strains exceeded a 1% difference, including *Halomonas alkaliantarctica* CRSS, *Vre*elandella *neptunia* DSM 15720, *Vreelandella olivaria* TYRC17, *Vreelandella utahensis* NBRC 102410,

Vreelandella azerica TBZ9T, *Vreelandella populi* MC, *Vreelandella vilamensis* DSM 21020T and finally *Vreelandella rituensis* TQ8S reaching a difference of 3.48%. The comparative genomic analysis revealed significant genetic diversity among the strains, indicating that *Vreelandella* sp. DE potentially represents a novel species. However, due to the complexity of the sample and the high probability of new species based on preliminary analysis, this identification is subjected to changes in the future after more precise analyses.

Table 3.4 – Pairwise comparisons of *Vreelandella* sp. DE genome with type strain genomes. The table below presents the pairwise dDDH values and G+C content between *Vreelandella* sp. DE and the selected type strain genomes. dDDH values are accompanied by their confidence intervals (C.I.) for the three distinct GBDP formulas (d_0, d_4 and d_6).

Type Strain	dDDH (d_0, %)	C.I. (d_0, %)	dDDH (d_4, %)	C.I. (d_4, %)	dDDH (d_6, %)	C.I. (d_6, %)	G+C content difference (%)
Vreelandella sulfidaeris DSM 15722	57.6	[54.0 - 61.2]	58.2	[55.4 - 60.9]	58.7	[55.5 - 61.9]	0.01
Vreelandella titanicae ATCC BAA-1257	42.8	[39.4 - 46.2]	27.3	[24.9 - 29.8]	37.9	[34.9 - 40.9]	0.82
Halomonas alkaliantarctica CRSS	45.6	[42.2 - 49.0]	27.0	[24.6 - 29.4]	39.7	[36.8 - 42.8]	1.03
Vreelandella glaciei DD 39	40.4	[37.0 - 43.8]	27.0	[24.6 - 29.5]	36.0	[33.1 - 39.1]	0.62
Vreelandella neptunia DSM 15720	44.3	[40.9 - 47.7]	26.8	[24.4 - 29.2]	38.8	[35.8 - 41.8]	1.20
Halomonas sedimenti QX-2	44.5	[41.1 - 47.9]	26.8	[24.5 - 29.3]	38.9	[35.9 - 41.9]	0.58
Halomonas maris QX-1	42.5	[39.1 - 45.9]	26.7	[24.3 - 29.1]	37.5	[34.5 - 40.5]	0.63
Vreelandella olivaria TYRC17	43.1	[39.8 - 46.6]	26.0	[23.7 - 28.5]	37.6	[34.7 - 40.7]	1.58
Vreelandella boliviensis DSM 15516	41.0	[37.6 - 44.5]	25.9	[23.6 - 28.4]	36.1	[33.2 - 39.2]	0.92
Vreelandella utahensis NBRC 102410	34.0	[30.6 - 37.5]	23.7	[21.4 - 26.1]	30.4	[27.4 - 33.5]	2.05
Vreelandella azerica TBZ9T	14.8	[11.9 - 18.2]	20.2	[18.0 - 22.6]	14.9	[12.5 - 17.8]	1.61
Vreelandella populi MC	20.2	[17.0 - 23.8]	20.2	[18.0 - 22.6]	19.4	[16.7 - 22.4]	1.22
Vreelandella rituensis TQ8S	15.0	[12.1 - 18.4]	19.8	[17.6 - 22.2]	15.1	[12.6 - 18.0]	3.48
Vreelandella vilamensis DSM 21020T	15.0	[12.1 - 18.4]	19.7	[17.5 - 22.1]	15.1	[12.6 - 17.9]	1.41

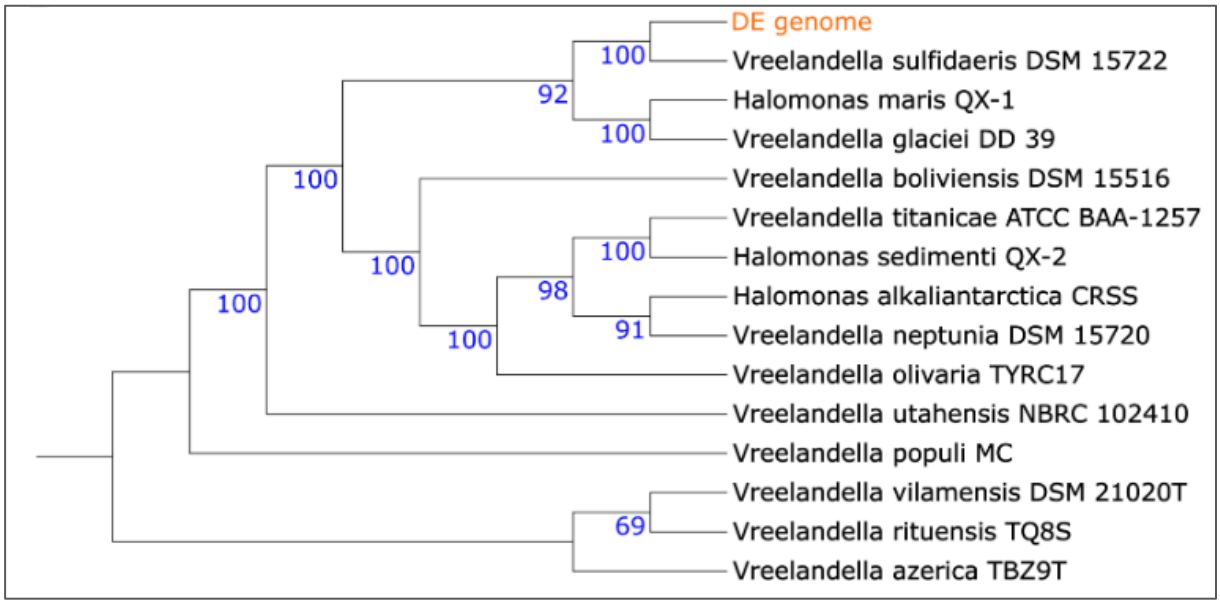

Figure 3.21 – GBDP-based phylogenomic tree. The phylogenomic tree was inferred using FastME 2.1.6.1 [133] based on GBDP distances derived from genome sequences. Branch lengths are scaled according to the GBDP distance formula d_5. Numbers above the branches represent GBDP pseudo-bootstrap support values greater than 60% from 100 replications, with an average branch support of 91.9%. The tree is midpoint-rooted. "DE genome" stands for *Vreelandella* sp. DE genome.

3.6.2 Functional Genomic Potential

Genome analysis revealed a promising functional potential genome due to the amount of plant growth-promoting traits (PGPT) genes, comprising 45% of the genes present in *Vreelandella* sp. DE genome as illustrated in Figure 3.22. It is noteworthy to highlight the presence of several bio-fertilization, phytohormone production and stress-relieving genes. Furthermore, was observed in Figure 3.23a the presence of various genes related with crucial nutrients acquisition and solubilization.

Several nitrogen fixation genes were found such as the entire *suf* system (*suf*A, *suf*B, *suf*C, *suf*D, *suf*E and *suf*S) related to nitrogenase biosynthesis. Additionally, genes related to phosphate solubilization were also found as the case of *pqq*B, *pqq*C, *pqq*D, *ppq*E and *gcd* for mineral phosphate and *phn*A, *phn*C, *phn*D, *phn*E and *phn*M for organic phosphate solubilization. Regarding potassium solubilization, genes including *ack*A, *mdh* and *ppc* were found. 19 different gene from *cys* system were found in *Vreelandella* sp. DE genome, these genes account for sulfate assimilation pathway. Furthermore, genes related to iron acquisition were also identified, such as the *ent*A, *ent*C and *ent*S connected with siderophore synthesis. Figure 3.23a also provided a closer view on the phytohormones production gene distribution. IAA production genes were noted, such as the *trp* system genes involved in the tryptophan biosynthetic pathway. Another group of genes related with phytohormones were the *mia*A, *mia*B and *mia*E related with the cytokinin synthesis. Moreover, genes of homologous of the ACCd such as *tdc*B and *dcy*D were reported. The genes *pss*A, *psl*B and *pel*F included in *Vreelandella* sp. DE genome are connected with the EPS and biofilm formation. The results summarized in Figure 3.23b indicated that more than 10% of the genes are involved in the neutralization of abiotic stresses. One mechanism to alleviate the salt-stress is through the production of osmoprotectants. In the *Vreelandella* sp. DE genome several genes related with these compounds production was identified, such as *tre*P, *tre*S, *tre*Y, *tre*Z and otsB, which are involved in the trehalose synthesis. Additionally, the genes *pro*A, *pro*B and *pro*C are related to proline synthesis. For the glycine betaine synthesis, the genes *bet*A and *bet*B were found. Moreover, *ect*A, *ect*B and *ect*C were among the genes connected to ectoine synthesis. Finally, the production of some polyamines, such as spermidine, may assist relieving salt-stress, for which the system of genes *spe* was identified. The antioxidant system is another mechanism utilized by bacteria to cope with salt-stress. Many genes involved with this mechanism were reported, such as *kat*E and *kat*G (catalase [CAT]), ahpC and ahpF (alkyl hydroperoxide reductase). Additionally, *gst*, *gpx* and *gor* are involved in glutathione metabolism. Genes related to ion transport were also identified. The *kdp* and

ktr systems are associated to K^+ uptake. Furthermore, *kef*A, *kef*B and *kef*C are connected with K^+/H^+ antiporter. Moreover, the system *mrp* is involved in Na^+/H^+ antiporters. Finally, *dna*J, *dna*K are relative to chaperones that regulate the folding and refolding processes of proteins under stress.

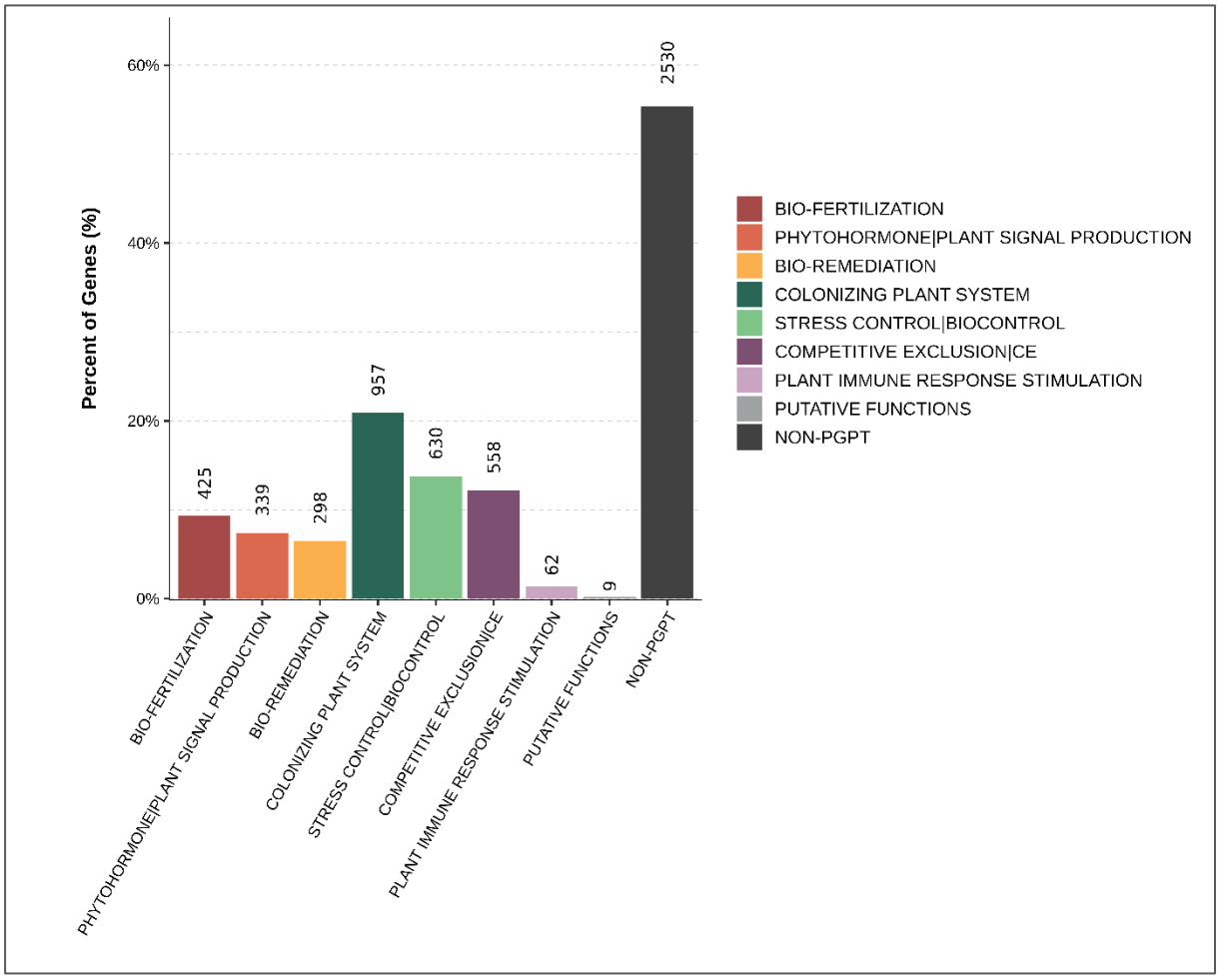

Figure 3.22 – PGPT genes presence in *Vreelandella* sp. DE genome. The column graph indicates the number as well as the percentage of genes in *Vreelandella* sp. DE genome for each PGPT category, according to PLaBAse database.

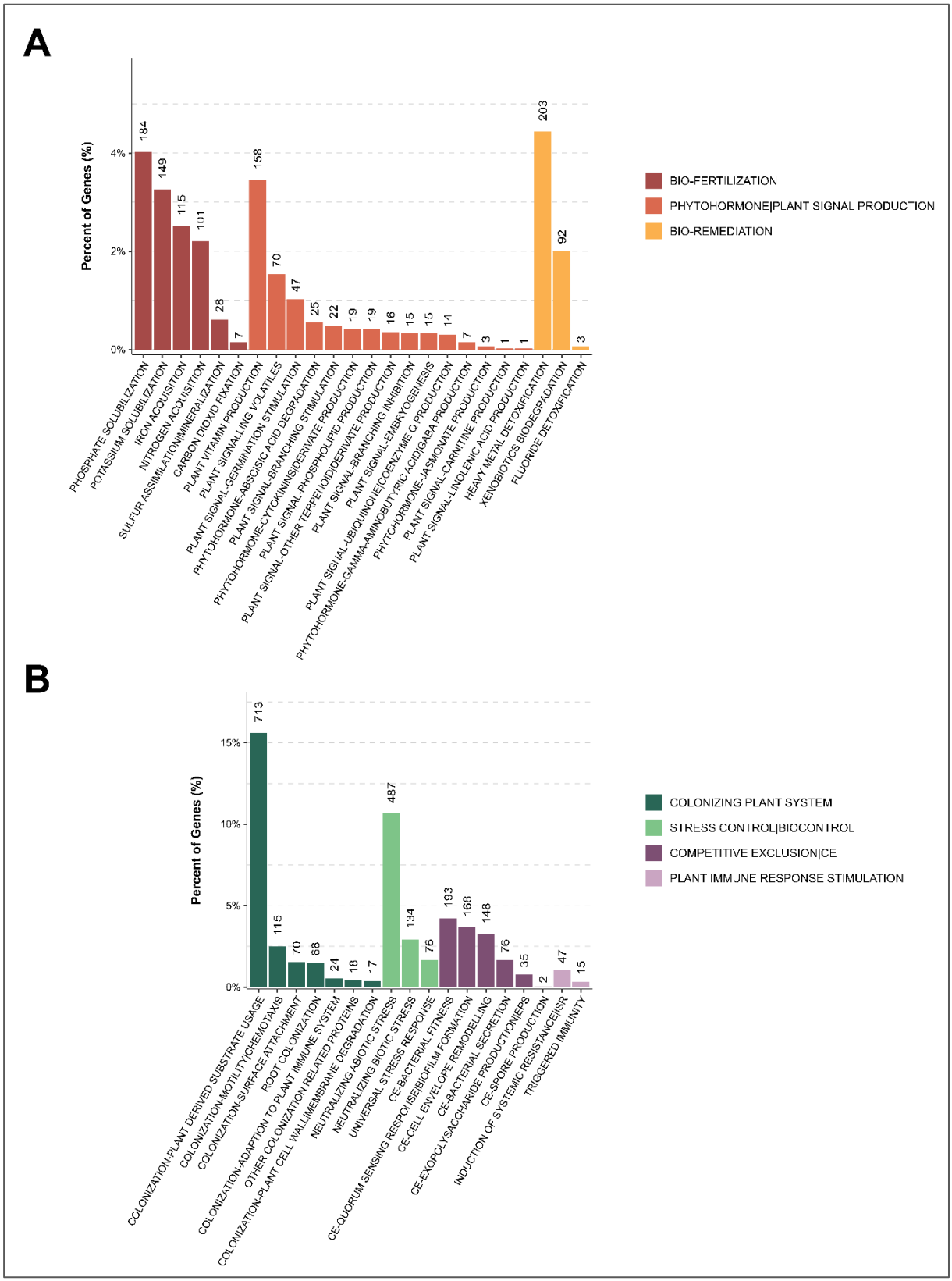

Figure 3.23 – Characterization of PGPT genes in *Vreelandella* sp. DE genome. The column graphs indicate the number as well as the percentage of genes in *Vreelandella* sp. DE genome for each PGPT subcategory (**A -** direct and **B -** indirect mechanisms), according to PLaBAse database.

3.7 Analyzing Salt-Stress-Relieving and Plant Growth-Promoting Metabolites Secreted and Produced by Halophile Beneficial Bacteria

A metabolomics analysis was conducted to elucidate the potential mechanisms employed by the candidate strains. The supernatant fraction contains compounds secreted by the strains, which may contribute to enhancing the growth and development of crop plants under salt-stress conditions. In contrast, the pellet fraction comprises compounds that enable the strains to tolerate and adapt to high salinity levels. This dual analysis provides an improved understanding of both the strains' beneficial effects on plants and their own survival strategies under saline stress.

In both the supernatant and pellet fractions, several metabolites were present in high concentrations across the three candidate strains, with some variation between them. In the supernatant, as demonstrated in Figure 3.24, several aminoacids, such as valine, leucine, isoleucine, pyroglutamic acid, methionine and phenylalanine were detected in all strains at high concentrations, exhibiting some strain-specific variations. Moreover, high levels of proline, an important osmoprotectant, were secreted by *I. loihiensis* EA and *V. salarius* GC, the same pattern was observed in lysine levels. Other metabolites from the aminoacids class, such as alanine and serine were present at high concentrations in *Vreelandella* sp. DE and *V. salarius* GC supernatants. While key metabolites in plant growth promoting and salt-stress mitigation, such as 4-aminobutyric acid (GABA) and trehalose were elevated in the same two strains. Furthermore, high concentrations of threonine were secreted by *Vreelandella* sp. DE and *I. loihiensis* EA. Additionally, the urea cycle intermediates citrulline, ornithine and arginine were found in higher concentrations in *I. loihiensis* EA. In the pellet fraction, as depicted in Figure 3.25. Alanine, pyroglutamic acid, glutamic acid, phenylalanine, hydroxyproline, lysine, glycerol-3-phosphate, hexadecanoic acid, valine, L-aspartic acid and isoleucine were abundant across all strains. The last three aminoacids with the addition of threonine present abundantly in *Vreelandella* sp. DE and *I. loihiensis* EA, may form the VTID complex, a complex to alleviate salt-stress effects. Moreover, threonine and 2-aminoadipic acid were elevated in both strains also. Additionally, GABA, trehalose, leucine and the urea cycle intermediates had higher concentrations in *Vreelandella* sp. DE and *V. salarius* GC. Besides that, proline and glutamine exhibited higher levels in *I. loihiensis* EA and *V. salarius* GC.

From the metabolomics analysis was also revealed a strong trend in the identified metabolites, suggesting their involvement in stress-protective roles. As demonstrated in Figure 3.26, approximately 75% of these identified metabolites were associated with bacterial defence mechanisms against various forms of abiotic stress, such as salinity, drought, oxidative damage, heavy metals and acid stress.

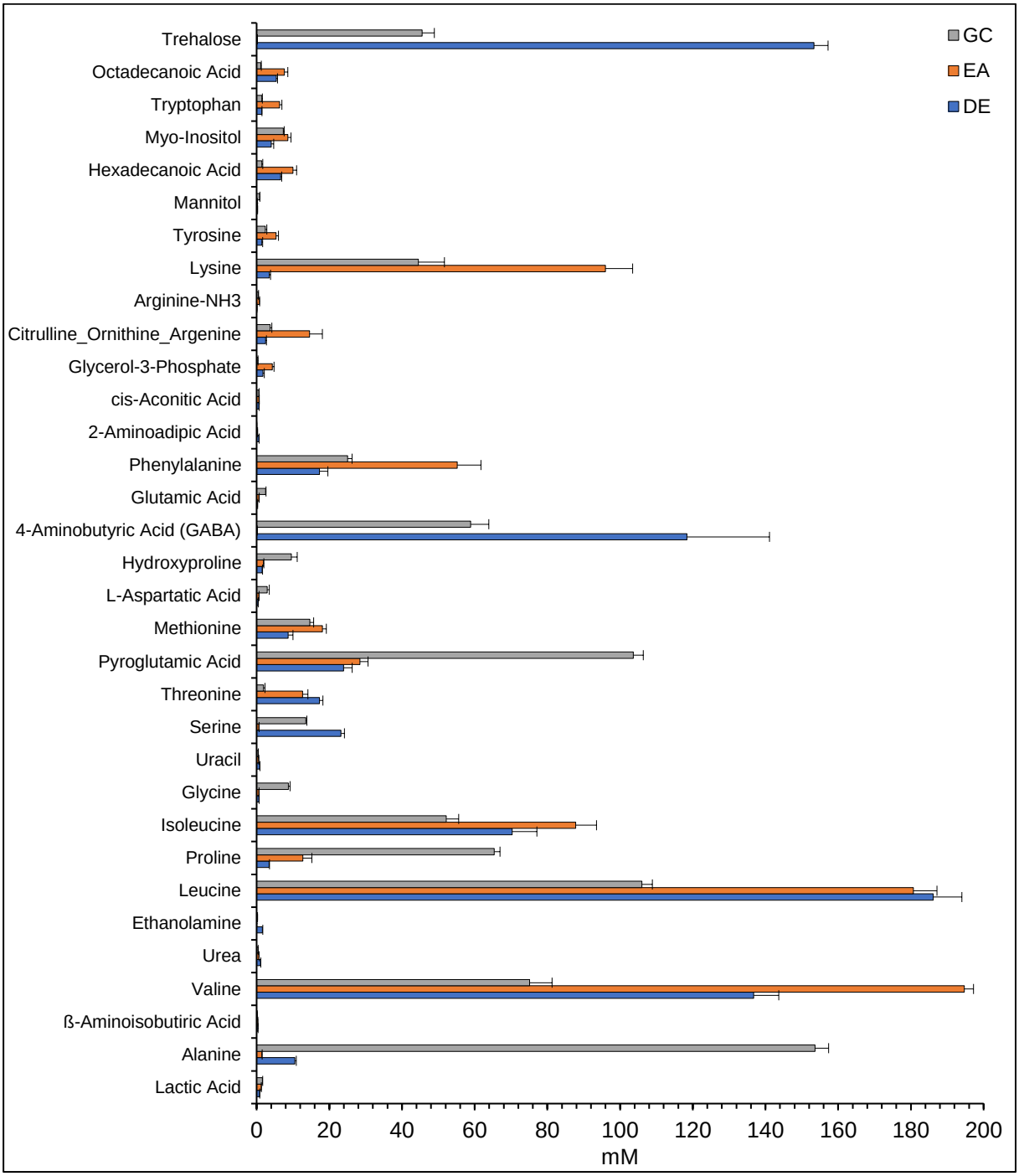

Figure 3.24 – Secreted bacterial metabolites. The bar graph indicates the concentrations of the metabolites in the supernatant fraction of the bacterial strains grown in LB supplemented with 2 M of NaCl. The blue bar is referent to the strain *Vreelandella* sp. DE, the orange bar to the strain *I. loihiensis* EA and the grey bar to the strain *V. salarius* GC. Error bars indicate standard deviation.

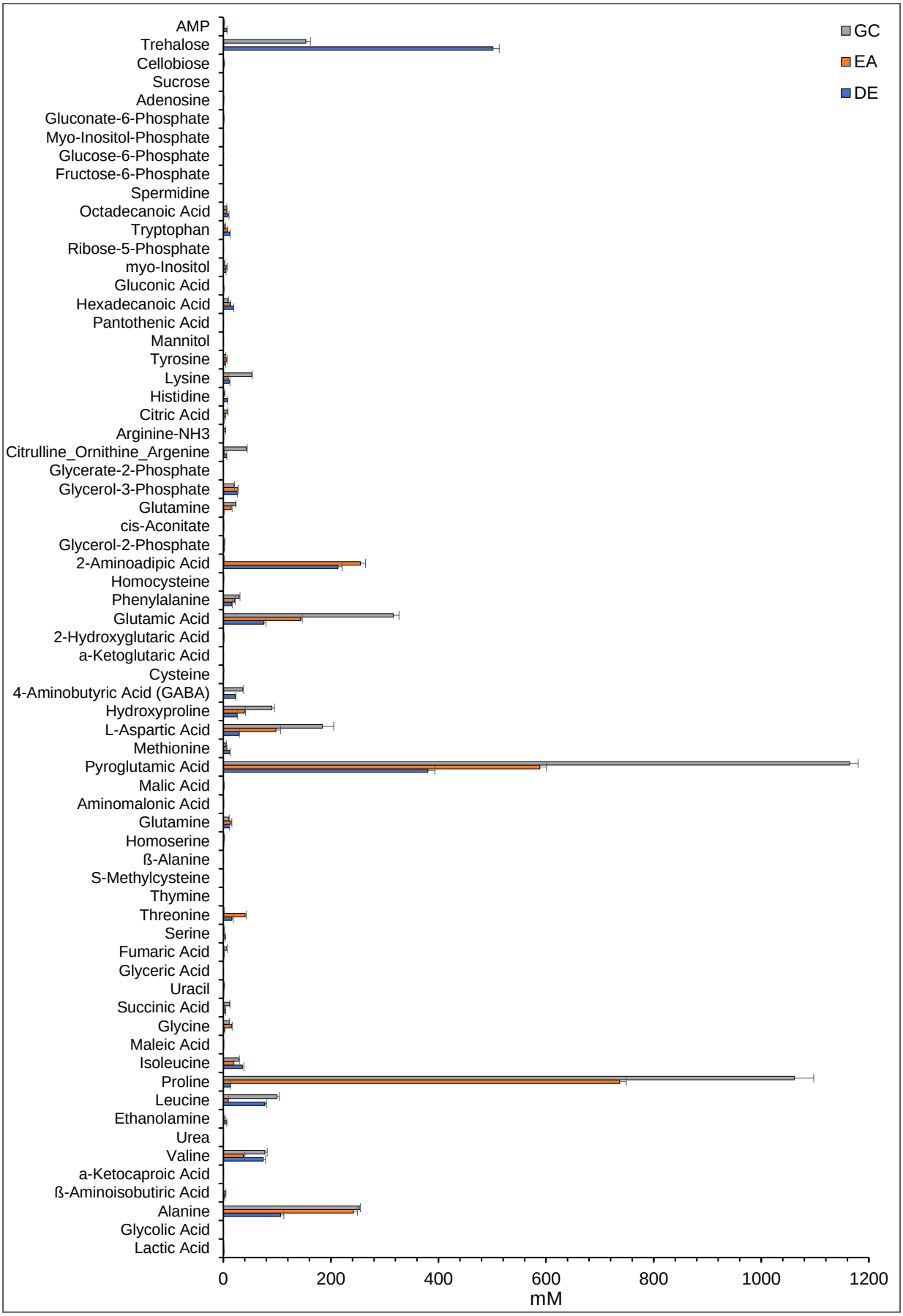
AMP
Trehalose
Cellobiose
Sucrose
Adenosine
Gluconate-6-Phosphate
Myo-Inositol-Phosphate
Glucose-6-Phosphate
Fructose-6-Phosphate
Spermidine
Octadecanoic Acid
Tryptophan
Ribose-5-Phosphate
myo-Inositol
Gluconic Acid
Hexadecanoic Acid
Pantothenic Acid
Mannitol
Tyrosine
Lysine
Histidine
Citric Acid
Arginine-NH3
Citrulline_Ornithine_Argenine
Glycerate-2-Phosphate
Glycerol-3-Phosphate
Glutamine
cis-Aconitate
Glycerol-2-Phosphate
2-Aminoadipic Acid
Homocysteine
Phenylalanine
Glutamic Acid
2-Hydroxyglutaric Acid
a-Ketoglutaric Acid
Cysteine
4-Aminobutyric Acid (GABA)
Hydroxyproline
L-Aspartic Acid
Methionine
Pyroglutamic Acid
Malic Acid
Aminomalonic Acid
Glutamine
Homoserine
ß-Alanine
S-Methylcysteine
Thymine
Threonine
Serine
Fumaric Acid
Glyceric Acid
Uracil
Succinic Acid
Glycine
Maleic Acid
Isoleucine
Proline
Leucine
Ethanolamine
Urea
Valine
a-Ketocaproic Acid
ß-Aminoisobutiric Acid
Alanine
Glycolic Acid
Lactic Acid
GC
EA
DE
0
200
400
600
800
1000
1200
mM

Figure 3.25 – Bacterial metabolites. The bar graph indicates the concentrations of the metabolites in the pellet fraction of the bacterial strains grown in LB supplemented with 2 M of NaCl. The blue bar is referent to the strain *Vreelandella* sp. DE, the orange bar to the strain *I. loihiensis* EA and the grey bar to the strain *V. salarius* GC. Many metabolites are not seen due to been present in really small concentrations, however they are illustrated in Figure 7.3. Error bars indicate standard deviation.

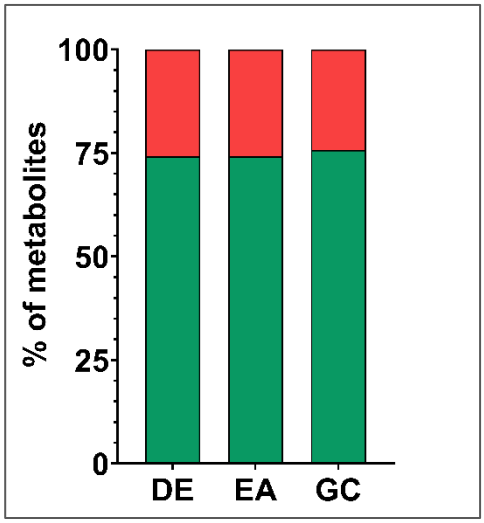

Figure 3.26 – Presence/absence of stress protecting metabolites. The column graph indicates the percentage of identified metabolites possessing (green sectors) and lacking (red sectors) stress-protecting roles for each strain. "DE" stands for the strain *Vreelandella* sp. DE, "EA" for the strain *I. loihiensis* EA and "GC" for the strain *V. salarius* GC.

All strains demonstrated a similar set of metabolites in both pellet and supernatant. However, the absence of ethanolamine and pantothenic acid was observed in *I. loihiensis* EA supernatant and pellet, respectively. Moreover, absence of cellobiose and S-methylcysteine in *Vreelandella* sp. DE and *V. salarius* GC pellet fractions, respectively, was noted.

The location of identified metabolites was summarized in Figure 3.27. The results indicated that half of the metabolites were present solely in pellet fraction. Besides, the remaining metabolites were located in both fractions, with the majority found at higher concentrations in the pellet, as in the case of glycine, pyroglutamic acid and proline. Nevertheless, some metabolites, such as leucine, isoleucine and urea exhibited higher concentrations in supernatant fractions. *Vreelandella* sp. DE and *V. salarius* GC demonstrated similar distributions of metabolite locations, despite having different compositions. Additionally, *I. loihiensis* EA displayed the most equitable distribution of metabolites located in both fractions in terms of location majority.

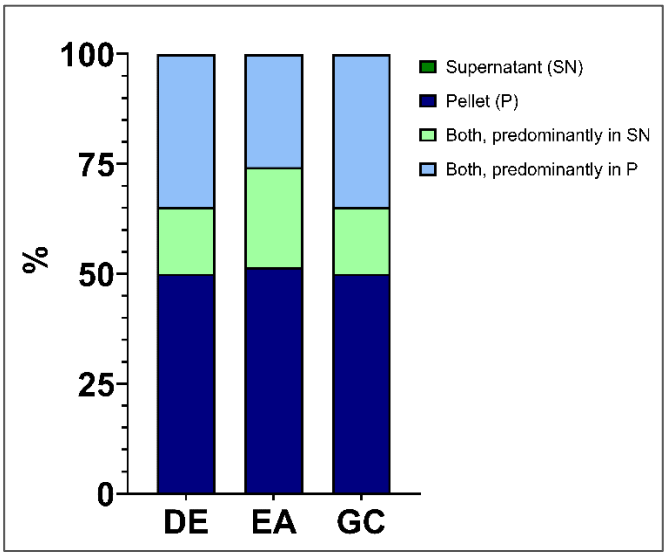

Figure 3.27 – Metabolites fraction location. The column graphs represent the relative distribution of each identified metabolite in the supernatant or pellet fraction for each strain. “DE” stands for the strain *Vreelandella* sp. DE, “EA” for the strain *I. loihiensis* EA and “GC” for the strain *V. salarius* GC. The dark green sectors refer to the metabolites identified only in the supernatant fraction, the dark blue sectors to the metabolites identified only in the pellet fraction, the light green sectors to the metabolites identified in both supernatant and pellet fractions, having higher concentration in supernatant and the light blue sectors to the metabolites identified in both supernatant and pellet fractions, having higher concentration in pellet.

All identified metabolites were classified into biomolecule categories to better understand the biomolecules distribution across supernatant and pellet fractions for each candidate strain. In terms of number of metabolites, few differences were identified as mentioned above. Ethanolamine (amine), pantothenic acid (organic acid), cellobiose (sugar) and S-methylcysteine (aminoacids) were the differential metabolites between strains. Furthermore, the metabolomics analysis revealed a predominance of the aminoacids class in both supernatant and pellet on number of metabolites and concentration for all strains, as illustrated in Figure 3.28. Additionally, the organic acids and sugar/sugar alcohols classes presented a similar number of identified metabolites and were more prevalent in the pellet fraction. The same occurred with the amines/amides class in *I. loihiensis* EA. Moreover, the nucleotides/nucleosides class is only present in the pellet. *Vreelandella* sp. DE exhibited the highest concentration of sugars/sugar alcohols, while *I. loihiensis* EA showed the lowest. However, *I. loihiensis* EA had the highest organic acids concentration. Regarding *Vreelandella* sp. DE, the pellet fraction demonstrated higher relative concentrations of sugars/sugar alcohols. Conversely, supernatant fraction of *I. loihiensis* EA demonstrated higher relative concentrations of organic acids. Lastly, amines, amides, nitrogen bases, nucleotides and nucleosides were present in notably low concentrations.

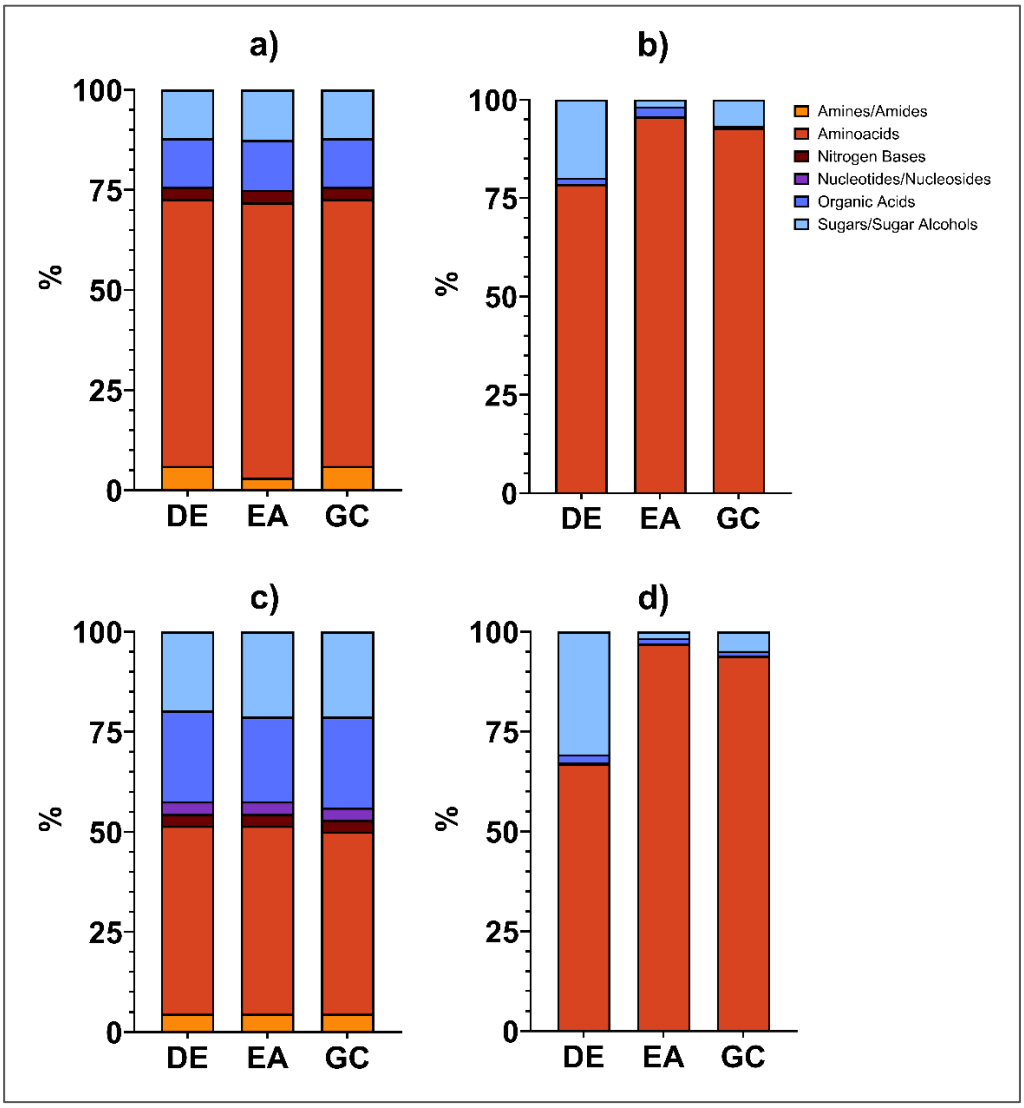

Figure 3.28 – Biomolecules distribution. The column graphs represent the relative distribution of each biomolecule class for each strain (amines/amides, aminoacids, nitrogen bases, nucleotides/nucleosides, organic acids and sugars/sugar alcohols), in which each of the identified metabolites were inserted. **a)** Number of identified metabolites belonging to each biomolecule class present in supernatant; **b)** sum of the concentration of the identified metabolites belonging to each biomolecule class present in supernatant; **c)** number of identified metabolites belonging to each biomolecule class present in pellet; **d)** sum of the concentration of the identified metabolites belonging to each biomolecule class present in pellet. “DE” stands for the strain *Vreelandella* sp. DE, “EA” for the strain *I. loihiensis* EA and “GC” for the strain *V. salarius* GC. The orange sector refers to amines/amides, the red to aminoacids, the dark red to nitrogen bases, the purple to nucleotides/nucleosides, the blue to organic acids and the light blue to sugars/sugar alcohols.

3.8 Transcriptomic Analysis of Plants Treated with Halophile Bacteria under Saline Stress

3.8.1 Phenotypical Changes of Maize Plants

To investigate the molecular impact of *Vreelandella* sp. DE treatment on maize plants, a transcriptomics analysis was performed. Firstly, phenotypical parameters were assessed two days after plant collection for RNA extraction to ensure that gene expression would manifest in the plant's phenotype. These results are quantified in Figure 3.29 and illustrated in Figure 3.30. Additionally, the effects of salt-stress on mock set were evident, with SL reduced by 44%. Furthermore, RL suffered a decrease of 31% and DW experienced an exponential decrease, losing more than half of its dry biomass. Regarding *Vreelandella* sp. DE treatment under salt-stress conditions, an overall enhancement was observed compared to the mock treatment, with SL increased by 50%. Moreover, RL improved by 73% and DW doubled. Besides, the effects of *Vreelandella* sp. DE treatment under control conditions and the effects of salinity on *Vreelandella* sp. DE treatment did not demonstrate significant alterations in the maize plants' phenotype.

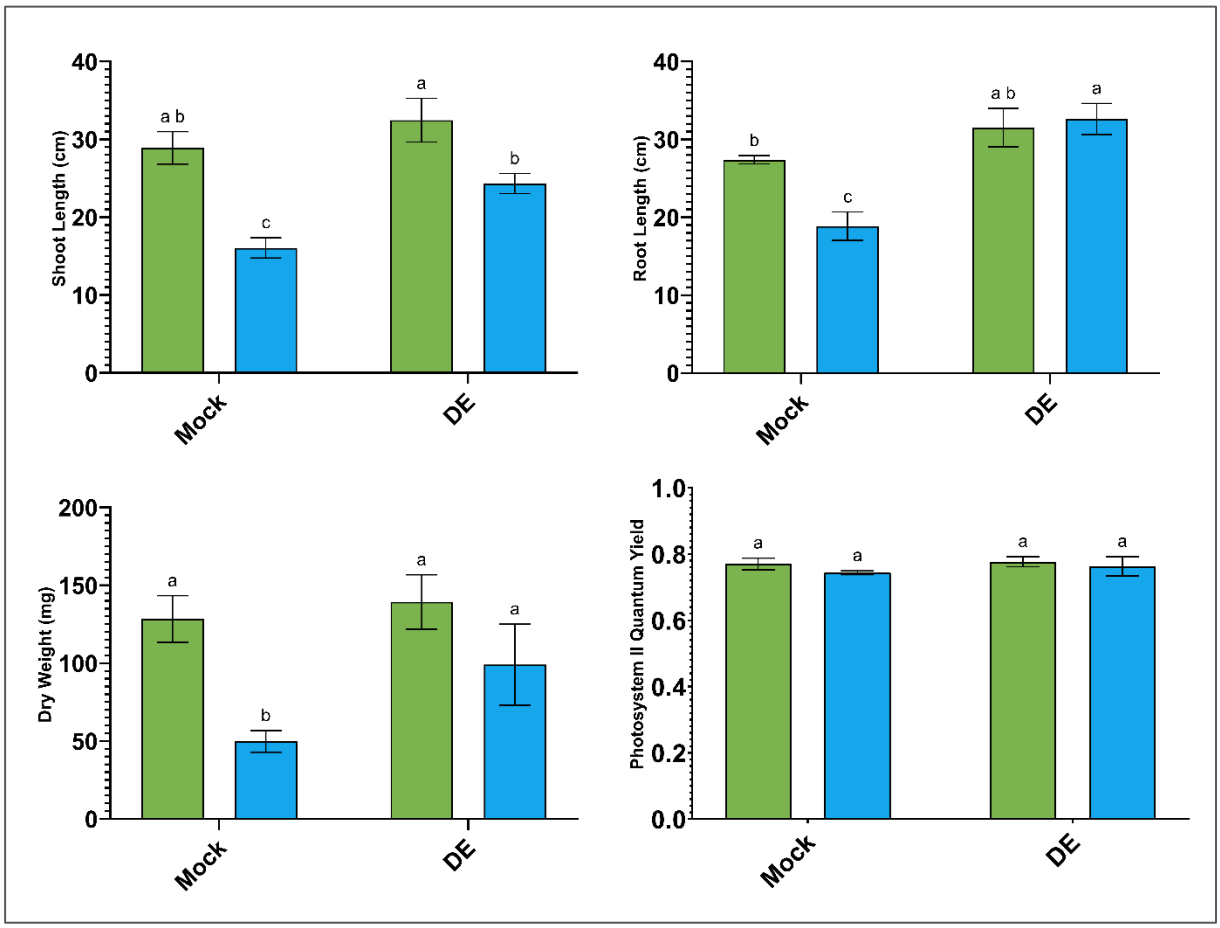

Figure 3.29 – Quantified phenotypical changes in maize plants after *Vreelandella* sp. DE treatment. The column graphs represent the shoot length, root length, full-plant dry weight biomass and photosystem II quantum yield recorded in maize after treatment with *Vreelandella* sp. DE, depicting the effects of the expressed genes analyzed by transcriptomics. The label "Mock" stands for mock treatment (without bacterial treatment) and "DE" for treatment using the strain *Vreelandella* sp. DE. The green columns indicate the control conditions, while the blue

bars depict the salt-stress conditions. The data sets (n = 3) were analyzed using a two-way ANOVA. Identical letters denote no statistically significant difference ($p < 0.05$). Error bars indicate standard deviation.

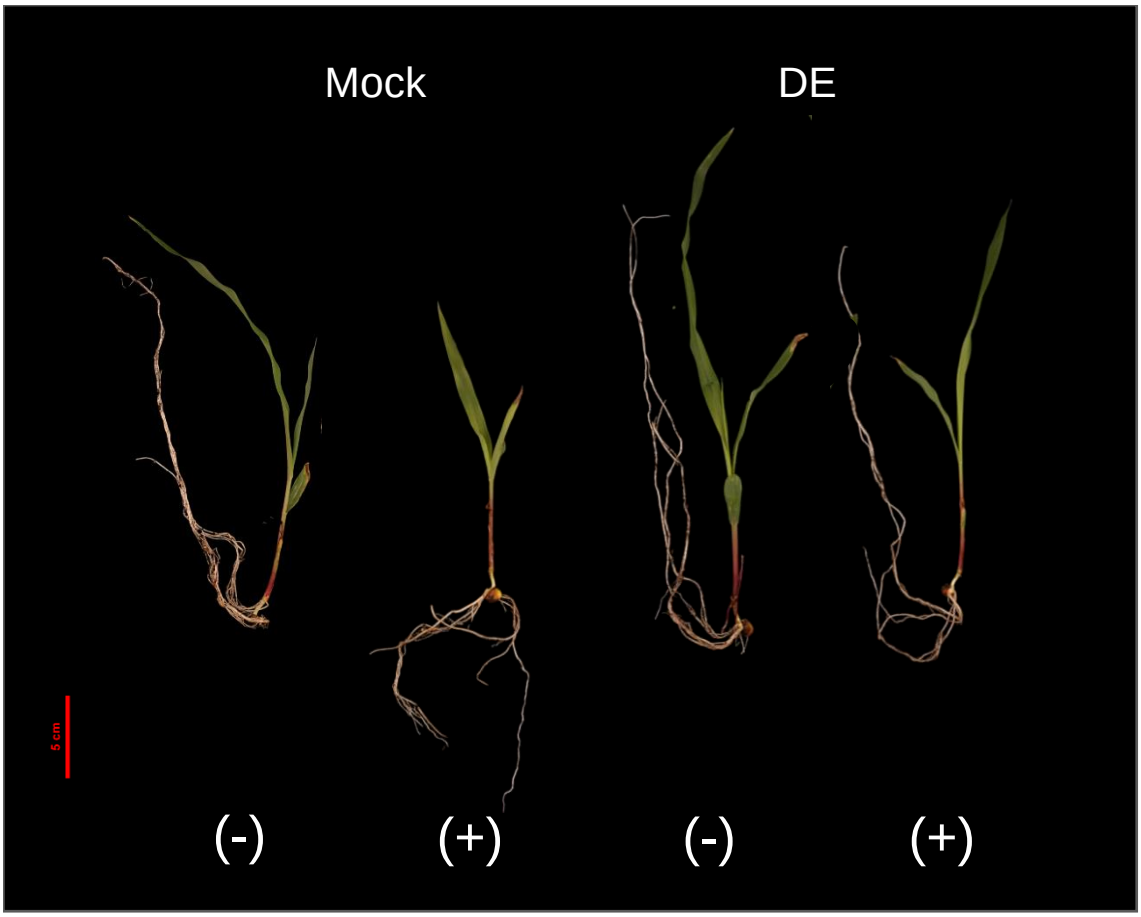

Figure 3.30 – Phenotypical changes in maize plants after *Vreelandella* sp. DE treatment. The complete plant images display the typical phenotype observed in maize plants following treatment with *Vreelandella* sp. DE, depicting the effects of the expressed genes analyzed by transcriptomics. The label “Mock” stands for mock treatment (without bacterial treatment) and “DE” for treatment using the strain *Vreelandella* sp. DE. Moreover, the label “-” indicates the control condition without salt-stress and “+” indicates the salt-stress condition.

3.8.2 Differentially Expressed Genes Functional Analysis

The RNA-seq analysis revealed a substantial number of differentially expressed genes (DEGs) across all comparisons of maize plants RNAs, as depicted in Figure 3.31. The mock set comparison demonstrated the lowest number of DEGs, with 255 down-regulated and 614 up-regulated genes under control conditions. Additionally, the *Vreelandella* sp. DE treatment set comparison exhibited 2379 down-regulated and 2486 up-regulated genes. Moreover, the mock treatment compared to *Vreelandella* sp. DE treatment under control conditions resulted in the largest number of DEGs, having 2850 down-regulated and 2590 up-regulated genes. Finally, 1897 down-regulated and 1451 up-regulated genes were recorded from the comparison between mock and *Vreelandella* sp. DE treatment under salt-stress conditions.

Besides, a considerable number of DEGs were observed among the various comparisons, as illustrated in Figure 3.32. Furthermore, of the 5306 DEGs present in the comparisons between treatment sets, 428 were found in both comparisons, while 4437 were exclusive to the *Vreelandella* sp. DE treatment set and 441 to mock set. Additionally, in total 7392 DEGs were found in the varying conditions comparisons, of which 1396 were found in treatment differences for both control and salt-stress

conditions. In addition, 4044 were verified only in treatment differences under control conditions and subsequently, 1952 were found exclusively in treatment differences under salt-stress conditions.

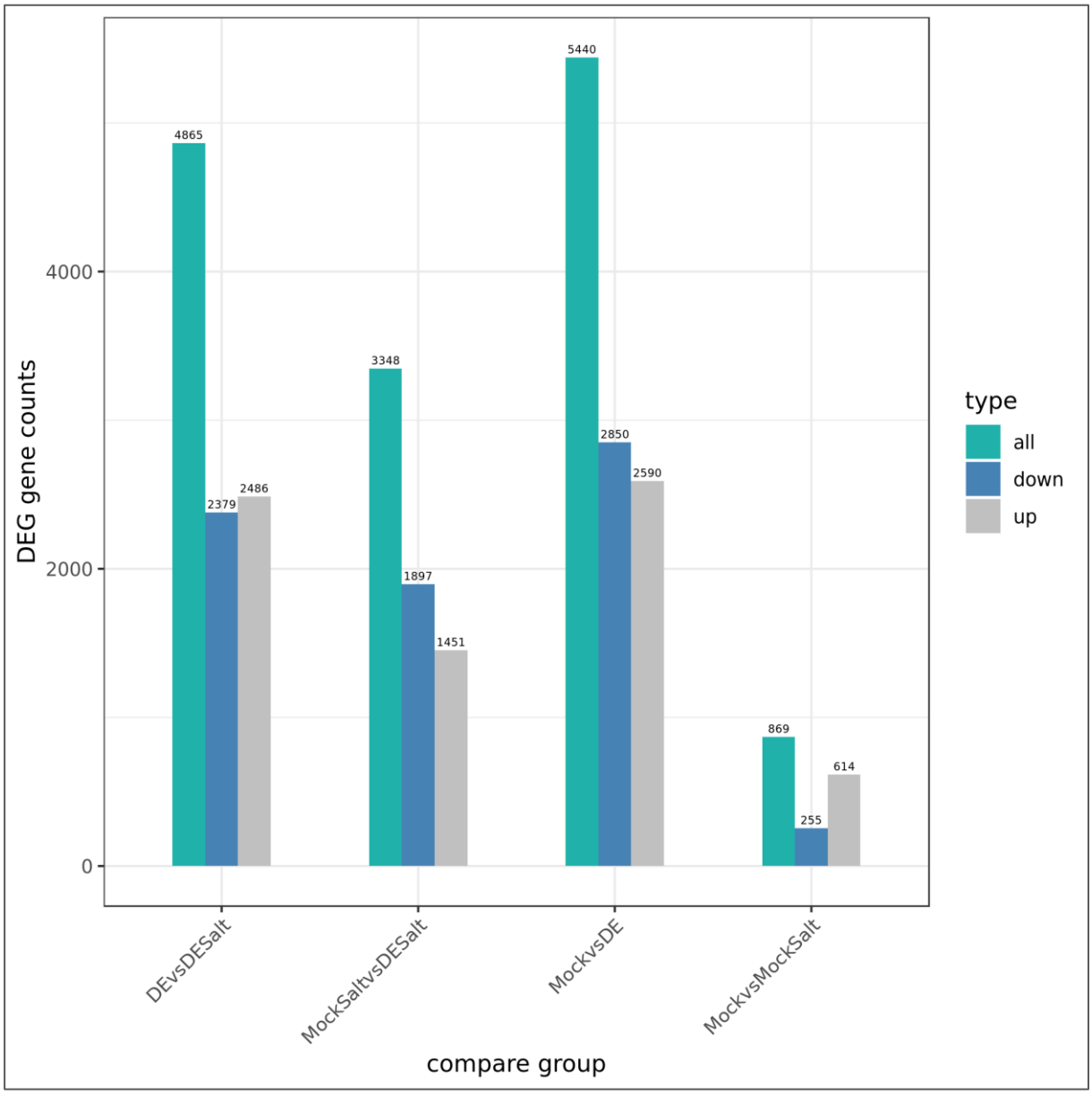

Figure 3.31 – Number of DEGs. The histogram illustrates the total number of DEGs (green column), the number of down-regulated expressed genes (blue column) and the number of up-regulated expressed genes (grey column). The label “Mock” stands for mock treatment (without bacterial treatment) under control conditions, “MockSalt” for mock treatment under salt-stress conditions, “DE” for treatment using the strain *Vreelandella* sp. DE under control conditions and “DESalt” for treatment using the strain *Vreelandella* sp. DE under salt-stress conditions. Moreover, the label “vs” indicates a comparison, wherein the up- and down-regulation are referent for the left term genes regarding the right term genes.

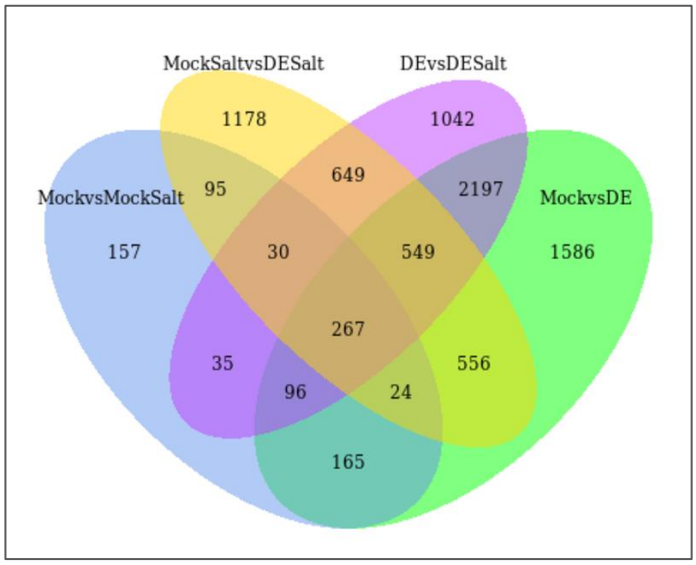

Figure 3.32 – Similarities between DEGs. The Venn diagram of differential expression highlights the distinct genes between the treatment and control groups. The total numbers within each circle represent the overall differentially expressed gene count in each group, while the overlapping section shows the number of differentially expressed genes common to both groups. The label “Mock” stands for mock treatment (without bacterial treatment) under control conditions, “MockSalt” for mock treatment under salt-stress conditions, “DE” for treatment using the strain *Vreelandella* sp. DE under control conditions and “DESalt” for treatment using the strain *Vreelandella* sp. DE under salt-stress conditions. Moreover, the label “vs” indicates a comparison.

Transcriptomics functional analysis revealed substantial differences in various molecular functions and metabolic pathways. Initially, as shown in Figure 3.33, salinity effects on mock treated maize plants demonstrated a down-regulation in DNA replication related genes, including enzymes, such as the DNA polymerase and primase, and replication factors. Additionally, a decreased expression of genes leading to several ribosomal subunits’ formation was observed. Regarding phytohormonal signal transduction, several genes were down-regulated, such as LOC103633549 and *aux*1, involved in IAA synthesis and influx, respectively. Conversely, some protein phosphatases encoding genes were up-regulated. The phenylpropanoid biosynthesis pathway demonstrated one of the highest significant enrichments, with down-regulated genes connected with enzymes production, such as cinnamyl-alcohol and coniferyl-aldehyde dehydrogenases. Moreover alanine, asparagine and glutamic acid metabolism was among the most significant enriched pathways exhibiting DEGs involved with enzymes production, as in the case of aspartate carbamoyl transferase-1 down-regulation and asparagine synthase and alanine transaminase up-regulation. Furthermore, ethylene responsive factors, such as A2P and ERF, were up-regulated regarding control set of plants, as well as genes related to stress-induced response, including anthocyanins, glutathione transferase, dehydrins, asparagine synthase and zeaxanthin epoxidase (ABA production) or polyamine oxidases. Conversely, energetic, growth and development regulation factors, such as RALFL33, gibberellin 3-oxidase, apyrase, GRF, GDSL esterase/lipase or alpha expansins were down-regulated by salinity. Moreover, structuring compounds and transporters for relevant compounds as rhamnose, hydroxyproline, mannose, critical aminoacids or xyloglucan compounds demonstrated a similar pattern.

Besides, the salt-stress impacts on *Vreelandella* sp. DE treated plants demonstrated a different set of most significant enrichment pathways, as illustrated in Figure 3.34. Several genes involved in the photosynthesis process and carbon fixation in photosynthetic organisms were down-regulated. These genes encompassed both PSI and PSII functions, light-harvesting complex I and II chlorophyll a/b binding proteins, Calvin cycle enzymes and many other proteins. Conversely, some genes were up-regulated, such as the one encoding the ferredoxin-4. In addition, DNA replication and ribosome were also present in the most significant enrichment pathways. Besides, it was noticed an upregulation of several growth-regulating factors (GRFs), beta-glucosidase, ACC oxidase, LEA proteins synthesis, antioxidant enzymes (oxidoreductases, superoxide dismutase (SODs), glutathione S-transferases (GSTs) and glutaredoxins), as well as the synthesis of proline, hydroxyproline, glutamic acid and other compounds that plants use for osmoprotection. These osmoprotectants were up-regulated even more when compared

to mock treated plants under salt conditions. However, many genes down-regulated by salinity in mock treated plants demonstrated an up-regulation in *Vreelandella* sp. DE treated plants when salt-stress affected.

In terms of treatments influences on maize plants under both control and salt-stress conditions, substantial functional differences were identified, as depicted in Figure 3.35 and Figure 3.36, respectively. In addition, *Vreelandella* sp. DE treated relative to mock treated plants exhibited an inverse pattern from the salinity effects in mock treatments. Several genes associated with photosynthetic processes and carbon fixation, which were previously downregulated under salt stress, were upregulated with *Vreelandella* sp. DE treatment. Inversely, other genes, such as the ferredoxin-4 encoding gene, exhibited decreased expression. However, genes connected to DNA replication demonstrated down-regulation, as occurred with salt-stress effects on mock treated maize plants. Furthermore, starch and sucrose metabolism was one of the most significant enrichment pathways. On the other hand, several genes encoding enzymes were up- and down-regulated. As the case of *TPS4*, *TPS5* and *TPS6* encoding for trehalose-6-phosphate synthase demonstrated a decreased expression. Conversely, the genes *SRA*, LOC100273093 and LOC103632655 exhibited an increased expression hampering trehalose 6-phosphate phosphatase production. Moreover, terpene synthases, expansins, fibre cell-long elongation factors, fatty acid elongases, beta glycosidases, cellulose synthases, xyloglucans synthesis, xyloglucans synthases, vegetative cell wall proteins accumulation (as gp1) or even flowering promotion factors related genes were up-regulated. In addition, many transporters were also upregulated in *Vreelandella* sp. DE treated plants (particularly ABC, polyol, aminoacid and sugar transport (as SWEET13b) transporters). Consistently, many phytohormone regulatory systems also increased their regulation, as demonstrated the upregulation of inositol-P synthases, auxin response proteins, IAA regulators and aminoacid receptors, ACC oxidases, gibberellin oxidases and brassinosteroid-regulators. Lastly, many nutrient-related regulators also shown an increased expression, mainly in the cases of N, including ammonium transporters, nitrilases and nitrate reductases, P with P transporters and S, such as sulfate transporter.

Finally, mock treated plants under saline conditions exhibited again a decreased expression of genes related to DNA replication in comparison to *Vreelandella* sp. DE treated. Furthermore, genes associated with base excision repair were up-regulated when compared to the mock treatment under salt-stress as reference. Additionally, benzoxazinoid and plant secondary metabolites biosynthesis, as well as valine, leucine and isoleucine degradation, were among the most significant enrichment pathways. Within these pathways, increased levels of expression were observed in genes encoding enzymes, such as indole-3-glycerol-phosphate lyase (LOC103644182 and *Igl*) and S-adenosylmethionine synthetase (LOC100282324), which are involved in the ethylene biosynthesis. Conversely, ACC oxidase was up-regulated, regulating the ethylene concentration. Besides, *Vreelandella* sp. DE treated plants demonstrated an increased expression of several stress-regulation factors as the synthesis of isoflavone monooxygenase and hydroxylases, senescence-induction factors, membrane integrity regulation factors, stress-response proteins and ABA response factors and degraders (aspartyl protease, L-ascorbate oxidases, L-asparaginases), production of chlorophyllase (chlorophyll degradation) and growth control activation factors. In addition, a notable amount of different antioxidant enzymes (peroxidase, chitinase, polyphenol oxidase, GSTs, phenylalanine ammonia-lyase, flavonoid monooxygenase, malate dehydrogenase, peroxidase, oxidoreductase and phosphoenolpyruvate (PEP) carboxylase), stress suppression factors (as chaperonins, cupredoxin, patatins, osmotin) and even specific growth inducing factors and nutrient related factors (GRFs, root cap proteins, germins, cellulose synthases, gibberellin synthesis, nitrate reductase, nitric oxide synthase). Finally, different stress-response compounds, including fasciclin, calnexin, remorin, pherophorin, akyrin, were upregulated in plants inoculated with *Vreelandella* sp. DE.

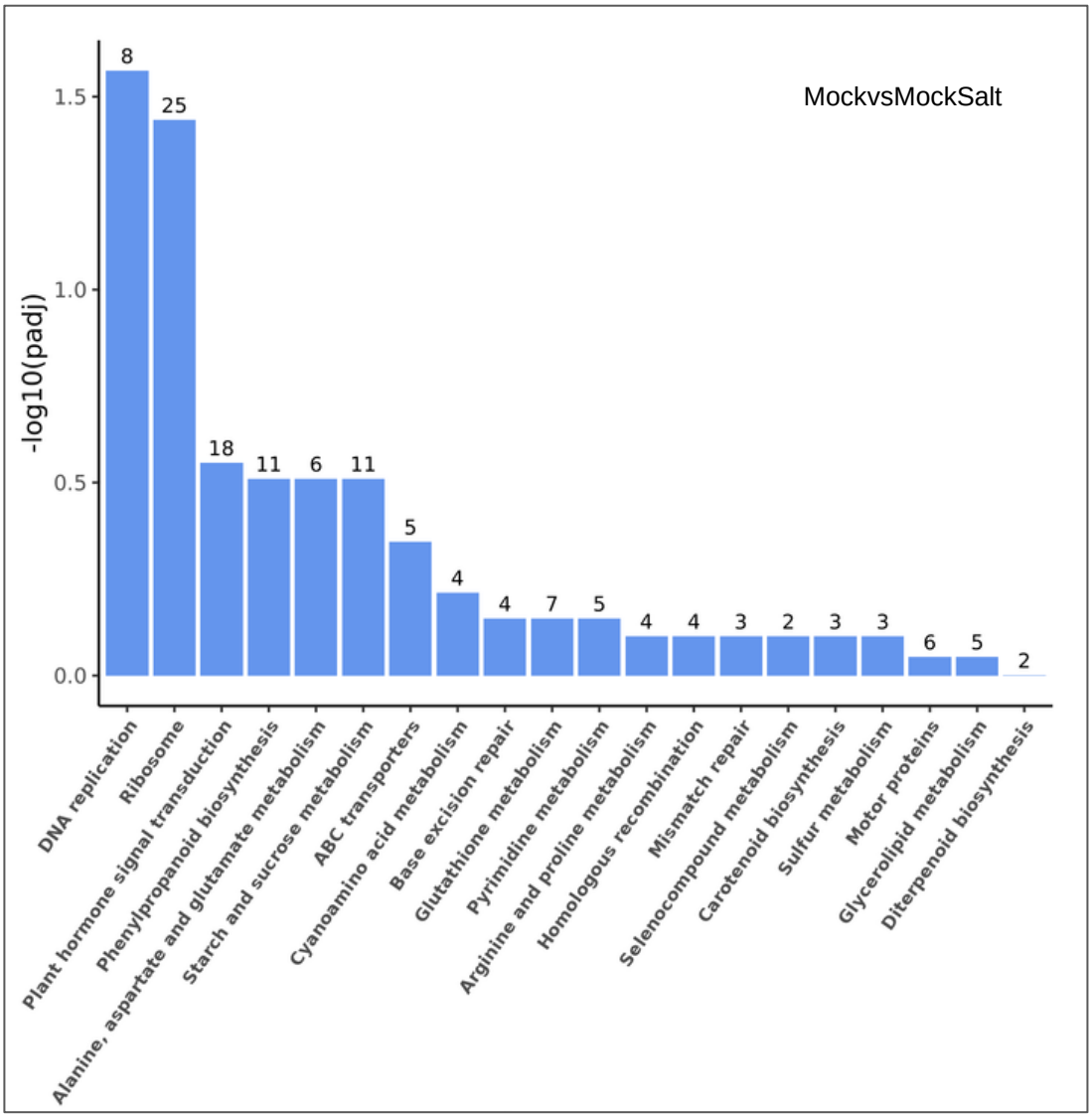

Figure 3.33 – Functional analysis of DEGs relative to mock set comparison. The column graph displays the 20 most significant KEGG pathways compared to the mock set. The x-axis represents the KEGG pathways, while the y-axis indicates the significance level of pathway enrichment, with higher values indicating greater significance. The values above each column represent the number of DEGs.

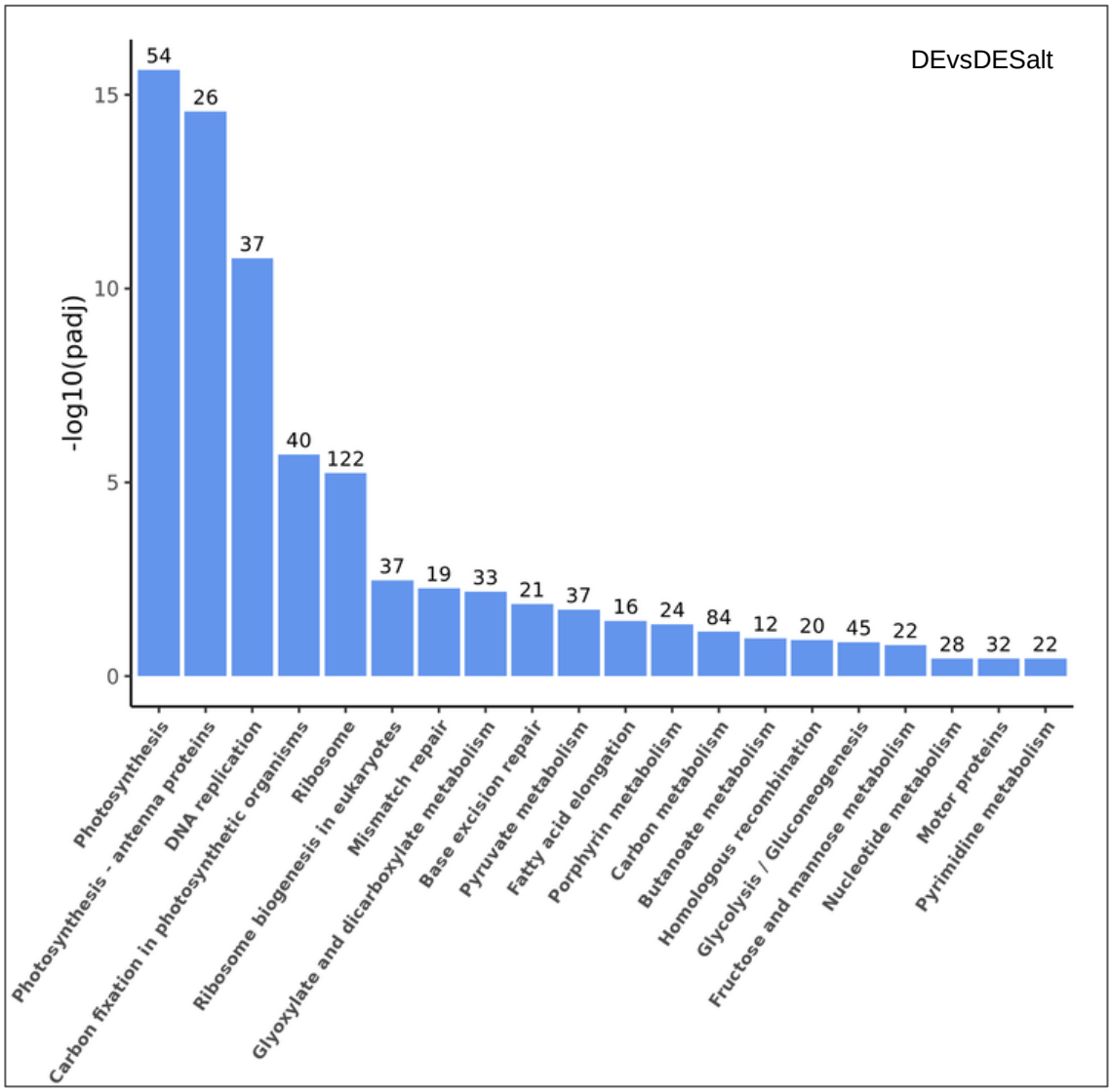

Figure 3.34 – Functional analysis of DEGs relative to *Vreelandella* sp. DE treatment set comparison. The column graph displays the 20 most significant KEGG pathways compared to the *Vreelandella* sp. DE treatment set. The x-axis represents the KEGG pathways, while the y-axis indicates the significance level of pathway enrichment, with higher values indicating greater significance. The values above each column represent the number of DEGs.

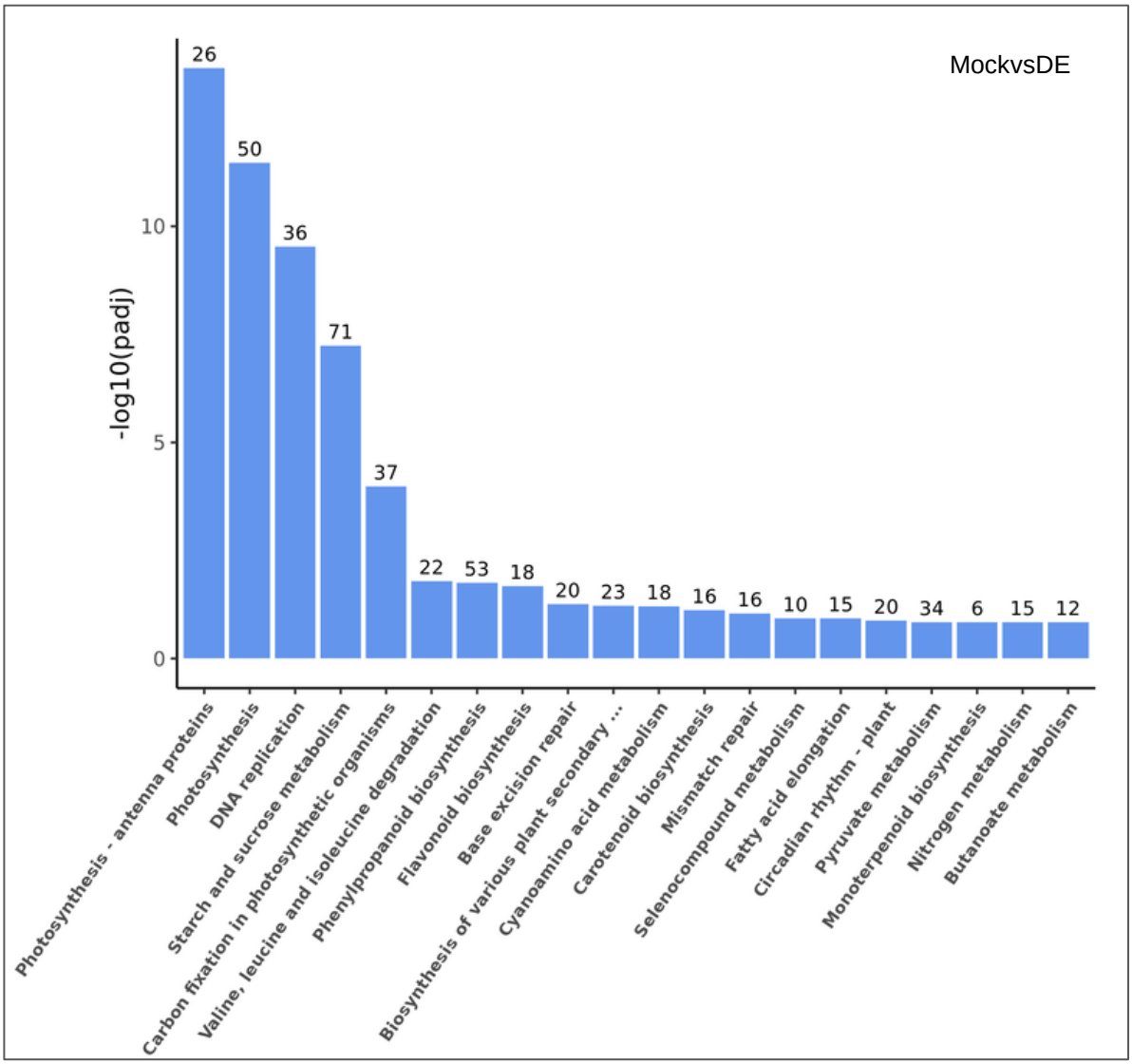

Figure 3.35 – Functional analysis of DEGs relative to *Vreelandella* sp. DE treatment under control conditions. The column graph illustrates the 20 most significant KEGG pathways relative to the *Vreelandella* sp. DE treatment under control conditions. The x-axis represents the KEGG pathways, while the y-axis indicates the significance level of pathway enrichment, with higher values indicating greater significance. The values above each column represent the number of DEGs.

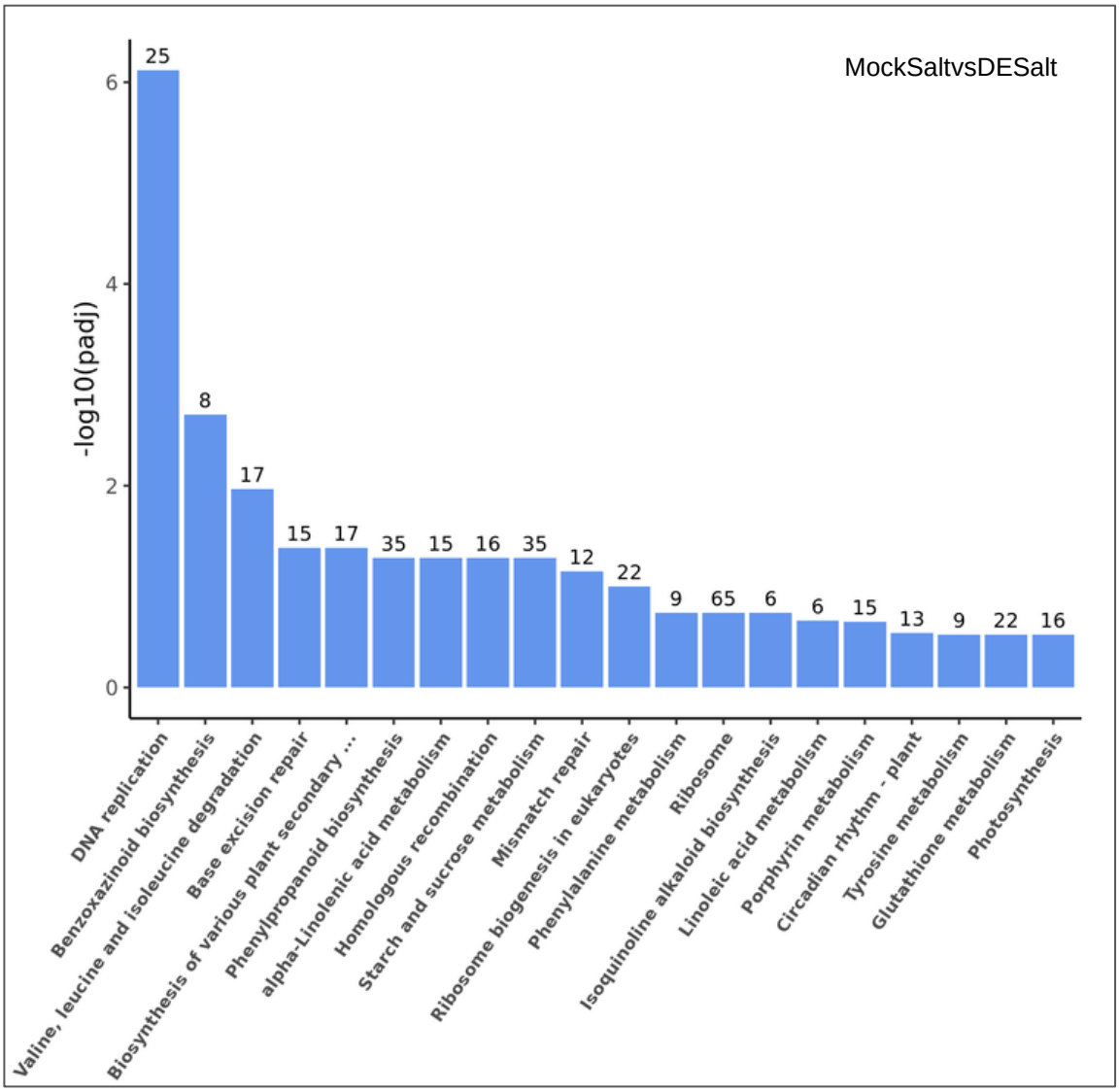

Figure 3.36 – Functional analysis of DEGs relative to *Vreelandella* sp. DE treatment under salt-stress conditions. The column graph illustrates the 20 most significant KEGG pathways relative to the *Vreelandella* sp. DE treatment under salt-stress conditions. The x-axis represents the KEGG pathways, while the y-axis indicates the significance level of pathway enrichment, with higher values indicating greater significance. The values above each column represent the number of DEGs.

4
DISCUSSION

Across the globe, soil salinization has been an increasing problem, mainly for the agricultural sector. In addition, numerous factors are contributing to the worsening of this issue, with evapotranspiration, precipitation and rising of groundwater levels being the main drivers of soil salinization [134], [135]. Furthermore, climate changes are intensifying the negative impacts of these factors, particularly in arid and semi-arid areas. Besides, farmlands are the areas most affected by saline soils [136]. Portugal's farmlands are not exempt from this phenomenon. Saline soils significantly affect important agricultural areas, such as Ribatejo, predominantly due to the advance of the salt wedge on the surrounding rivers [21], [137]. Moreover, it is projected that Ribatejo will experience reduced precipitation and even higher temperatures in the future, which will increase the salinity in the soils, thus leading to threatening challenges to regional crop sustainability [138]. As a result, the agricultural industry is faced with an urgent challenge to develop methods for mitigating soil salinization in order to maintain crops sustainability. This is essential for meeting the expanding needs of an expanding global population. Hence, the rationale for this project was that the utilization of adapted microbiota accustomed to thriving in saline environments may assist crops in coping with salt-stress conditions.

To test this proposition, bacteria from Iberian saltpans and salt flats were collected and isolated in highly saline conditions to form a halophile/halotolerant collection. Therefore, several halophile species were discovered, such as *Idiomarina loihiensis* and *Salinivibrio costicola* [139], [140]. Common species in saline environments, including *Oceanobacillus picturae* and *Planococcus rifietoensis* were also identified [141], [142], [143], [144], [145], [146]. Additionally, the growth in significantly higher concentrations of NaCl substantially altered the composition of the culturable bacteria collection compared to a collection sampled from the same locations [20]. *Bacillus atrophaeus* and *Priestia megaterium* are the only species present in both collections, suggesting that the majority of the bacteria isolated are dependent on high salinity levels for growth. Additionally, the bacterial community diversity in soil 6 aligns with the typically observed Shannon diversity index values for culturable bacteria (1.5-2.6) [147], [148]. However, the remaining soils exhibited lower diversity than is customary, indicating the possibility that high salinity reduces bacterial biodiversity [149]. Furthermore, saline soils demonstrated a higher population abundance than the gypsic ones, which may be attributed with the adaptive evolution of bacteria to thrive under saline environments [150]. Consequently, a large number of different halophile strains were isolated. In evaluating and identifying the most promising candidate strains for several approaches, a key focus was on verifying their effectiveness in stressing conditions. Although many researchers employ *in vitro* testing to efficiently assess each strain's general capabilities, this method may not necessarily predict similar outcomes in plants, particularly under stressing environments [151], [152], [153], [154]. Consequently, it was decided to incorporate salt stress into the screening tests as a distinguishing element, in line with an emerging contextualizing trend in the field [6], [155]. Hence, bacterial strains were selected with varying characteristics to capture a broad spectrum of mechanisms that could enhance crop resilience under salt stress. This selection approach aligns with previous studies that emphasize the importance of trait diversity in addressing environmental challenges [156], [157].

The candidate strain *Kushneria marisflavi* AA, was selected for its remarkable antioxidant production, significantly exceeding 9 mM of antioxidants equivalents. This feature is noteworthy, as it surpasses the concentration typically produced by known high antioxidant producers such as *Bifidobacterium longum*, a lactic acid bacteria recognized for its antioxidant capabilities [158]. The elevated antioxidant levels produced suggest a strong potential for mitigating oxidative stress in plants through the

regulation of ROS levels [159]. Additionally, *Kushneria marisflavi* was reported to enhance the salt-stress resilience of sunflower (*Helianthus annuus*), lettuce (*Lactuca sativa*) and barley (*Hordeum vulgare*) by Szymańska and collaborators [160]. Another strain selected as a candidate was *Vreelandella* sp. DE due to its exceptional biofilm production, nitrogen fixation and sulfur oxidation under high salinity conditions. The ability to form robust biofilms is critical in alleviating ionic toxicity and osmotic stress, as the biofilm acts as a physical barrier, protecting plant roots [61], [161]. Notably, the biofilm production of *Vreelandella* sp. DE far exceeds the typical values seen in various *Pseudomonas* species, which average around OD_{550nm} = 0.6 [162]. Additionally, nitrogen fixation, which is rarely observed in pure cultures under salt-stress [163], it is of paramount importance as nitrogen is the most critical nutrient for plants and is scarce under saline conditions [164]. Besides, the sulfur oxidizing capability provides the advantage of supplying not only this macronutrient, which is substantially involved in protein synthesis, but also exhibits a synergistic effect on various other essential nutrients which may be associated with the nitrogen fixation ability [82]. The strain *Idiomarina loihiensis* EA emerged as a candidate due to its high production of auxins, which are key growth phytohormones with a fundamental role in root architecture [165], [166]. Its auxin production surpasses that of *Azospirillum brasilense* (30 µg/mL of IAA equivalents), which is known to enhance plant growth through auxins production [167], [168]. This may elucidate the observed development of a more branched root system in maize plants inoculated with *Idiomarina loihiensis* EA. *Virgibacillus salarius* GC was also selected for its manganese solubilizing capabilities. In addition, manganese is an essential micronutrient involved in PSII functions [169]. Moreover, *Idiomarina abyssalis* IA was selected due to its capacity to produce siderophores, which are iron-scavenging compounds that inhibit infection by phytopathogens [170]. *Planococcus citreus ID* was selected for its notable phosphate-solubilizing capacity, a crucial trait for enhancing plant growth and development [171]. Notably, *Planococcus citreus* ID demonstrated phosphate solubilization at levels comparable to high-performing bacteria (40 mg/mL of PO_4^- equivalents), even under salt stress, which typically diminishes this ability [172]. *Rossellomorea aquimaris* 104 is one of the calcium-solubilizing bacteria, so it was selected. Hence, calcium is an essential micronutrient related to signalling processes, including salt-stress tolerance [173]. Furthermore, Li and Jiang reported that *Rossellomorea aquimaris* was capable of alleviating salt-stress in maize seedlings [50], the same pattern was verified in maize plants inoculated with *Rossellomorea aquimaris* 104, reinforcing the efficacy of this strain as PGPB under salt-stress conditions. *Halobacillus faecis* 109 was another strain selected as a candidate since it was capable to grow in an ACC-only carbon and nitrogen source medium, suggesting the presence of ACCd, an enzyme that regulates ethylene (stress hormone) levels through the breakdown of ACC (ethylene precursor) [174], [175]. This strain demonstrated a significant capacity to regulate ethylene levels, given that it exceeded the performance of several ACCd-producing bacteria [176], [177]. Nonetheless, ACCd production may be sufficient to improve the salt resilience in monocots, as observed in maize seedlings, since monocots typically demonstrate lower ethylene stress sensitivity [178]. *Bacillus swezeyi* 119 was also chosen as a candidate due to its exceptional proline secretion and capacity to produce exopolysaccharides. Proline is an important antioxidant and osmoprotectant that reduces cell water potential and aids sustaining turgor pressure [179]. Furthermore, EPS are associated with biofilm formation and have similar functions, including the formation of a physical barrier around the roots, providing resistance to osmotic stress and a protective role against ionic toxicity [180]. Finally, the strain *Oceanobacillus picturae* 123 was chosen as it excelled in potassium solubilization. Furthermore, potassium solubilization plays a crucial role in plant nutrition [181]. Besides, it was reported to aid in coping with osmotic stress [182]. Moreover, enhanced maize root length in plants treated with *Oceanobacillus picturae* 123 could be derived from this specific trait [183]. Therefore, the selection and characterization of halophile and halotolerant bacterial strains capable of thriving in saline conditions, coupled with their PGPT such as antioxidants and osmoprotectants production, biofilm formation and nutrient availability, underscores their potential as robust bioinoculants. These strains may facilitate the development of bioinoculants specifically tailored for saline environments, offering a sustainable approach to enhancing crop resilience and productivity under salt stress.

Besides the candidate strains' performance on the diverse PGPT tests, a remarkable salt-stress resilience was observed in the candidate strains. *Vreelandella* sp. DE and *Idiomarina loihiensis* EA distinguish themselves from the remaining strains due to their affinity for higher salinity levels. Moreover, several mechanisms developed through adaptation to highly saline environments may elucidate this impressive capability. Both strains possess a substantially elevated amount of aminoacids in their composition, which are related with salt-stress resilience [184], [185]. Additionally, proline and alanine function as osmoprotectants [186], [187], [188]. Furthermore, glutamic acid and GABA signalling modulates stress-related responses, such as ethylene and ROS regulation [186], [189], [190]. Pyroglutamic acid,

phenylalanine, valine, threonine, isoleucine and L-aspartic acid are all aminoacids involved in the enhancement of the antioxidant system and the production of important metabolites against salt-stress nefarious effects, such as proline, glutamic acid and GABA mentioned previously [191], [192]. Besides, the latter four aminoacids form the VTID complex that alleviates salt-stress due to increasing antioxidant enzymes activity (CAT and SOD), reducing malondialdehyde (MDA) an oxidative stress marker and increasing the levels of osmoprotectants [193]. Consequently, *Idiomarina loihiensis* EA demonstrated a salt-stress relieving mechanism more focused on proline as the major osmolyte and a higher aminoacid content. Conversely, *Vreelandella* sp. DE demonstrated a salinity tolerance focused on trehalose as major osmolyte. Trehalose provides an alternative source of carbon and energy. Additionally, its chemical properties, including strong water affinity, absence of internal hydrogen bonds formation, non-hygroscopic glass formation and chemical stability render it one of the major osmoprotectants [194]. These results demonstrate the existence of alternative strategies for coping with saline environments. However, the candidate strains isolated from the hypergypsic soils (*Rossellomorea aquimaris* 104 and *Halobacillus faecis* 109) belong to the group in which the salinity threshold is lower, reinforcing the notion that there is species adaptation to the surrounding environment. Hence, the candidate strains exhibited promising results in a variety of tests and salt-stress resilience, leading to the identification of a diverse set of bacteria with the potential to aid crops in thriving in highly saline environments.

Maize (*Zea mays*) and tomato (*Solanum lycopersicum*) are two of the major crops cultivated in the Ribatejo region [23]. Additionally, maize a monocotyledon (monocot) is one of the most significant crops regarding human and animal nutrition [195]. Furthermore, tomato a dicotyledon (dicot) is one of the most relevant fleshy fruit crops and it has been utilized as a model plant [196]. Therefore, they were selected as plant models.

Early-stage biotreatment tests were conducted as a second and more accurate screening to assess candidate strains' potential in enhancing maize and tomato growth and resilience under salt-stress conditions. Initially, both crops were subjected to the same salinity level. However, the fragile structure of tomato seedlings led to their death while stress was applied, thus necessitating a reduction in salinity. In addition, early-stage tests were extended in tomato plants to provide a clearer phenotype. Interestingly, while almost all biotreatments were effective in enhancing the photosystem II quantum yield in tomato plants, which is relevant due to this parameter's connection with plant viability [197], [198], no significant changes were reported in maize, this may be related with retarded phenotypic changes of the QY under salt-stress conditions [199]. Additionally, the differences between maize sets may be attributed to the climatic conditions experienced during the experiment [200]. Another interesting aspect noted was the effects of salinity on uninoculated tomato seedlings, which demonstrated higher growth under saline conditions. This phenomenon has been previously reported [201], [202], although further studies are needed to elucidate it. Furthermore, *Vreelandella* sp. DE functional genomic analysis demonstrated the presence of some genes related with root colonization, potentially providing it the capacity of chemotaxis towards the roots (*che* gene cluster), motility (*flh*D and *flh*C) and secondary attachment to roots (*lap*A). However, the absence of genes related to root primary attachment was noted, as well as some other genes reported to be crucial for root colonization without losing the biofilm forming capabilities, such as *abr*B, *sig*H, *sig*D, *nrf*A and *yus*V, thus resulting in the poor root colonization capacity [203], [204]. Besides the candidate strains have not proven capable of colonizing the plant roots, they are able to enhance plant growth and alleviate salt-stress through alternative mechanisms, such as the secretion of exudates [205], [206], [207]. Furthermore, early-stage tests do not always predict the final outcome of PGPB effects on crops [208]. Therefore, long-term biotreatment tests were conducted to better predict the candidate strains' influence on maize and tomato plants under field conditions. For this purpose, *Vreelandella* sp. DE, *Idiomarina loihiensis* EA and *Virgibacillus salarius* GC were select to proceed to the subsequent stage. This selection was based on the two strains exhibiting the highest SL in tomato plants under salt-stress conditions (*Idiomarina loihiensis* EA and *Virgibacillus salarius* GC). Additionally, among the strains that enhanced tomato plants to a more advanced developmental stage, *Vreelandella* sp. DE demonstrated the highest SL in maize plants under saline conditions. Moreover, this characteristic, in conjunction with a significant increase in RL, contributed to its selection as a biotreatment for the maize plants transcriptomics analysis. Furthermore, due to time constraints and the need for clearer phenotypes in tomato plants, the transcriptomic analysis was exclusively conducted on the maize model plant.

Long-term biotreatment tests have yielded highly promising results. Notably, treatments with *Vreelandella* sp. DE and *Idiomarina loihiensis* EA enhanced or maintained both plants' overall growth in saline conditions, which may be attributed to the preference of these strains for higher salinity levels [209]. Besides, the strains may be assisting the plants through various mechanisms, including the

secretion of bacterial exudates. Hence, a metabolomic analysis of the metabolites secreted by the candidate strains under saline conditions was conducted, to investigate the potential of these compounds to enhance plant growth under saline conditions. It was pertinent to test under saline environments because salinity affects bacterial metabolism [210], [211]. *Vreelandella* sp. DE and *Virgibacillus salarius* GC treatments exhibited similar effects on maize plants. Interestingly, some metabolites secreted in high amounts only by these two strains were reported to have beneficial effects on plants. For instance, trehalose and GABA were reported to enhance plant growth and salt-resilience through mediation of various physiological and molecular processes, such as regulation of osmotic potential, antioxidant systems, carbon and nitrogen metabolism, phytohormones, improvement of membrane integrity and nutrient uptake [212], [213], [214], [215], [216]. Additionally, the aminoacids alanine and serine presented a similar pattern, both are involved in the synthesis of several biomolecules, such as other aminoacids, nitrogen bases, phospholipids and sphingolipids, required for cell proliferation, which may be associated with a more robust stem in maize plants under stress [217], [218]. Moreover, these aminoacids have been associated with abiotic stresses, with alanine functioning as an osmoprotectant, as well as a precursor of antioxidants and other osmoprotectants [188], [219], [220]. Furthermore, substantially lower levels of secreted trehalose and GABA by *Virgibacillus salarius* GC in comparison with *Vreelandella* sp. DE may be connected with the inefficacy of *Virgibacillus salarius* GC treatment on tomato plants, suggesting that these metabolites are crucial for plant salt tolerance enhancement. Conversely, the strain *Idiomarina loihiensis* EA did not demonstrate the secretion of high levels of these metabolites. It apparently improves plants' salt-tolerance through the secretion of high concentrations of diverse aminoacids, such as phenylalanine, lysine and proline. These aminoacids have the capacity to increase the antioxidants levels and produce many molecules relevant for plant development and defence against salinity, such as osmoprotectants, of which proline is one of the most significant [221], [222], [223]. Additionally, *Vreelandella* sp. DE genomic analysis revealed an interesting set of functional genes related to PGPTs, including nutrient acquisition and solubilization, phytohormones production and salt-stress neutralization, such as osmoprotectants and antioxidants production. The presence of these genes may be associated with the biotreatment efficacy on plants [224]. Remarkably, the entire *suf* system was identified in *Vreelandella* sp. DE, which encodes for an Fe-S cluster and is crucial for nitrogenase biosynthesis, mainly under stress conditions [225], [226], thus suggesting a potential mechanism for nitrogen fixation under high salinity levels. This phenomenon is significant because salt stress typically inhibits nitrogenase biosynthesis, thereby reducing its activity. For instance, Tripathi and colleagues demonstrated that nitrogenase biosynthesis and activity in *Azospirillum brasilense* were completely inhibited by the presence of 350 mM NaCl [227]. Salinity stress is known to adversely affect nitrogen cycling, including nitrogen fixation, which consequently decreases nitrogen availability in soil [228]. Given this context, the capacity of *Vreelandella* sp. DE to perform nitrogen fixation under high salinity is highly relevant for enhancing crop growth in saline environments.

Nevertheless, the transcriptomics analysis provided further insights into the effects of salinity and *Vreelandella* sp. DE treatment on maize plants. Salinity led to a decrease in gene expression in mock treated maize plants, thus down-regulating genes encoding for ribosome formation, which plays a crucial role in translation processes, resulting in a decrease of proteins production [229]. Moreover, the expression of genes related to DNA replication was decreased, hampering cell division, hence leading to decreased tissue development, contributing to reduced SL and RL [230]. Additionally, the decreased expression of the gene LOC100282482 encoding for aspartate carbamoyltransferase 1 impedes the pyrimidine biosynthesis, which are nitrogen bases needed for nucleotide formation [231]. Conversely, expression of genes related to DNA replication was increased by salinity in plants treated with *Vreelandella* sp. DE, which may explain an enhanced growth of maize plants in the long-term biotreatment tests under saline over control conditions. However, early-stage tests demonstrated the opposite trend, suggesting that plants are still acclimating to the saline environment. Furthermore, salinity exhibited a diminishing of expression of genes related to IAA synthesis and influx in mock treated plants, which is a crucial growth phytohormone, also serving to explain a reduction in overall plant growth [232]. Moreover, enzymes involved in lignocellulose biosynthesis, such as cinnamyl-alcohol dehydrogenase and coniferyl-aldehyde dehydrogenase exhibited their genes expression LOC100216819 and *rf2f,* respectively, down-regulated resulting in a diminution of rigidity and strength in plant cell walls, which renders plants more vulnerable to salt-stress [233], [234]. Besides, genes encoding for asparagine synthase were up-regulated, suggesting that asparagine accumulation may function as a plant response to salt-stress by serving as a nitrogen reserve used for protein synthesis [235]. Additionally, the expression of genes encoding for enzymes involved in glutamic acid biosynthesis, such as aspartate and alanine transaminases were found up-regulated in *Vreelandella* sp. DE and both treatments, respectively. These

enzymes have similar functions and are important not only due to the glutamic acid synthesis, but also due to the balance of the C:N ratio through reversible reactions of ketoacids to aminoacids [236]. In addition, salinity effects on *Vreelandella* sp. DE treated plants led to enhanced expression of genes encoding for PEP carboxylase (*pep*7 and LOC100384708), an important enzyme in abiotic stress response by regulating root growth and stress markers, which may have a substantial impact on root development [237]. Furthermore, significant alterations in gene expression of mock set plants in comparison with *Vreelandella* sp. DE treated were identified in both control and salt-stress conditions. Notably, a substantial number of genes related to several photosynthesis processes and carbon fixation in photosynthetic organisms were up-regulated by *Vreelandella* sp. DE treatment under control conditions, although genes related specifically to the ferredoxin-4 were down-regulated, more studies about this protein function are needed to elucidate the causality of this event. Interestingly, many genes encoding for enzymes involved in sucrose metabolism were up-regulated by *Vreelandella* sp. DE treatment, highlighting the trehalose-6-phosphatase, that will convert trehalose-6-phosphate (T6P) into 2 molecules of trehalose. Reduction of T6P is important because it inhibits the sucrose non-fermenting 1-related protein kinase1 (SnRK1) complex that plays a crucial role in plant growth, mainly in root development. However, T6P is relevant for starch biosynthesis and other molecular functions. Hence, sucrose, a T6P precursor, levels are increased by sucrose-phosphate synthase and sucrose-6-phosphate phosphatase. Additionally, starch synthetase was up-regulated as well to mitigate the lower levels of T6P and higher levels of trehalose that breaks the starch molecules, which results in a dynamic metabolism more efficient in plant growth [238], [239], [240]. Remarkably, *Vreelandella* sp. DE treatment under salt-stress conditions demonstrated not only an up-regulation of gene associated with DNA replication as it enhanced several genes connected to base excision repair, but this is also a crucial process to prevent DNA lesions that are more frequent under stress conditions, thus enhancing plant growth and resilience as mentioned above [241]. Furthermore, genes involved in valine, leucine and isoleucine degradation were down-regulated, which demonstrates a better coping with salt-stress, given that during stress, aminoacids are consumed as alternative fuel sources for respiration [242]. Remarkably, genes encoding for several enzymes involved in plant enhancement under saline conditions were identified, such as S-adenosylmethionine synthetase through the production of polyamines (spermidine and spermine) that alleviate salinity stress [243]. Interestingly, ACC oxidase was upregulated in order to regulate the ethylene levels crucial to regulate the salt-stress effects on plants [244]. The cytochrome P450 also was reported to increase salt tolerance in plants [245]. Besides, indole-3-glycerol-phosphate lyase, indole-2-monooxygenase and 3-hydroxyindolin-2-one monooxygenase are associated with auxins biosynthesis, which are important for plant growth as previously mentioned [246], [247]. Furthermore, the upregulation of several stress-regulating and stress-supressing factors are contributing for a better coping with salinity by plants inoculated with *Vreelandella* sp. DE. Additionally, the increasing expression of various antioxidant enzymes are also associated with salt-stress mitigation, as well as the stress-response compounds up-regulation. Lastly, growth inducing and nutrient related factors led to an enhanced plant growth.

To combat the challenges posed by salinization, the adoption of sustainable and reliable approaches is necessary. A strategic use of locally available resources has the potential to greatly advance the development of novel bioformulations. These bioformulations would be designed to align more effectively with environmental conditions, employing a range of adaptive mechanisms. Given the intricacies of salt-stress, solutions must extend beyond simple growth promotion and incorporate more advanced, multifaceted strategies. Nevertheless, additional research is required in this field to support the development of bioformulations designed to surpass this stressing conditions. This may rely on the use of microbial consortia to improve bacterial performance [248], the evaluation of full-cycle responses in both plants and fruits, up-scale field trials with diverse crops and further investigation on the mechanisms underlying plant-microbe interactions. All these steps are essential to find a solution to overcome the major problem of soil salinization in agriculture.

5

CONCLUSIONS

Soil salinization has been a major issue for agricultural productivity, due to the substantial reduction in yield across several crops. This phenomenon implies the urgent need to find alternative solutions to mitigate soil salinity impacts on crops. Bioformulations could potentially be a sustainable and effective solution to achieve this goal. To do so, a total of 54 strains were isolated from saltpans/salt flats located in the Iberian Peninsula. However, soil biodiversity was notably low across samples, likely reflecting the impact of salinity on reducing microbial diversity. Furthermore, saline soils presented a higher abundance of halophile/halotolerant bacteria compared to gypsic soils. In order to have a more effective selection to develop a novel bioformulation, strains performance was assessed under saline stress conditions. On this purpose, ten candidate strains were selected for exhibiting the highest performance in one or more of the desirable traits. Remarkably, the strains *Vreelandella* sp. DE and *Idiomarina loihiensis* EA, which demonstrated the highest salt-affinity also demonstrated the highest number of desirable plant growth-promoting traits. Furthermore, metabolomics analysis revealed the presence of different strategies to overcome salinity stress, with *Vreelandella* sp. DE producing high levels of trehalose and *Idiomarina loihiensis* EA showing an elevated proline production. Besides, both strains demonstrated a high aminoacid content in their metabolism, which is linked with salt tolerance. Additionally, *Vreelandella* sp. DE contained in its genome a varied set of genes related to the tested plant growth-promoting traits, which helps explaining its high performance across the different tests. Moreover, the diverse biotreatments have relied on different strategies for plant enhancement, which resulted in varied phenotypical aspects. As expected, *Vreelandella* sp. DE and *Idiomarina loihiensis* EA treatments were the most effective enhancing crops growth under saline conditions. In maize, both *Vreelandella* sp. DE and *Idiomarina loihiensis* EA significantly enhanced growth, with shoot length increasing by 57% and 33%, respectively. Dry weight was notably higher, with *Vreelandella* sp. DE quadrupling and *Idiomarina loihiensis* EA doubling it. Photosystem II quantum yield was maintained in both treatments, indicating stable photosynthetic efficiency under saline conditions. Similarly, in tomato, both strains showed substantial growth improvements in shoot and root length, with *Vreelandella* sp. DE and *Idiomarina loihiensis* EA increasing the dry weight by 15- and 17-fold, respectively and were also capable of maintaining the photosystem II quantum yield. Hence, these results present promising perspectives for testing these biotreatments in full-cycle plant tests to evaluate the effects on crop productivity. Therefore, there is a need to better understand the mechanisms underlying plant-microbe interactions, to comprehend how the strains can aid crops in better coping with salt-stress. In this regard, omics approaches were conducted on both bacterial strains and plants, including genomics, metabolomics and transcriptomics. Furthermore, metabolomics exhibited the presence of several metabolites involved in stress-tolerance and with plant growth-promoting capabilities being produced and secreted by bacterial strains, as well as the use of alternative strategies among the candidate strains. For instance, *Idiomarina loihiensis* EA secreted a higher level of aminoacids comparing to other candidates, including proline, phenylalanine and lysine. Along with-it remarkable auxin production may be connected with both maize and tomato enhancement. Conversely, *Vreelandella* sp. DE secretes GABA, trehalose and some aminoacids, such as alanine and serine. These metabolites enhance plant growth and salt-resilience through mediation of various physiological and molecular processes, of which the cell proliferation as well as phospholipids and sphingolipids production may be associated with sturdier stems in maize plants under stress. Lastly, the transcriptomics analysis conducted has shown the influence of

Vreelandella sp. DE treatment in maize plants' gene expression, highlighting the overexpression of genes related to DNA replication and repair as well as osmoprotectants and auxins biosynthesis, antioxidants enzymes, growth-inducing and nutrient related factors, while reducing the expression of genes associated with stress, such as aminoacids consumption as alternative energy source. Upcoming trials might involve the preparation of consortia bioformulations, plant full-cycle biotreatment tests, field trials evaluating plant's productivity and fruits nutritional value using diverse crops to ensure the efficacy of these promising candidates. Additionally, comparative genomics between candidates may be valuable to identify potential molecular markers. Besides, metabolomics in plants treated with different biotreatments may encompass another strategy to better comprehend the bacterial influence on plants to mitigate salt-stress.

6

BIBLIOGRAPHY

[1] R. Bulgari, G. Franzoni, and A. Ferrante, 'Biostimulants application in horticultural crops under abiotic stress conditions', 2019, *MDPI AG*. doi: 10.3390/agronomy9060306.

[2] A. Gull, A. A. Lone, and N. U. I. Wani, 'Biotic and abiotic stresses in plants', *Abiotic and biotic stress in plants*, vol. 7, pp. 1–9, 2019.

[3] S. Sachdev, S. A. Ansari, M. I. Ansari, M. Fujita, and M. Hasanuzzaman, 'Abiotic stress and reactive oxygen species: Generation, signaling, and defense mechanisms', *Antioxidants*, vol. 10, no. 2, pp. 1–37, Feb. 2021, doi: 10.3390/antiox10020277.

[4] A. and A. M. M. and M.-R. and S. T. O. and A. P. Rasool Saiema and Hameed, 'Salt Stress: Causes, Types and Responses of Plants', in *Ecophysiology and Responses of Plants under Salt Stress*, M. M. and P. M. N. V Ahmad Parvaiz and Azooz, Ed., New York, NY: Springer New York, 2013, pp. 1–24. doi: 10.1007/978-1-4614-4747-4_1.

[5] K. Butcher, A. F. Wick, T. DeSutter, A. Chatterjee, and J. Harmon, 'Soil Salinity: A Threat to Global Food Security', *Agron J*, vol. 108, no. 6, pp. 2189–2200, 2016, doi: 10.2134/agronj2016.06.0368.

[6] G. Ondrasek *et al.*, 'Salt Stress in Plants and Mitigation Approaches', *Plants*, vol. 11, no. 6, Mar. 2022, doi: 10.3390/plants11060717.

[7] T. Song *et al.*, 'Metabolomic analysis of alfalfa (Medicago sativa L.) root-symbiotic rhizobia responses under alkali stress', *Front Plant Sci*, vol. 8, Jul. 2017, doi: 10.3389/fpls.2017.01208.

[8] S. S. Gill and N. Tuteja, 'Reactive oxygen species and antioxidant machinery in abiotic stress tolerance in crop plants', *Plant Physiology and Biochemistry*, vol. 48, no. 12, pp. 909–930, Dec. 2010, doi: 10.1016/j.plaphy.2010.08.016.

[9] G. Zhao *et al.*, 'Nitrate reductase-dependent nitric oxide is crucial for multi-walled carbon nanotube-induced plant tolerance against salinity', *Nanoscale*, vol. 11, no. 21, pp. 10511–10523, Jun. 2019, doi: 10.1039/c8nr10514f.

[10] S. Zhao, Q. Zhang, M. Liu, H. Zhou, C. Ma, and P. Wang, 'Regulation of plant responses to salt stress', *Int J Mol Sci*, vol. 22, no. 9, May 2021, doi: 10.3390/ijms22094609.

[11] P. Ahmad, M. M. Azooz, and M. N. V Prasad, *Salt stress in plants*, vol. 10. Springer, 2013. doi: 10.1007/978-1-4614-6108-1.

[12] P. Shrivastava and R. Kumar, 'Soil salinity: A serious environmental issue and plant growth promoting bacteria as one of the tools for its alleviation', *Saudi J Biol Sci*, vol. 22, no. 2, pp. 123–131, Mar. 2015, doi: 10.1016/j.sjbs.2014.12.001.

[13] M. Qadir *et al.*, 'Economics of salt-induced land degradation and restoration', *Nat Resour Forum*, vol. 38, no. 4, pp. 282–295, Nov. 2014, doi: 10.1111/1477-8947.12054.

[14] F. FAO, 'The future of food and agriculture: alternative pathways to 2050', *Food and Agriculture Organization of the United Nations Rome*, p. 228, 2018.

[15] A. Tomaz, P. Palma, P. Alvarenga, and M. C. Gonçalves, 'Chapter 13 - Soil salinity risk in a climate change scenario and its effect on crop yield', in *Climate Change and Soil Interactions*, M. N. V. Prasad and M. Pietrzykowski, Eds., Elsevier, 2020, pp. 351–396. doi: 10.1016/B978-0-12-818032-7.00013-8.

[16] B. Okur and N. Örçen, ‘Chapter 12 - Soil salinization and climate change’, in *Climate Change and Soil Interactions*, M. N. V. Prasad and M. Pietrzykowski, Eds., Elsevier, 2020, pp. 331–350. doi: 10.1016/B978-0-12-818032-7.00012-6.
[17] L. A. Richards, *Diagnosis and improvement of saline and alkali soils*, no. 60. US Government Printing Office, 1954.
[18] K. Negacz, Ž. Malek, A. de Vos, and P. Vellinga, ‘Saline soils worldwide: Identifying the most promising areas for saline agriculture’, *J Arid Environ*, vol. 203, Aug. 2022, doi: 10.1016/j.jaridenv.2022.104775.
[19] I. N. Daliakopoulos *et al.*, ‘The threat of soil salinity: A European scale review’, *Science of the Total Environment*, vol. 573, pp. 727–739, Dec. 2016, doi: 10.1016/j.scitotenv.2016.08.177.
[20] T. Gil *et al.*, ‘Isolation and Characterization of Culturable Osmotolerant Microbiota in Hypersaline and Hypergypsic Soils as New Treatment for Osmotic Stress in Plants’, *Soil Syst*, vol. 7, no. 4, Dec. 2023, doi: 10.3390/soilsystems7040086.
[21] T. B. Ramos *et al.*, ‘Soil salinity assessment using vegetation indices derived from Sentinel-2 multispectral data. application to Lezíria Grande, Portugal’, *Agric Water Manag*, vol. 241, Nov. 2020, doi: 10.1016/j.agwat.2020.106387.
[22] A. J. Alvim and J. C. Martins, ‘Diagnóstico do estádio evolutivo de alguns solos salinos da Lezíria Grande de VF de Xira e sugestões para o melhoramento da sua utilização’, *Pedologia, Oeiras*, vol. 23, no. 2, pp. 1–43, 1988.
[23] ABLGVFX - Associação de Beneficiários da Lezíria Grande de Vila Franca de Xira, ‘Agriculture’, ABLGVFX - Associação de Beneficiários da Lezíria Grande de Vila Franca de Xira. [Online]. Available: https://www.ablgvfx.pt/agricultura.php
[24] C. M. Grieve, S. R. Grattan, and E. V. Maas, ‘Plant Salt Tolerance’, in *Agricultural Salinity Assessment and Management*, 2nd ed., W. W. Wallender and K. K. Tanji, Eds., Reston, VA: ASCE, 2012, ch. 13, pp. 405–459.
[25] N. Katerji, J. W. Van Hoorn, A. Hamdy, and M. Mastrorilli, ‘Salt tolerance classification of crops according to soil salinity and to water stress day index’, *Agric Water Manag*, vol. 43, pp. 99–109, Feb. 2000, doi: 10.1016/s0378-3774(99)00048-7.
[26] T. Su *et al.*, ‘Autophagy: An Intracellular Degradation Pathway Regulating Plant Survival and Stress Response’, *Front Plant Sci*, vol. 11, Feb. 2020, doi: 10.3389/fpls.2020.00164.
[27] S. Shabala, ‘Learning from halophytes: Physiological basis and strategies to improve abiotic stress tolerance in crops’, *Ann Bot*, vol. 112, no. 7, pp. 1209–1221, Nov. 2013, doi: 10.1093/aob/mct205.
[28] T. Horie, I. Karahara, and M. Katsuhara, ‘Salinity tolerance mechanisms in glycophytes: An overview with the central focus on rice plants’, *Rice*, vol. 5, no. 1, 2012, doi: 10.1186/1939-8433-5-11.
[29] Y. Himabindu, T. Chakradhar, M. C. Reddy, A. Kanygin, K. E. Redding, and T. Chandrasekhar, ‘Salt-tolerant genes from halophytes are potential key players of salt tolerance in glycophytes’, *Environ Exp Bot*, vol. 124, pp. 39–63, Apr. 2016, doi: 10.1016/j.envexpbot.2015.11.010.
[30] M. Ashraf, ‘Tolerance of some potential forage grasses from arid regions of Pakistan to salinity and drought’, in *Biosaline Agriculture and Salinity Tolerance in Plants*, M. Öztürk, Y. Waisel, M. A. Khan, and G. Görk, Eds., Basel: Birkhäuser Basel, 2006, pp. 15–27.
[31] C. Forni, D. Duca, and B. R. Glick, ‘Mechanisms of plant response to salt and drought stress and their alteration by rhizobacteria’, *Plant Soil*, vol. 410, no. 1–2, pp. 335–356, Jan. 2017, doi: 10.1007/s11104-016-3007-x.
[32] R. Pushpavalli, J. D. Berger, N. C. Turner, K. H. M. Siddique, T. D. Colmer, and V. Vadez, ‘Cross-tolerance for drought, heat and salinity stresses in chickpea (Cicer arietinum L.)’, *J Agron Crop Sci*, vol. 206, no. 3, pp. 405–419, Jun. 2020, doi: 10.1111/jac.12393.
[33] M. Khataar, M. H. Mohhamadi, and F. Shabani, ‘Soil salinity and matric potential interaction on water use, water use efficiency and yield response factor of bean and wheat’, *Sci Rep*, vol. 8, no. 1, Dec. 2018, doi: 10.1038/s41598-018-20968-z.
[34] F. M. Howari, P. C. Goodell, and S. Miyamoto, ‘Spectral Properties of Salt Crusts Formed on Saline Soils’, *J Environ Qual*, vol. 31, no. 5, pp. 1453–1461, Sep. 2002, doi: 10.2134/jeq2002.1453.
[35] E. Van Zelm, Y. Zhang, and C. Testerink, ‘Salt Tolerance Mechanisms of Plants’, *Annu Rev Plant Biol*, vol. 71, no. 1, pp. 403–433, Mar. 2020, doi: 10.1146/annurev-arplant-050718.
[36] J. Shumilina *et al.*, ‘Glycation of plant proteins: Regulatory roles and interplay with sugar signalling?’, *Int J Mol Sci*, vol. 20, no. 9, May 2019, doi: 10.3390/ijms20092366.

[37] R. Munns and M. Tester, ‘Mechanisms of salinity tolerance’, *Annu Rev Plant Biol*, vol. 59, pp. 651–681, 2008, doi: 10.1146/annurev.arplant.59.032607.092911.
[38] A. Gupta *et al.*, ‘Mechanistic Insights of Plant Growth Promoting Bacteria Mediated Drought and Salt Stress Tolerance in Plants for Sustainable Agriculture’, *Int J Mol Sci*, vol. 23, no. 7, Apr. 2022, doi: 10.3390/ijms23073741.
[39] N. S. Muchate, G. C. Nikalje, N. S. Rajurkar, P. Suprasanna, and T. D. Nikam, ‘Plant Salt Stress: Adaptive Responses, Tolerance Mechanism and Bioengineering for Salt Tolerance’, *Botanical Review*, vol. 82, no. 4, pp. 371–406, Dec. 2016, doi: 10.1007/s12229-016-9173-y.
[40] J. M. Cheeseman, ‘The evolution of halophytes, glycophytes and crops, and its implications for food security under saline conditions’, *New Phytologist*, vol. 206, no. 2, pp. 557–570, Apr. 2015, doi: 10.1111/nph.13217.
[41] J. Mammadov, R. Buyyarapu, S. K. Guttikonda, K. Parliament, I. Y. Abdurakhmonov, and S. P. Kumpatla, ‘Wild relatives of maize, rice, cotton, and soybean: Treasure troves for tolerance to biotic and abiotic stresses’, *Front Plant Sci*, vol. 9, Jun. 2018, doi: 10.3389/fpls.2018.00886.
[42] W. Sun *et al.*, ‘Comparative transcriptomic profiling of a salt-tolerant wild tomato species and a salt-sensitive tomato cultivar’, *Plant Cell Physiol*, vol. 51, no. 6, pp. 997–1006, Jun. 2010, doi: 10.1093/pcp/pcq056.
[43] H. Singh, P. Kumar, A. Kumar, M. C. Kyriacou, G. Colla, and Y. Rouphael, ‘Grafting tomato as a tool to improve salt tolerance’, *Agronomy*, vol. 10, no. 2, Feb. 2020, doi: 10.3390/agronomy10020263.
[44] M. Kordrostami and B. Rabiei, ‘Salinity Stress Tolerance in Plants: Physiological, Molecular, and Biotechnological Approaches’, in *Plant Abiotic Stress Tolerance: Agronomic, Molecular and Biotechnological Approaches*, M. Hasanuzzaman, K. R. Hakeem, K. Nahar, and H. F. Alharby, Eds., Cham: Springer International Publishing, 2019, pp. 101–127. doi: 10.1007/978-3-030-06118-0_4.
[45] M. S. Afridi *et al.*, ‘Biotechnological approaches in agriculture and environmental management - bacterium Kocuria rhizophila 14ASP as heavy metal and salt- tolerant plant growth- promoting strain’, doi: 10.1007/s11756-021-00826-6/Published.
[46] V. Poria *et al.*, ‘Plant Growth-Promoting Bacteria (PGPB) integrated phytotechnology: A sustainable approach for remediation of marginal lands’, *Front Plant Sci*, vol. 13, Oct. 2022, doi: 10.3389/fpls.2022.999866.
[47] K. K. Bhise and P. B. Dandge, ‘Mitigation of salinity stress in plants using plant growth promoting bacteria’, *Symbiosis*, vol. 79, no. 3, pp. 191–204, Nov. 2019, doi: 10.1007/s13199-019-00638-y.
[48] M. Numan *et al.*, ‘Plant growth promoting bacteria as an alternative strategy for salt tolerance in plants: A review’, *Microbiol Res*, vol. 209, pp. 21–32, Apr. 2018, doi: 10.1016/j.micres.2018.02.003.
[49] Y. Gao, H. Zou, B. Wang, and F. Yuan, ‘Progress and Applications of Plant Growth-Promoting Bacteria in Salt Tolerance of Crops’, *Int J Mol Sci*, vol. 23, no. 13, Jul. 2022, doi: 10.3390/ijms23137036.
[50] H. Q. Li and X. W. Jiang, ‘Inoculation with plant growth-promoting bacteria (PGPB) improves salt tolerance of maize seedling’, *Russian Journal of Plant Physiology*, vol. 64, no. 2, pp. 235–241, Mar. 2017, doi: 10.1134/S1021443717020078.
[51] P. Sánchez *et al.*, ‘The synergy of halotolerant PGPB and mauran mitigates salt stress in tomato (Solanum lycopersicum) via osmoprotectants accumulation’, *Physiol Plant*, vol. 175, no. 6, p. e14111, Nov. 2023, doi: 10.1111/ppl.14111.
[52] L. Rajput, A. Imran, F. Mubeen, and F. Y. Hafeez, ‘SALT-TOLERANT PGPR STRAIN PLANOCOCCUS RIFIETOENSIS PROMOTES THE GROWTH AND YIELD OF WHEAT (TRITICUM AESTIVUM L.) CULTIVATED IN SALINE SOIL’, *Pak. J. Bot*, vol. 45, no. 6, pp. 1955–1962, 2013.
[53] Y. Pii, T. Mimmo, N. Tomasi, R. Terzano, S. Cesco, and C. Crecchio, ‘Microbial interactions in the rhizosphere: beneficial influences of plant growth-promoting rhizobacteria on nutrient acquisition process. A review’, *Biol Fertil Soils*, vol. 51, no. 4, pp. 403–415, May 2015, doi: 10.1007/s00374-015-0996-1.
[54] M. Y. Alzate Zuluaga *et al.*, ‘Can Inoculation With the Bacterial Biostimulant Enterobacter sp. Strain 15S Be an Approach for the Smarter P Fertilization of Maize and Cucumber Plants?’, *Front Plant Sci*, vol. 12, Aug. 2021, doi: 10.3389/fpls.2021.719873.
[55] P. Chang *et al.*, ‘Plant Growth-Promoting Bacteria Facilitate the Growth of Barley and Oats in Salt-Impacted Soil: Implications for Phytoremediation of Saline Soils’, *Int J Phytoremediation*, vol. 16, no. 11, pp. 1133–1147, Nov. 2014, doi: 10.1080/15226514.2013.821447.

[56] Y. Pii *et al.*, 'Modulation of Fe acquisition process by Azospirillum brasilense in cucumber plants', *Environ Exp Bot*, vol. 130, pp. 216–225, 2016, doi: 10.1016/j.envexpbot.2016.06.011.
[57] B. R. Glick', Z. Cheng', J. Czarny', and J. Duan, 'Promotion of plant growth by ACC deaminase-producing soil bacteria', in *New Perspectives and Approaches in Plant Growth-Promoting Rhizobacteria Research*, Springer eBooks, 2007, pp. 329–339. doi: 10.1007/978-1-4020-6776-1_8.
[58] A. H. Naing, T. T. Maung, and C. K. Kim, 'The ACC deaminase-producing plant growth-promoting bacteria: Influences of bacterial strains and ACC deaminase activities in plant tolerance to abiotic stress', *Physiol Plant*, vol. 173, no. 4, pp. 1992–2012, Dec. 2021, doi: 10.1111/ppl.13545.
[59] R. Çakmakçı, G. Mosber, A. H. Milton, F. Alatürk, and B. Ali, 'The Effect of Auxin and Auxin-Producing Bacteria on the Growth, Essential Oil Yield, and Composition in Medicinal and Aromatic Plants', *Curr Microbiol*, vol. 77, no. 4, pp. 564–577, Apr. 2020, doi: 10.1007/s00284-020-01917-4.
[60] Y. Li, M. Narayanan, X. Shi, X. Chen, Z. Li, and Y. Ma, 'Biofilms formation in plant growth-promoting bacteria for alleviating agro-environmental stress', *Science of the Total Environment*, vol. 907, Jan. 2024, doi: 10.1016/j.scitotenv.2023.167774.
[61] N. Ajijah, A. Fiodor, A. K. Pandey, A. Rana, and K. Pranaw, 'Plant Growth-Promoting Bacteria (PGPB) with Biofilm-Forming Ability: A Multifaceted Agent for Sustainable Agriculture', *Diversity (Basel)*, vol. 15, no. 1, Jan. 2023, doi: 10.3390/d15010112.
[62] W. A. Kasim, R. M. Gaafar, R. M. Abou-Ali, M. N. Omar, and H. M. Hewait, 'Effect of biofilm forming plant growth promoting rhizobacteria on salinity tolerance in barley', *Annals of Agricultural Sciences*, vol. 61, no. 2, pp. 217–227, Dec. 2016, doi: 10.1016/j.aoas.2016.07.003.
[63] M. M. Haque *et al.*, 'Halotolerant biofilm-producing rhizobacteria mitigate seawater-induced salt stress and promote growth of tomato', *Sci Rep*, vol. 12, no. 1, Dec. 2022, doi: 10.1038/s41598-022-09519-9.
[64] H.-C. Flemming, J. Wingender, U. Szewzyk, P. Steinberg, S. A. Rice, and S. Kjelleberg, 'Biofilms: an emergent form of bacterial life', *Nat Rev Microbiol*, vol. 14, no. 9, pp. 563–575, 2016, doi: 10.1038/nrmicro.2016.94.
[65] M. A. Khan *et al.*, 'Halotolerant bacteria mitigate the effects of salinity stress on soybean growth by regulating secondary metabolites and molecular responses', *BMC Plant Biol*, vol. 21, no. 1, Dec. 2021, doi: 10.1186/s12870-021-02937-3.
[66] A. de A. Santos, J. A. G. da Silveira, A. Bonifacio, A. C. Rodrigues, and M. do V. B. Figueiredo, 'Antioxidant response of cowpea co-inoculated with plant growth-promoting bacteria under salt stress', *Brazilian Journal of Microbiology*, vol. 49, no. 3, pp. 513–521, Jul. 2018, doi: 10.1016/j.bjm.2017.12.003.
[67] D. Y. Sharavin, 'CROP PRODUCTION HALOTOLERANT PHOSPHATE SOLUBILIZING IAA-SYNTHESIZING REPRESENTATIVES OF PANTOEA GENUS PROMOTE PROLINE SYNTHESIS IN WHEAT SEEDLINGS UNDER SALT STRESS', *Journal of Agriculture and Environment*, vol. 2, no. 18, p. 2021, doi: 10.23649/jae.2021.2.18.3.
[68] M. Neshat, A. Abbasi, A. Hosseinzadeh, M. R. Sarikhani, D. Dadashi Chavan, and A. Rasoulnia, 'Plant growth promoting bacteria (PGPR) induce antioxidant tolerance against salinity stress through biochemical and physiological mechanisms', *Physiology and Molecular Biology of Plants*, vol. 28, no. 2, pp. 347–361, Feb. 2022, doi: 10.1007/s12298-022-01128-0.
[69] M. Singh, 'Proline and Salinity Tolerance in Plants', *Biochem Pharmacol (Los Angel)*, vol. 03, no. 06, 2014, doi: 10.4172/2167-0501.1000e170.
[70] Kaur G and B. Ns, 'Modulation of proline metabolism under drought and salt stress conditions in wheat seedlings', *Indian J Biochem Biophys*, vol. 55, pp. 114–124, 2018.
[71] G. Santoyo, J. M. Sánchez-Yáñez, and S. de los Santos-Villalobos, 'Methods for Detecting Biocontrol and Plant Growth-Promoting Traits in Rhizobacteria', in *Methods in Rhizosphere Biology Research*, D. Reinhardt and A. K. Sharma, Eds., Singapore: Springer Singapore, 2019, pp. 133–149. doi: 10.1007/978-981-13-5767-1_8.
[72] A. F. Scavino and R. O. Pedraza, 'The Role of Siderophores in Plant Growth-Promoting Bacteria', in *Bacteria in Agrobiology: Crop Productivity*, D. K. Maheshwari, M. Saraf, and A. Aeron, Eds., Berlin, Heidelberg: Springer Berlin Heidelberg, 2013, pp. 265–285. doi: 10.1007/978-3-642-37241-4_11.
[73] J. Fukami, P. Cerezini, and M. Hungria, 'Azospirillum: benefits that go far beyond biological nitrogen fixation', *AMB Express*, vol. 8, no. 1, Dec. 2018, doi: 10.1186/s13568-018-0608-1.

[74] N. A. Di Benedetto *et al.*, 'The role of plant growth promoting bacteria in improving nitrogen use efficiency for sustainable crop production: A focus on wheat', *AIMS Microbiol*, vol. 3, no. 3, pp. 413–434, 2017, doi: 10.3934/microbiol.2017.3.413.
[75] E. Wickert, J. Marcondes, M. V. Lemos, and E. G. M. Lemos, 'Nitrogen assimilation in Citrus based on CitEST data mining', *Genet Mol Biol*, vol. 30, pp. 810–818, Jan. 2007, doi: 10.1590/S1415-47572007000500009.
[76] Y. F. Wang and J. D. Gu, 'Effects of allylthiourea, salinity, and pH on ammonia/ammonium-oxidizing prokaryotes in mangrove sediment incubated in laboratory microcosms', *Appl Microbiol Biotechnol*, vol. 98, no. 7, pp. 3257–3274, 2014, doi: 10.1007/s00253-013-5399-3.
[77] E. T. Alori, B. R. Glick, and O. O. Babalola, 'Microbial phosphorus solubilization and its potential for use in sustainable agriculture', *Front Microbiol*, vol. 8, Jun. 2017, doi: 10.3389/fmicb.2017.00971.
[78] M. Billah, M. Khan, A. Bano, T. U. Hassan, A. Munir, and A. R. Gurmani, 'Phosphorus and phosphate solubilizing bacteria: Keys for sustainable agriculture', *Geomicrobiol J*, vol. 36, no. 10, pp. 904–916, Nov. 2019, doi: 10.1080/01490451.2019.1654043.
[79] M. Ahmad, S. M. Nadeem, M. Naveed, and Z. A. Zahir, 'Potassium-Solubilizing Bacteria and Their Application in Agriculture', in *Potassium Solubilizing Microorganisms for Sustainable Agriculture*, V. S. Meena, B. R. Maurya, J. P. Verma, and R. S. Meena, Eds., New Delhi: Springer India, 2016, pp. 293–313. doi: 10.1007/978-81-322-2776-2_21.
[80] E. Bakhshandeh, H. Pirdashti, and K. S. Lendeh, 'Phosphate and potassium-solubilizing bacteria effect on the growth of rice', *Ecol Eng*, vol. 103, pp. 164–169, Jun. 2017, doi: 10.1016/j.ecoleng.2017.03.008.
[81] N. Joshi, R. Gothalwal, M. Singh, and K. Dave, 'Novel sulphur-oxidizing bacteria consummate sulphur deficiency in oil seed crop', *Arch Microbiol*, vol. 203, no. 1, Jan. 2021, doi: 10.1007/s00203-020-02009-4.
[82] V. Rajagopal and P. Ramakrishnan, 'Sulphur Oxidizing Bacteria and Pulse Nutrition-A Review', *World Journal of Agricultural Sciences*, vol. 5, no. 3, pp. 270–278, 2009.
[83] P. K. Hepler, 'Calcium: A Central Regulator of Plant Growth and Development', *Plant Cell*, vol. 17, no. 8, pp. 2142–2155, Aug. 2005, doi: 10.1105/tpc.105.032508.
[84] J. Bañuls and E. Primo-Millo, 'Salinity-calcium interactions on growth and ionic concentration of Citrus plants', *Plant Soil*, vol. 133, pp. 39–46, May 1991, doi: 10.1007/BF00011897.
[85] A. Ijaz *et al.*, 'Insights Into Manganese Solubilizing Bacillus spp. for Improving Plant Growth and Manganese Uptake in Maize', *Front Plant Sci*, vol. 12, Nov. 2021, doi: 10.3389/fpls.2021.719504.
[86] S. B. Schmidt and S. Husted, 'The biochemical properties of manganese in plants', *Plants*, vol. 8, no. 10, Oct. 2019, doi: 10.3390/plants8100381.
[87] A. Ventosa, J. Joaqui´, J. J. Nieto, and A. Oren, 'Biology of Moderately Halophilic Aerobic Bacteria', *MICROBIOLOGY AND MOLECULAR BIOLOGY REVIEWS*, vol. 62, no. 2, pp. 504–544, 1998, doi: 10.1128/mmbr.62.2.504-544.1998.
[88] H. Etesami and G. A. Beattie, 'Mining halophytes for plant growth-promoting halotolerant bacteria to enhance the salinity tolerance of non-halophytic crops', *Front Microbiol*, vol. 9, no. FEB, Feb. 2018, doi: 10.3389/fmicb.2018.00148.
[89] C. Petrillo *et al.*, 'Genomic and Physiological Characterization of Bacilli Isolated From Salt-Pans With Plant Growth Promoting Features', *Front Microbiol*, vol. 12, Sep. 2021, doi: 10.3389/fmicb.2021.715678.
[90] J. Pérez-Inocencio, G. Iturriaga, C. L. Aguirre-Mancilla, M. S. Vásquez-Murrieta, M. A. Lastiri-Hernández, and D. Álvarez-Bernal, 'Reduction in Salt Stress Due to the Action of Halophilic Bacteria That Promote Plant Growth in Solanum lycopersicum', *Microorganisms*, vol. 11, no. 11, Nov. 2023, doi: 10.3390/microorganisms11112625.
[91] S. Navarro-Torre *et al.*, 'Sustainable agricultural management of saline soils in arid and semi-arid Mediterranean regions through halophytes, microbial and soil-based technologies', *Environ Exp Bot*, vol. 212, Aug. 2023, doi: 10.1016/j.envexpbot.2023.105397.
[92] A. Mauceri *et al.*, 'Integrated omics approach reveals the molecular pathways activated in tomato by Kocuria rhizophila, a soil plant growth-promoting bacterium', *Plant Physiology and Biochemistry*, vol. 210, May 2024, doi: 10.1016/j.plaphy.2024.108609.
[93] K. K. Meena *et al.*, 'Abiotic stress responses and microbe-mediated mitigation in plants: The omics strategies', *Front Plant Sci*, vol. 8, Feb. 2017, doi: 10.3389/fpls.2017.00172.

[94] R. M. Shelake, D. Pramanik, and J. Y. Kim, 'Exploration of plant-microbe interactions for sustainable agriculture in CRISPR era', *Microorganisms*, vol. 7, no. 8, Aug. 2019, doi: 10.3390/microorganisms7080269.
[95] S. M. Zamanzadeh-Nasrabadi, F. Mohammadiapanah, M. Hosseini-Mazinani, and S. Sarikhan, 'Salinity stress endurance of the plants with the aid of bacterial genes', *Front Genet*, vol. 14, 2023, doi: 10.3389/fgene.2023.1049608.
[96] I. Mellidou *et al.*, 'Comparative Transcriptomics and Metabolomics Reveal an Intricate Priming Mechanism Involved in PGPR-Mediated Salt Tolerance in Tomato', *Front Plant Sci*, vol. 12, Aug. 2021, doi: 10.3389/fpls.2021.713984.
[97] G. Dif *et al.*, 'Performance of halotolerant bacteria associated with Sahara-inhabiting halophytes Atriplex halimus L. and Lygeum spartum L. ameliorate tomato plant growth and tolerance to saline stress: from selective isolation to genomic analysis of potential determinants', *World J Microbiol Biotechnol*, vol. 38, no. 1, Jan. 2022, doi: 10.1007/s11274-021-03203-2.
[98] M. Y. Alzate Zuluaga *et al.*, 'The adaptive metabolomic profile and functional activity of tomato rhizosphere are revealed upon PGPB inoculation under saline stress', *Environ Exp Bot*, vol. 189, Sep. 2021, doi: 10.1016/j.envexpbot.2021.104552.
[99] A. Kumar, S. Singh, A. K. Gaurav, S. Srivastava, and J. P. Verma, 'Plant Growth-Promoting Bacteria: Biological Tools for the Mitigation of Salinity Stress in Plants', *Front Microbiol*, vol. 11, Jul. 2020, doi: 10.3389/fmicb.2020.01216.
[100] Z. Degon *et al.*, 'Azospirillum brasilense improves rice growth under salt stress by regulating the expression of key genes involved in salt stress response, abscisic acid signaling, and nutrient transport, among others', *Frontiers in Agronomy*, vol. 5, 2023, doi: 10.3389/fagro.2023.1216503.
[101] B. Wicke *et al.*, 'The global technical and economic potential of bioenergy from salt-affected soils', *Energy Environ Sci*, vol. 4, no. 8, pp. 2669–2681, 2011, doi: 10.1039/C1EE01029H.
[102] J. Sánchez, M. D. Curt, and J. Fernández, 'Approach to the potential production of giant reed in surplus saline lands of Spain', *GCB Bioenergy*, vol. 9, no. 1, pp. 105–118, Jan. 2017, doi: 10.1111/gcbb.12329.
[103] M. Niza-Costa, A. S. Rodríguez-dos Santos, I. Rebelo-Romão, M. V. Ferrer, C. Sequero López, and J. I. Vílchez, 'Geographically Disperse, Culturable Seed-Associated Microbiota in Forage Plants of Alfalfa (Medicago sativa L.) and Pitch Clover (Bituminaria bituminosa L.): Characterization of Beneficial Inherited Strains as Plant Stress-Tolerance Enhancers', *Biology (Basel)*, vol. 11, no. 12, Dec. 2022, doi: 10.3390/biology11121838.
[104] A. Ambrosini and L. M. P. Passaglia, 'Plant Growth–Promoting Bacteria (PGPB): Isolation and Screening of PGP Activities', *Curr Protoc Plant Biol*, vol. 2, no. 3, pp. 190–209, Sep. 2017, doi: 10.1002/pb.20054.
[105] B. M. Coffey and G. G. Anderson, 'Biofilm Formation in the 96-Well Microtiter Plate', 2014, pp. 631–641. doi: 10.1007/978-1-4939-0473-0_48.
[106] Mu'minah, Baharuddin, H. Subair, and Fahruddin, 'Isolation and Screening Bacterial Exopolysaccharide (EPS) from Potato Rhizosphere in Highland and the Potential as a Producer Indole Acetic Acid (IAA)', *Procedia Food Sci*, vol. 3, pp. 74–81, 2015, doi: 10.1016/j.profoo.2015.01.007.
[107] T. Takao, F. Kitatani, N. Watanabe, A. Yagi, and K. Sakata, 'A Simple Screening Method for Antioxidants and Isolation of Several Antioxidants Produced by Marine Bacteria from Fish and Shellfish', *Biosci Biotechnol Biochem*, vol. 58, no. 10, pp. 1780–1783, 1994, doi: 10.1271/bbb.58.1780.
[108] G. Goswami *et al.*, 'Proline confers acid stress tolerance to Bacillus megaterium G18', *Sci Rep*, vol. 12, no. 1, Dec. 2022, doi: 10.1038/s41598-022-12709-0.
[109] N. K. Arora and M. Verma, 'Modified microplate method for rapid and efficient estimation of siderophore produced by bacteria', *3 Biotech*, vol. 7, no. 6, Dec. 2017, doi: 10.1007/s13205-017-1008-y.
[110] T. Sulistiyani, S. Meliah, and T. R. Sulistiyani, 'Isolation and Characterization of Nitrogen Fixing Endophytic Bacteria Associated with Sweet Sorghum (Sorghum bicolor)', in *The SATREPS Conference*, Nov. 2017, pp. 110–117.
[111] B. X. Zheng *et al.*, 'Identification and characterization of inorganic-phosphate-solubilizing bacteria from agricultural fields with a rapid isolation method', *AMB Express*, vol. 8, no. 1, Dec. 2018, doi: 10.1186/s13568-018-0575-6.

[112] M. V. S. RAJAWAT, S. SINGH, S. P. TYAGI, and A. K. SAXENA, 'A Modified Plate Assay for Rapid Screening of Potassium-Solubilizing Bacteria', Oct. 01, 2016, *Institute of Soil Science*. doi: 10.1016/S1002-0160(15)60080-7.
[113] M. Y. Hidayat, H. M. Saud, and A. A. Samsudin, 'Isolation and characterisation of sulphur oxidizing bacteria isolated from hot spring in Malaysia for biological deodorisation of hydrogen sulphide in chicken Manure', *Media Peternakan Fakultas Peternakan Institut Pertanian Bogor*, vol. 40, no. 3, pp. 178–187, 2017, doi: 10.5398/medpet.2017.40.3.178.
[114] S. M. Tamilselvi, C. Thiyagarajan, and S. Uthandi, 'Calcite dissolution by brevibacterium sp. SOTI06: A futuristic approach for the reclamation of calcareous sodic soils', *Front Plant Sci*, vol. 7, no. DECEMBER2016, Dec. 2016, doi: 10.3389/fpls.2016.01828.
[115] T. Gil *et al.*, 'Comparing native and non-native seed-isolated strains for drought resilience in maize (Zea mays L.)', *Plant Stress*, vol. 12, Jun. 2024, doi: 10.1016/j.stress.2024.100462.
[116] V. J. Ignacio, Y. Yang, D. Yi, and H. Zhang, 'Measurements of root colonized bacteria species', *Bio Protoc*, vol. 11, no. 7, Apr. 2021, doi: 10.21769/BioProtoc.3976.
[117] C. A. Schneider, W. S. Rasband, and K. W. Eliceiri, 'NIH Image to ImageJ: 25 years of image analysis', *Nat Methods*, vol. 9, no. 7, pp. 671–675, 2012, doi: 10.1038/nmeth.2089.
[118] M. Kolmogorov, J. Yuan, Y. Lin, and P. A. Pevzner, 'Assembly of long, error-prone reads using repeat graphs', *Nat Biotechnol*, vol. 37, no. 5, pp. 540–546, May 2019, doi: 10.1038/s41587-019-0072-8.
[119] B. J. Walker *et al.*, 'Pilon: An integrated tool for comprehensive microbial variant detection and genome assembly improvement', *PLoS One*, vol. 9, no. 11, Nov. 2014, doi: 10.1371/journal.pone.0112963.
[120] B. Langmead and S. L. Salzberg, 'Fast gapped-read alignment with Bowtie 2', *Nat Methods*, vol. 9, no. 4, pp. 357–359, Apr. 2012, doi: 10.1038/nmeth.1923.
[121] A. Gurevich, V. Saveliev, N. Vyahhi, and G. Tesler, 'QUAST: Quality assessment tool for genome assemblies', *Bioinformatics*, vol. 29, no. 8, pp. 1072–1075, Apr. 2013, doi: 10.1093/bioinformatics/btt086.
[122] D. H. Parks, M. Imelfort, C. T. Skennerton, P. Hugenholtz, and G. W. Tyson, 'CheckM: Assessing the quality of microbial genomes recovered from isolates, single cells, and metagenomes', *Genome Res*, vol. 25, no. 7, pp. 1043–1055, Jul. 2015, doi: 10.1101/gr.186072.114.
[123] M. Seppey, M. Manni, and E. M. Zdobnov, 'BUSCO: Assessing genome assembly and annotation completeness', in *Methods in Molecular Biology*, vol. 1962, Humana Press Inc., 2019, pp. 227–245. doi: 10.1007/978-1-4939-9173-0_14.
[124] T. Seemann, 'Prokka: Rapid prokaryotic genome annotation', *Bioinformatics*, vol. 30, no. 14, pp. 2068–2069, Jul. 2014, doi: 10.1093/bioinformatics/btu153.
[125] J. P. Meier-Kolthoff and M. Göker, 'TYGS is an automated high-throughput platform for state-of-the-art genome-based taxonomy', *Nat Commun*, vol. 10, no. 1, Dec. 2019, doi: 10.1038/s41467-019-10210-3.
[126] B. Buchfink, C. Xie, and D. H. Huson, 'Fast and sensitive protein alignment using DIAMOND', *Nat Methods*, vol. 12, no. 1, pp. 59–60, Jan. 2014, doi: 10.1038/nmeth.3176.
[127] S. Patz, A. Gautam, M. Becker, S. Ruppel, P. Rodríguez-Palenzuela, and D. H. Huson, 'PLaBAse: A comprehensive web resource for analyzing the plant growth-promoting potential of plant-associated bacteria', *bioRxiv*, Dec. 2021, doi: 10.1101/2021.12.13.472471.
[128] J. Kopka, A. Fernie, W. Weckwerth, Y. Gibon, and M. Stitt, 'Metabolite profiling in plant biology: platforms and destinations', *Genome Biol*, vol. 5, no. 109, pp. 1–9, 2004, doi: 10.1186/gb-2004-5-6-109.
[129] O. Fiehn, J. Kopka, P. Dörmann, T. Altmann, R. N. Trethewey, and L. Willmitzer, 'Metabolite profiling for plant functional genomics', *Nat Biotechnol*, vol. 18, no. 11, pp. 1757–1161, Nov. 2000, doi: 10.1038/81137.
[130] A. Afifah, P. Nounurai, R. S. Ferniah, H. P. Kusumaningrum, D. Wulandari, and A. Budiharjo, 'An optimised trizol-based protocol for the improvement of rna extraction yield of tomato stem', *Pertanika J Trop Agric Sci*, vol. 44, no. 3, pp. 673–684, Aug. 2021, doi: 10.47836/pjtas.44.3.10.
[131] M. Pertea, G. M. Pertea, C. M. Antonescu, T. C. Chang, J. T. Mendell, and S. L. Salzberg, 'StringTie enables improved reconstruction of a transcriptome from RNA-seq reads', *Nat Biotechnol*, vol. 33, no. 3, pp. 290–295, 2015, doi: 10.1038/nbt.3122.
[132] A. Subramanian *et al.*, 'Gene set enrichment analysis: A knowledge-based approach for interpreting genome-wide expression profiles', in *National Academy of Sciences*, Sep. 2005, pp. 15545–15550. doi: 10.1073/pnas.0506580102.

[133] V. Lefort, R. Desper, and O. Gascuel, 'FastME 2.0: A comprehensive, accurate, and fast distance-based phylogeny inference program', *Mol Biol Evol*, vol. 32, no. 10, pp. 2798–2800, Oct. 2015, doi: 10.1093/molbev/msv150.
[134] A. Hassani, A. Azapagic, and N. Shokri, 'Global predictions of primary soil salinization under changing climate in the 21st century', *Nat Commun*, vol. 12, no. 1, Dec. 2021, doi: 10.1038/s41467-021-26907-3.
[135] Y. Gao, J. Chen, H. Qian, H. Wang, W. Ren, and W. Qu, 'Hydrogeochemical characteristics and processes of groundwater in an over 2260 year irrigation district: A comparison between irrigated and nonirrigated areas', *J Hydrol (Amst)*, vol. 606, p. 127437, 2022, doi: 10.1016/j.jhydrol.2022.127437.
[136] Y. Zhang *et al.*, 'Characterization of soil salinization and its driving factors in a typical irrigation area of Northwest China', *Science of the Total Environment*, vol. 837, Sep. 2022, doi: 10.1016/j.scitotenv.2022.155808.
[137] M. C. Paz, M. Farzamian, A. M. Paz, N. L. Castanheira, M. C. Gonçalves, and F. M. Santos, 'Assessing soil salinity dynamics using time-lapse electromagnetic conductivity imaging', *SOIL*, vol. 6, no. 2, pp. 499–511, Oct. 2020, doi: 10.5194/soil-6-499-2020.
[138] C. Yang, H. Fraga, W. Van Ieperen, and J. A. Santos, 'Assessment of irrigated maize yield response to climate change scenarios in Portugal', *Agric Water Manag*, vol. 184, pp. 178–190, Apr. 2017, doi: 10.1016/j.agwat.2017.02.004.
[139] H. Benmebarek and K. Kharroub, 'Production Assay and Partial Characterization of a Protease Production Assay and Partial Characterization of a Protease Produced by Idiomarina loihiensis, a Moderately Halophilic Bacterium Strain', in *The 2nd International Electronic Conference on Microbiology*, Nov. 2023. doi: 10.3390/ECM2023-16464.
[140] D. Zhu, S. Cui, and S. Nagata, 'Isolation and characterization of salt-sensitive mutants of the moderately halophilic bacterium Salinivibrio costicola subsp. yaniae', *Biosci Biotechnol Biochem*, vol. 72, no. 8, pp. 1977–1982, 2008, doi: 10.1271/bbb.70652.
[141] N. Kumar Arora *et al.*, 'Halo-tolerant plant growth promoting rhizobacteria for improving productivity and remediation of saline soils', *J Adv Res*, vol. 26, pp. 69–82, Nov. 2020, doi: 10.1016/j.jare.2020.07.003.
[142] A. Sanjay, N. P. Purvi, J. V. Meghna, and G. R. G., 'Isolation and characterization of endophytic bacteria colonizing halophyte and other salt tolerant plant species from coastal Gujarat', *Afr J Microbiol Res*, vol. 8, no. 17, pp. 1779–1788, Apr. 2014, doi: 10.5897/ajmr2013.5557.
[143] S. Tripathi, S. Barua, and K. Chakrabarti, 'Site specific bioinoculants for sustainable agriculture in coastal saline soil', in *Halophiles: Biodiversity and Sustainable Exploitation*, Springer International Publishing, 2015, pp. 209–234. doi: 10.1007/978-3-319-14595-2_8.
[144] F. Orhan and M. Gulluce, 'Isolation and Characterization of Salt-Tolerant Bacterial Strains in Salt-Affected Soils of Erzurum, Turkey', *Geomicrobiol J*, vol. 32, no. 6, pp. 521–529, Jul. 2015, doi: 10.1080/01490451.2014.962674.
[145] M. A. Siddikee, P. S. Chauhan, R. Anandham, G.-H. Han, and T.-M. Sa, 'Isolation, characterization, and use for plant growth promotion under salt stress, of ACC deaminase-producing halotolerant bacteria derived from coastal soil', *J Microbiol Biotechnol*, vol. 20, no. 11, pp. 1577–1584, 2010.
[146] F. Orhan and M. Gulluce, 'Isolation and characterization of salt-tolerant bacterial strains in salt-affected soils of East Anatolian region', *Geomicrobiol J*, vol. 32, no. 1, pp. 10–16, 2015.
[147] A. Rani, S. Porwal, R. Sharma, A. Kapley, H. J. Purohit, and V. C. Kalia, 'Assessment of microbial diversity in effluent treatment plants by culture dependent and culture independent approaches', *Bioresour Technol*, vol. 99, no. 15, pp. 7098–7107, Oct. 2008, doi: 10.1016/j.biortech.2008.01.003.
[148] S. Venkatachalam, V. Gowdaman, and S. R. Prabagaran, 'Culturable and Culture-Independent Bacterial Diversity and the Prevalence of Cold-Adapted Enzymes from the Himalayan Mountain Ranges of India and Nepal', *Microb Ecol*, vol. 69, no. 3, pp. 472–491, Apr. 2015, doi: 10.1007/s00248-014-0476-4.
[149] J. Yang, L. Ma, H. Jiang, G. Wu, and H. Dong, 'Salinity shapes microbial diversity and community structure in surface sediments of the Qinghai-Tibetan Lakes', *Sci Rep*, vol. 6, Apr. 2016, doi: 10.1038/srep25078.
[150] Y. Q. Li *et al.*, 'Bacterial community in saline farmland soil on the Tibetan plateau: responding to salinization while resisting extreme environments', *BMC Microbiol*, vol. 21, no. 1, Dec. 2021, doi: 10.1186/s12866-021-02190-6.

[151] J. I. Rilling, J. J. Acuña, P. Nannipieri, F. Cassan, F. Maruyama, and M. A. Jorquera, 'Current opinion and perspectives on the methods for tracking and monitoring plant growth–promoting bacteria', *Soil Biol Biochem*, vol. 130, pp. 205–219, 2019, doi: 10.1016/j.soilbio.2018.12.012.
[152] Y. Bashan, L. E. de-Bashan, S. R. Prabhu, and J. P. Hernandez, 'Advances in plant growth-promoting bacterial inoculant technology: Formulations and practical perspectives (1998-2013)', *Plant Soil*, vol. 378, pp. 1–33, May 2014, doi: 10.1007/s11104-013-1956-x.
[153] M. Vocciante, M. Grifoni, D. Fusini, G. Petruzzelli, and E. Franchi, 'The Role of Plant Growth-Promoting Rhizobacteria (PGPR) in Mitigating Plant's Environmental Stresses', *Applied Sciences (Switzerland)*, vol. 12, no. 3, Feb. 2022, doi: 10.3390/app12031231.
[154] S. Subramanian, A. Souleimanov, and D. L. Smith, 'Thuricin17 Production and Proteome Differences in Bacillus thuringiensis NEB17 Cell-Free Supernatant Under NaCl Stress', *Front Sustain Food Syst*, vol. 5, Mar. 2021, doi: 10.3389/fsufs.2021.630628.
[155] R. P. Singh, P. Jha, and P. N. Jha, 'The plant-growth-promoting bacterium Klebsiella sp. SBP-8 confers induced systemic tolerance in wheat (Triticum aestivum) under salt stress', *J Plant Physiol*, vol. 184, pp. 57–67, Jul. 2015, doi: 10.1016/j.jplph.2015.07.002.
[156] S. Timmusk, T. Pall, S. Raz, A. Fetsiukh, and E. Nevo, 'The potential for plant growth-promoting bacteria to impact crop productivity in future agricultural systems is linked to understanding the principles of microbial ecology', *Front Microbiol*, vol. 14, 2023, doi: 10.3389/fmicb.2023.1141862.
[157] A. Pedrinho *et al.*, 'Soil microbial diversity plays an important role in resisting and restoring degraded ecosystems', *Plant Soil*, vol. 500, no. 1–2, pp. 325–349, Jul. 2024, doi: 10.1007/s11104-024-06489-x.
[158] K. A. Hussein, A. K. Niamah, and K. R. Majeed, 'ANTIMICROBIAL, ANTIOXIDANT, AND OPTIMAL CONDITION FOR EXOPOLYSACCHARIDES SECRATED FROM NEW LOCAL STRAIN-ISOLATE Bifidobacterium longum subsp. infantis strain Iraq-Basrah 3', *Journal of Microbiology, Biotechnology and Food Sciences*, vol. 14, no. 2, Aug. 2024, doi: 10.55251/jmbfs.10761.
[159] M. Hasanuzzaman *et al.*, 'Regulation of ascorbate-glutathione pathway in mitigating oxidative damage in plants under abiotic stress', *Antioxidants*, vol. 8, no. 9, Sep. 2019, doi: 10.3390/antiox8090384.
[160] S. Szymańska, M. I. Lis, A. Piernik, and K. Hrynkiewicz, 'Pseudomonas stutzeri and Kushneria marisflavi Alleviate Salinity Stress-Associated Damages in Barley, Lettuce, and Sunflower', *Front Microbiol*, vol. 13, Mar. 2022, doi: 10.3389/fmicb.2022.788893.
[161] O. Brokate, J. Papenbrock, and A. E. Turcios, 'Biofilm-forming microorganisms in the rhizosphere to improve plant growth: Coping with abiotic stress and environmental pollution', *Applied Soil Ecology*, vol. 202, Oct. 2024, doi: 10.1016/j.apsoil.2024.105591.
[162] A. Ueda and H. Saneoka, 'Characterization of the Ability to Form Biofilms by Plant-Associated Pseudomonas Species', *Curr Microbiol*, vol. 70, no. 4, pp. 506–513, Feb. 2015, doi: 10.1007/s00284-014-0749-7.
[163] H. H. Zahran, 'Diversity, adaptation and activity of the bacterial flora in saline environments', *Biol Fertil Soils*, vol. 25, pp. 211–223, Sep. 1997, doi: 10.1007/s003740050306.
[164] M. Akhtar, F. Hussain, M. Y. Ashraf, T. M. Qureshi, J. Akhter, and A. R. Awan, 'Influence of Salinity on Nitrogen Transformations in Soil', *Commun Soil Sci Plant Anal*, vol. 43, no. 12, pp. 1674–1683, Jun. 2012, doi: 10.1080/00103624.2012.681738.
[165] G. E. Schaller, A. Bishopp, and J. J. Kieber, 'The yin-yang of hormones: Cytokinin and auxin interactions in plant development', *Plant Cell*, vol. 27, no. 1, pp. 44–63, 2015, doi: 10.1105/tpc.114.133595.
[166] J. Brumos *et al.*, 'Local Auxin Biosynthesis Is a Key Regulator of Plant Development', *Dev Cell*, vol. 47, no. 3, pp. 306-318.e5, Nov. 2018, doi: 10.1016/j.devcel.2018.09.022.
[167] M. Malhotra and S. Srivastava, 'Stress-responsive indole-3-acetic acid biosynthesis by Azospirillum brasilense SM and its ability to modulate plant growth', *Eur J Soil Biol*, vol. 45, no. 1, pp. 73–80, Jan. 2009, doi: 10.1016/j.ejsobi.2008.05.006.
[168] T. M. Tien, M. H. Gaskins, and D. H. Hubbell3, 'Plant Growth Substances Produced by Azospirillum brasilense and Their Effect on the Growth of Pearl Millet (Pennisetum americanum L.)t', *Appl Environ Microbiol*, vol. 37, no. 5, pp. 1016–1024, 1979, [Online]. Available: https://journals.asm.org/journal/aem
[169] S. Alejandro, S. Höller, B. Meier, and E. Peiter, 'Manganese in Plants: From Acquisition to Subcellular Allocation', *Front Plant Sci*, vol. 11, Mar. 2020, doi: 10.3389/fpls.2020.00300.
[170] A. Aznar *et al.*, 'Scavenging iron: A novel mechanism of plant immunity activation by microbial siderophores', *Plant Physiol*, vol. 164, no. 4, pp. 2167–2183, 2014, doi: 10.1104/pp.113.233585.

[171] D. KOUR *et al.*, 'Biodiversity, current developments and potential biotechnological applications of phosphorus-solubilizing and -mobilizing microbes: A review', *Pedosphere*, vol. 31, no. 1, pp. 43–75, Feb. 2021, doi: 10.1016/S1002-0160(20)60057-1.
[172] M. A. Malboobi *et al.*, 'Solubilization of organic and inorganic phosphates by three highly efficient soil bacterial isolates', *World J Microbiol Biotechnol*, vol. 25, no. 8, pp. 1471–1477, Jul. 2009, doi: 10.1007/s11274-009-0037-z.
[173] M. R. Hadi and N. Karimi, 'THE ROLE OF CALCIUM IN PLANTS' SALT TOLERANCE', *J Plant Nutr*, vol. 35, no. 13, pp. 2037–2054, Oct. 2012, doi: 10.1080/01904167.2012.717158.
[174] B. R. Glick, 'Modulation of plant ethylene levels by the bacterial enzyme ACC deaminase', *FEMS Microbiol Lett*, vol. 251, no. 1, pp. 1–7, Oct. 2005, doi: 10.1016/j.femsle.2005.07.030.
[175] R. P. Singh, G. M. Shelke, A. Kumar, and P. N. Jha, 'Biochemistry and genetics of ACC deaminase: A weapon to "stress ethylene" produced in plants', *Front Microbiol*, vol. 6, no. SEP, 2015, doi: 10.3389/fmicb.2015.00937.
[176] K. Chookietwattana and K. Maneewan, 'Selection of efficient salt-tolerant bacteria containing ACC deaminase for promotion of tomato growth under salinity stress', *Soil Environ*, vol. 31, no. 1, pp. 30–36, 2012, [Online]. Available: www.se.org.pkhttp://www.sss-pakistan.org
[177] P. Kumari and V. Khanna, 'ACC-deaminase and EPS production by salt tolerant rhizobacteria augment growth in Chickpea under salinity stress', *International Journal of Bio-resource and Stress Management*, vol. 6, no. 5, p. 558, 2015, doi: 10.5958/0976-4038.2015.00084.6.
[178] G. Holguin and B. R. Glick, 'Expression of the ACC deaminase gene from enterobacter cloacae UW4 in Azospirillum brasilense', *Microb Ecol*, vol. 41, no. 3, pp. 281–288, 2001, doi: 10.1007/s002480000040.
[179] U. K. Ghosh, M. N. Islam, M. N. Siddiqui, X. Cao, and M. A. R. Khan, 'Proline, a multifaceted signalling molecule in plant responses to abiotic stress: understanding the physiological mechanisms', *Plant Biol*, vol. 24, no. 2, pp. 227–239, Mar. 2022, doi: 10.1111/plb.13363.
[180] H. Naseem and A. Bano, 'Role of plant growth-promoting rhizobacteria and their exopolysaccharide in drought tolerance of maize', *J Plant Interact*, vol. 9, no. 1, pp. 689–701, 2014, doi: 10.1080/17429145.2014.902125.
[181] H. Etesami, S. Emami, and H. A. Alikhani, 'Potassium solubilizing bacteria (KSB): Mechanisms, promotion of plant growth, and future prospects-a review', *J Soil Sci Plant Nutr*, vol. 17, no. 4, pp. 897–911, 2017, doi: 10.4067/S0718-95162017000400005.
[182] M. A. Ahanger and R. M. Agarwal, 'Potassium up-regulates antioxidant metabolism and alleviates growth inhibition under water and osmotic stress in wheat (Triticum aestivum L)', *Protoplasma*, vol. 254, no. 4, pp. 1471–1486, Jul. 2017, doi: 10.1007/s00709-016-1037-0.
[183] M. Imran *et al.*, 'Inoculation of potassium solubilizing bacteria with different potassium fertilization sources mediates maize growth and productivity', *Pak J Agric Sci*, vol. 57, no. 4, pp. 1045–1055, Jul. 2020, doi: 10.21162/PAKJAS/20.9788.
[184] M. F. Edbeib, R. A. Wahab, and F. Huyop, 'Halophiles: biology, adaptation, and their role in decontamination of hypersaline environments', *World J Microbiol Biotechnol*, vol. 32, no. 8, Aug. 2016, doi: 10.1007/s11274-016-2081-9.
[185] Y. Wang *et al.*, 'Comparative transcriptome and metabolome profiling reveal molecular mechanisms underlying OsDRAP1-mediated salt tolerance in rice', *Sci Rep*, vol. 11, no. 1, Dec. 2021, doi: 10.1038/s41598-021-84638-3.
[186] S. H. Saum and V. Müller, 'Salinity-dependent switching of osmolyte strategies in a moderately halophilic bacterium: Glutamate induces proline biosynthesis in Halobacillus halophilus', *J Bacteriol*, vol. 189, no. 19, pp. 6968–6975, Oct. 2007, doi: 10.1128/JB.00775-07.
[187] B. Faiza, Z. karam Halima, and K. Nour-Eddine, 'Physiological responses of salt stress and osmoprotection with proline in two strains of lactococci isolated from camel's milk in Southern Algeria', *Afr J Biotechnol*, vol. 10, no. 83, pp. 19429–19435, Dec. 2011, doi: 10.5897/AJB11.1807.
[188] N. N. Joghee and G. Jayaraman, 'Metabolomic characterization of halophilic bacterial isolates reveals strains synthesizing rare diaminoacids under salt stress', *Biochimie*, vol. 102, no. 1, pp. 102–111, 2014, doi: 10.1016/j.biochi.2014.02.015.
[189] C. Chang, B. Wang, L. Shi, Y. Li, L. Duo, and W. Zhang, 'Alleviation of salt stress-induced inhibition of seed germination in cucumber (Cucumis sativus L.) by ethylene and glutamate', *J Plant Physiol*, vol. 167, no. 14, pp. 1152–1156, Sep. 2010, doi: 10.1016/j.jplph.2010.03.018.
[190] A. M. Kinnersley and F. J. Turano, 'Gamma aminobutyric acid (GABA) and plant responses to stress', *CRC Crit Rev Plant Sci*, vol. 19, no. 6, pp. 479–509, 2000, doi: 10.1080/07352680091139277.

[191] F. Cui *et al.*, 'Identification of metabolites and transcripts involved in salt stress and recovery in peanut', *Front Plant Sci*, vol. 9, Feb. 2018, doi: 10.3389/fpls.2018.00217.
[192] A. K. G. Atteya, R. S. El-Serafy, K. M. El-Zabalawy, A. Elhakem, and E. A. E. Genaidy, 'Exogenously Supplemented Proline and Phenylalanine Improve Growth, Productivity, and Oil Composition of Salted Moringa by Up-Regulating Osmoprotectants and Stimulating Antioxidant Machinery', *Plants*, vol. 11, no. 12, Jun. 2022, doi: 10.3390/plants11121553.
[193] K. Wu *et al.*, 'Metabolomics analysis reveals enhanced salt tolerance in maize through exogenous Valine-Threonine-Isoleucine-Aspartic acid application', *Front Plant Sci*, vol. 15, 2024, doi: 10.3389/fpls.2024.1374142.
[194] J. C. Argüelles, 'Physiological roles of trehalose in bacteria and yeasts: A comparative analysis', *Arch Microbiol*, vol. 174, no. 4, pp. 217–224, 2000, doi: 10.1007/s002030000192.
[195] S. A. Tanumihardjo, L. McCulley, R. Roh, S. Lopez-Ridaura, N. Palacios-Rojas, and N. S. Gunaratna, 'Maize agro-food systems to ensure food and nutrition security in reference to the Sustainable Development Goals', *Glob Food Sec*, vol. 25, p. 100327, 2020, doi: 10.1016/j.gfs.2019.100327.
[196] T. Tohge, L. P. De Souza, and A. R. Fernie, 'Current understanding of the pathways of flavonoid biosynthesis in model and crop plants', *J Exp Bot*, vol. 68, no. 15, pp. 4013–4028, Jul. 2017, doi: 10.1093/jxb/erx177.
[197] S. Puthiyaveetil *et al.*, 'Significance of the photosystem II Core phosphatase PBCP for plant viability and protein repair in thylakoid membranes', *Plant Cell Physiol*, vol. 55, no. 7, pp. 1245–1254, 2014, doi: 10.1093/pcp/pcu062.
[198] A. A. Ghotbi-Ravandi, M. Shahbazi, M. Pessarakli, and M. Shariati, 'Monitoring the photosystem II behavior of wild and cultivated barley in response to progressive water stress and rehydration using OJIP chlorophyll a fluorescence transient', *J Plant Nutr*, vol. 39, no. 8, pp. 1174–1185, Jul. 2016, doi: 10.1080/01904167.2015.1047522.
[199] H. M. Kalaji, Govindjee, K. Bosa, J. Kościelniak, and K. Żuk-Gołaszewska, 'Effects of salt stress on photosystem II efficiency and CO2 assimilation of two Syrian barley landraces', *Environ Exp Bot*, vol. 73, pp. 64–72, 2011, doi: 10.1016/j.envexpbot.2010.10.009.
[200] J. Amikuzuno and S. A. Donkoh, 'CLIMATE VARIABILITY AND YIELDS OF MAJOR STAPLE FOOD CROPS IN NORTHERN GHANA', *Afr Crop Sci J*, vol. 20, pp. 349–360, 2012.
[201] C. Kapadia *et al.*, 'Halotolerant microbial consortia for sustainable mitigation of salinity stress, growth promotion, and mineral uptake in tomato plants and soil nutrient enrichment', *Sustainability (Switzerland)*, vol. 13, no. 15, Aug. 2021, doi: 10.3390/su13158369.
[202] C. E. da S. Oliveira *et al.*, 'Can saline irrigation improve the quality of tomato fruits?', *Agron J*, vol. 114, no. 2, pp. 900–914, Mar. 2022, doi: 10.1002/agj2.21003.
[203] H. E. Knights, B. Jorrin, T. L. Haskett, and P. S. Poole, 'Deciphering bacterial mechanisms of root colonization', *Environ Microbiol Rep*, vol. 13, no. 4, pp. 428–444, Aug. 2021, doi: 10.1111/1758-2229.12934.
[204] K. Dietel, B. Beator, A. Budiharjo, B. Fan, and R. Borriss, 'Bacterial Traits Involved in colonization of Arabidopsis thaliana roots by Bacillus amyloliquefaciens FZB42', *Plant Pathol J (Faisalabad)*, vol. 29, no. 1, pp. 59–66, 2013, doi: 10.5423/PPJ.OA.10.2012.0155.
[205] M. Ansari *et al.*, 'Microbial Exudates as Biostimulants: Role in Plant Growth Promotion and Stress Mitigation', *J Xenobiot*, vol. 13, no. 4, pp. 572–603, Dec. 2023, doi: 10.3390/jox13040037.
[206] G. A. Jana, B. R. Glick, and M. W. Yaish, 'Chapter 14 - Salt tolerance in plants: Using OMICS to assess the impact of plant growth-promoting bacteria (PGPB)', in *Mitigation of Plant Abiotic Stress by Microorganisms*, G. Santoyo, A. Kumar, M. Aamir, and S. Uthandi, Eds., Academic Press, 2022, pp. 299–320. doi: 10.1016/B978-0-323-90568-8.00014-6.
[207] S. Tiwari, 'An Outline of Plant–Microbe Interactions for Stress Management', in *Plant-Microbe Interaction and Stress Management*, P. Singh Chauhan, S. K. Tewari, and S. Misra, Eds., Singapore: Springer Nature Singapore, 2024, pp. 21–28. doi: 10.1007/978-981-97-4239-4_2.
[208] M. A. Hossain, M. S. Hossain, and M. Akter, 'Challenges faced by plant growth-promoting bacteria in field-level applications and suggestions to overcome the barriers', *Physiol Mol Plant Pathol*, vol. 126, Jul. 2023, doi: 10.1016/j.pmpp.2023.102029.
[209] S. DasSarma and P. DasSarma, 'Halophiles and their enzymes: Negativity put to good use', *Curr Opin Microbiol*, vol. 25, pp. 120–126, Jun. 2015, doi: 10.1016/j.mib.2015.05.009.
[210] S. H. Seo, S. E. Park, E. J. Kim, K. I. Lee, C. S. Na, and H. S. Son, 'A GC-MS based metabolomics approach to determine the effect of salinity on Kimchi', *Food Research International*, vol. 105, pp. 492–498, Mar. 2018, doi: 10.1016/j.foodres.2017.11.069.

[211] H. M. Dawson *et al.*, 'Microbial metabolomic responses to changes in temperature and salinity along the western Antarctic Peninsula', *ISME Journal*, vol. 17, no. 11, pp. 2035–2046, Nov. 2023, doi: 10.1038/s41396-023-01475-0.
[212] G. Iturriaga, R. Suárez, and B. Nova-Franco, 'Trehalose metabolism: From osmoprotection to signaling', *Int J Mol Sci*, vol. 10, no. 9, pp. 3793–3810, Sep. 2009, doi: 10.3390/ijms10093793.
[213] M. Nawaz *et al.*, 'Trehalose: a promising osmo-protectant against salinity stress—physiological and molecular mechanisms and future prospective', *Mol Biol Rep*, vol. 49, no. 12, pp. 11255–11271, Dec. 2022, doi: 10.1007/s11033-022-07681-x.
[214] A. K. Sarkar and S. Sadhukhan, 'Imperative role of trehalose metabolism and trehalose-6-phosphate signaling on salt stress responses in plants', *Physiol Plant*, vol. 174, no. 1, Jan. 2022, doi: 10.1111/ppl.13647.
[215] S. A. Dabravolski and S. V. Isayenkov, 'The Role of the γ-Aminobutyric Acid (GABA) in Plant Salt Stress Tolerance', *Horticulturae*, vol. 9, no. 2, Feb. 2023, doi: 10.3390/horticulturae9020230.
[216] M. I. R. Khan *et al.*, 'Role of GABA in plant growth, development and senescence', *Plant Gene*, vol. 26, Jun. 2021, doi: 10.1016/j.plgene.2021.100283.
[217] M. Alfosea-Simón *et al.*, 'Physiological, Nutritional and Metabolomic Responses of Tomato Plants After the Foliar Application of Amino Acids Aspartic Acid, Glutamic Acid and Alanine', *Front Plant Sci*, vol. 11, Jan. 2021, doi: 10.3389/fpls.2020.581234.
[218] R. Ros, J. Muñoz-Bertomeu, and S. Krueger, 'Serine in plants: Biosynthesis, metabolism, and functions', *Trends Plant Sci*, vol. 19, no. 9, pp. 564–569, 2014, doi: 10.1016/j.tplants.2014.06.003.
[219] Z. Zhang, C. Mao, Z. Shi, and X. Kou, 'The amino acid metabolic and carbohydrate metabolic pathway play important roles during salt-stress response in tomato', *Front Plant Sci*, vol. 8, Jul. 2017, doi: 10.3389/fpls.2017.01231.
[220] P. B. K. Kishor *et al.*, 'Lysine, Lysine-Rich, Serine, and Serine-Rich Proteins: Link Between Metabolism, Development, and Abiotic Stress Tolerance and the Role of ncRNAs in Their Regulation', *Front Plant Sci*, vol. 11, Dec. 2020, doi: 10.3389/fpls.2020.546213.
[221] A. K. G. Atteya, R. S. El-Serafy, K. M. El-Zabalawy, A. Elhakem, and E. A. E. Genaidy, 'Exogenously Supplemented Proline and Phenylalanine Improve Growth, Productivity, and Oil Composition of Salted Moringa by Up-Regulating Osmoprotectants and Stimulating Antioxidant Machinery', *Plants*, vol. 11, no. 12, Jun. 2022, doi: 10.3390/plants11121553.
[222] Q. Yang, D. Zhao, and Q. Liu, 'Connections Between Amino Acid Metabolisms in Plants: Lysine as an Example', *Front Plant Sci*, vol. 11, Jun. 2020, doi: 10.3389/fpls.2020.00928.
[223] A. El Moukhtari, C. Cabassa-Hourton, M. Farissi, and A. Savouré, 'How Does Proline Treatment Promote Salt Stress Tolerance During Crop Plant Development?', *Front Plant Sci*, vol. 11, Jul. 2020, doi: 10.3389/fpls.2020.01127.
[224] G. Santoyo, G. Moreno-Hagelsieb, M. del Carmen Orozco-Mosqueda, and B. R. Glick, 'Plant growth-promoting bacterial endophytes', *Microbiol Res*, vol. 183, pp. 92–99, Feb. 2016, doi: 10.1016/j.micres.2015.11.008.
[225] Q. Li, Y. Li, X. Li, and S. Chen, 'Identification of genes involved in fe–s cluster biosynthesis of nitrogenase in paenibacillus polymyxa wly78', *Int J Mol Sci*, vol. 22, no. 7, Apr. 2021, doi: 10.3390/ijms22073771.
[226] C. Ayala-Castro, A. Saini, and F. W. Outten, 'Fe-S Cluster Assembly Pathways in Bacteria', *Microbiology and Molecular Biology Reviews*, vol. 72, no. 1, pp. 110–125, Mar. 2008, doi: 10.1128/mmbr.00034-07.
[227] A. K. Tripathi, T. Nagarajan, S. C. Verma, and D. Le Rudulier, 'Inhibition of biosynthesis and activity of nitrogenase in Azospirillum brasilense Sp7 under salinity stress', *Curr Microbiol*, vol. 44, no. 5, pp. 363–367, May 2002, doi: 10.1007/s00284-001-0022-8.
[228] X. Li *et al.*, 'High Salinity Inhibits Soil Bacterial Community Mediating Nitrogen Cycling', *Microb Ecol*, vol. 87, no. 21, Oct. 2021, doi: 10.1128/AEM.01366-21.
[229] A. Rozov *et al.*, 'Importance of potassium ions for ribosome structure and function revealed by long-wavelength X-ray diffraction', *Nat Commun*, vol. 10, no. 1, Dec. 2019, doi: 10.1038/s41467-019-10409-4.
[230] P. Gong *et al.*, 'SAMBA controls cell division rate during maize development', *Plant Physiol*, vol. 188, no. 1, pp. 411–424, Jan. 2022, doi: 10.1093/plphys/kiab514.
[231] H. Shibata, H. Ochiai, Y. Sawa, and S. Miyoshi, 'Localization of Carbamoylphosphate Synthetase and Aspartate Carbamoyltransferase in Chloroplasts', *Plant Physiol*, vol. 80, pp. 126–129, Jan. 1986, doi: 10.1104/pp.80.1.126.

[232] M. Zhang *et al.*, 'Physiological and transcriptomic analysis uncovers salinity stress mechanisms in a facultative crassulacean acid metabolism plant Dendrobium officinale', *Front Plant Sci*, vol. 13, Oct. 2022, doi: 10.3389/fpls.2022.1028245.
[233] M. Tronchet, C. BalaguÉ, T. Kroj, L. Jouanin, and D. Roby, 'Cinnamyl alcohol dehydrogenases-C and D, key enzymes in lignin biosynthesis, play an essential role in disease resistance in Arabidopsis', *Mol Plant Pathol*, vol. 11, no. 1, pp. 83–92, Jan. 2010, doi: 10.1111/j.1364-3703.2009.00578.x.
[234] A. P. Ferro *et al.*, 'Inhibition of Zea mays coniferyl aldehyde dehydrogenase by daidzin: A potential approach for the investigation of lignocellulose recalcitrance', *Process Biochemistry*, vol. 90, pp. 131–138, Mar. 2020, doi: 10.1016/j.procbio.2019.11.024.
[235] C. Kaya, S. Aydemir, O. Sonmez, M. Ashraf, and M. Dikilitas, 'Regulation of growth and some key physiological processes in salt-stressed maize (Zea mays L.) plants by exogenous application of asparagine and glycerol', *Acta Bot. Croat*, vol. 72, no. 1, p. 2013, 2013.
[236] A. Ullah, M. Li, J. Noor, A. Tariq, Y. Liu, and L. Shi, 'Effects of salinity on photosynthetic traits, ion homeostasis and nitrogen metabolism in wild and cultivated soybean', *PeerJ*, vol. 2019, no. 12, 2019, doi: 10.7717/peerj.8191.
[237] A. B. Feria *et al.*, 'Phosphoenolpyruvate carboxylase (PEPC) and PEPC-kinase (PEPC-k) isoenzymes in Arabidopsis thaliana: role in control and abiotic stress conditions', *Planta*, vol. 244, no. 4, pp. 901–913, Oct. 2016, doi: 10.1007/s00425-016-2556-9.
[238] J. Ponnu, V. Wahl, and M. Schmid, 'Trehalose-6-phosphate: Connecting plant metabolism and development', *Front Plant Sci*, vol. 2, no. NOV, Nov. 2011, doi: 10.3389/fpls.2011.00070.
[239] C. M. Figueroa and J. E. Lunn, 'A tale of two sugars: Trehalose 6-phosphate and sucrose', *Plant Physiol*, vol. 172, no. 1, pp. 7–27, Sep. 2016, doi: 10.1104/pp.16.00417.
[240] T. Albi, M. T. Ruiz, P. De Los Reyes, F. Valverde, and J. M. Romero, 'Characterization of the sucrose phosphate phosphatase (SPP) isoforms from Arabidopsis thaliana and role of the S6PPc domain in dimerization', *PLoS One*, vol. 11, no. 11, Nov. 2016, doi: 10.1371/journal.pone.0166308.
[241] T. Roldán-Arjona, R. R. Ariza, and D. Córdoba-Cañero, 'DNA Base Excision Repair in Plants: An Unfolding Story With Familiar and Novel Characters', *Front Plant Sci*, vol. 10, Aug. 2019, doi: 10.3389/fpls.2019.01055.
[242] P. Schertl, L. Danne, and H. P. Braun, '3-hydroxyisobutyrate dehydrogenase is involved in both, valine and isoleucine degradation in arabidopsis thaliana', *Plant Physiol*, vol. 175, no. 1, pp. 51–61, Sep. 2017, doi: 10.1104/pp.17.00649.
[243] I. M. Ahmed *et al.*, 'The Barley S-Adenosylmethionine Synthetase 3 Gene HvSAMS3 Positively Regulates the Tolerance to Combined Drought and Salinity Stress in Tibetan Wild Barley', *Cells*, vol. 9, no. 6, Jun. 2020, doi: 10.3390/cells9061530.
[244] M. Houben and B. Van de Poel, '1-aminocyclopropane-1-carboxylic acid oxidase (ACO): The enzyme that makes the plant hormone ethylene', *Front Plant Sci*, vol. 10, May 2019, doi: 10.3389/fpls.2019.00695.
[245] X. Liang *et al.*, 'Metabolomics-driven gene mining and genetic improvement of tolerance to salt-induced osmotic stress in maize', *New Phytologist*, vol. 230, no. 6, pp. 2355–2370, Jun. 2021, doi: 10.1111/nph.17323.
[246] A. Richter *et al.*, 'Indole-3-glycerolphosphate synthase, a branchpoint for the biosynthesis of tryptophan, indole, and benzoxazinoids in maize', *Plant Journal*, vol. 106, no. 1, pp. 245–257, Apr. 2021, doi: 10.1111/tpj.15163.
[247] H. Li *et al.*, 'Transcriptomic profiling of the high-vigour maize (Zea mays L.) hybrid variety response to cold and drought stresses during seed germination', *Sci Rep*, vol. 11, no. 1, Dec. 2021, doi: 10.1038/s41598-021-98907-8.
[248] O. S. Olanrewaju and O. O. Babalola, 'Bacterial consortium for improved maize (Zea mays l.) production', *Microorganisms*, vol. 7, no. 11, Nov. 2019, doi: 10.3390/microorganisms7110519.

7

ANNEXES

7.1 Halophile/Halotolerant Bacterial Collection

Table 7.1 – List of isolated strains and morphological characteristics. The table indicates the sample code. species name determined through the comparison of 16S rRNA sequences with the National Library of Medicine BLAST database and morphology of bacterial colonies in five parameters (colour. texture. elevation. margin and propagation) following the guidelines of PathElective. UI stands for “Unidentified”.

Sample	Species	Morphology				
		Colour	Texture	Elevation	Margin	Propagation
AA	*Kushneria marisflavi*	orange	viscid	flat	entire	moderate
AB	*Halomonas elongata*	white	viscid	raised	entire	large
AC	UI	white	viscid	crateriform	entire	moderate
BC	*Bacillus atrophaeus*	light brown	viscid	draughtsman	entire	large
DA	*Halobacillus faecis*	yellow	smooth	flat	entire	moderate
DD	*Virgibacillus salarius*	white	dull	flat	filiform	large
DE	*Vreelandella* sp.	white	smooth	raised	curled	large
DF	UI	white	mucoid	flat	entire	moderate
EA	*Idiomarina loihiensis*	white/cream	viscid	raised	lobate	moderate
EB	UI					
EC	UI	cream	mucoid	raised	entire	moderate
ED	UI					
EE	*Marinobacter persicus*	light yellow	transparent	flat	filiform	moderate
EF	UI	white	viscid	flat	entire	moderate
EG	UI					
FA	*Halobacillus trueperi*	yellow	smooth	crateriform	entire	small
FD	*Halomonas glaciei*	brown	dry	raised	filiform	large
FE	*Halobacillus sediminis*	white	dull	raised	entire	moderate
GA	*Oceanobacillus picturae*	yellow	smooth	flat	entire	puntiform
GB	*Alkalibacterium putridalgicola*	white	smooth	umbonate	entire	large
GC	*Virgibacillus salarius*	white	dull	umbonate	serrate	large
GD	UI	white	viscid	draughtsman	undulate	small
HA	*Salinivibrio costicola*	white	smooth	crateriform	entire	moderate
HB	*Idiomarina abyssalis*	white	smooth	raised	entire	large

HC	*Halomonas taeanensis*	white	viscid	crateriform	entire	moderate
IA	*Idiomarina abyssalis*	white	smooth	raised	entire	large
IC	*Pseudalkalibacillus hwajinpoensis*	white/cream	smooth	raised	entire	small
ID	*Planococcus citreus*	orange	smooth	convex	entire	moderate
IF	*Oceanobacillus picturae*	white	smooth	flat	undulate	moderate
IG	*Halobacillus trueperi*	yellow	smooth	draughtsman	entire	moderate
101	*Bacillus halotolerans*					
102	UI	cream	smooth	flat	entire	small
103	*Halobacillus faecis*	transparent	smooth	flat	entire	small
104	*Rossellomorea aquimaris*	white	smooth	flat	undulate	small
105	UI	white	smooth	flat	entire	puntiform
106	UI					
107	*Oceanobacillus picturae*	white	smooth	draughtsman	undulate	moderate
108	UI					
109	*Halobacillus faecis*	light orange	smooth	crateriform	entire	moderate
110	*Halobacillus faecis*	light orange/yellow	viscid	flat	entire	large
111	*Alkalicoccobacillus gibsonii*	white	viscid	raised	entire	small
112	*Candida* sp.	orange	viscid	raised	entire	puntiform
113	*Planococcus rifietoensis*	orange	viscid	raised	entire	moderate
114	*Candida parapsilosis*	white	dull	flat	entire	moderate
115	*Oceanobacillus kimchii*	white	viscid	raised	entire	moderate
116	*Paraliobacillus sediminis*					
117	*Penicillium chrysogenum*	transparent	smooth	flat	entire	moderate
118	UI					
119	*Bacillus swezeyi*	white	mucoid	raised	entire	large
120	*Halobacillus faecis*					
121	*Priestia megaterium*					
122	*Candida parapsilosis*	white	dull	crateriform	entire	moderate
123	*Oceanobacillus picturae*	white	smooth	raised	filiform	moderate
124	*Rossellomorea vietnamensis*	white	smooth	raised	filiform	moderate

7.2 Strains Performance under High Salinity Levels

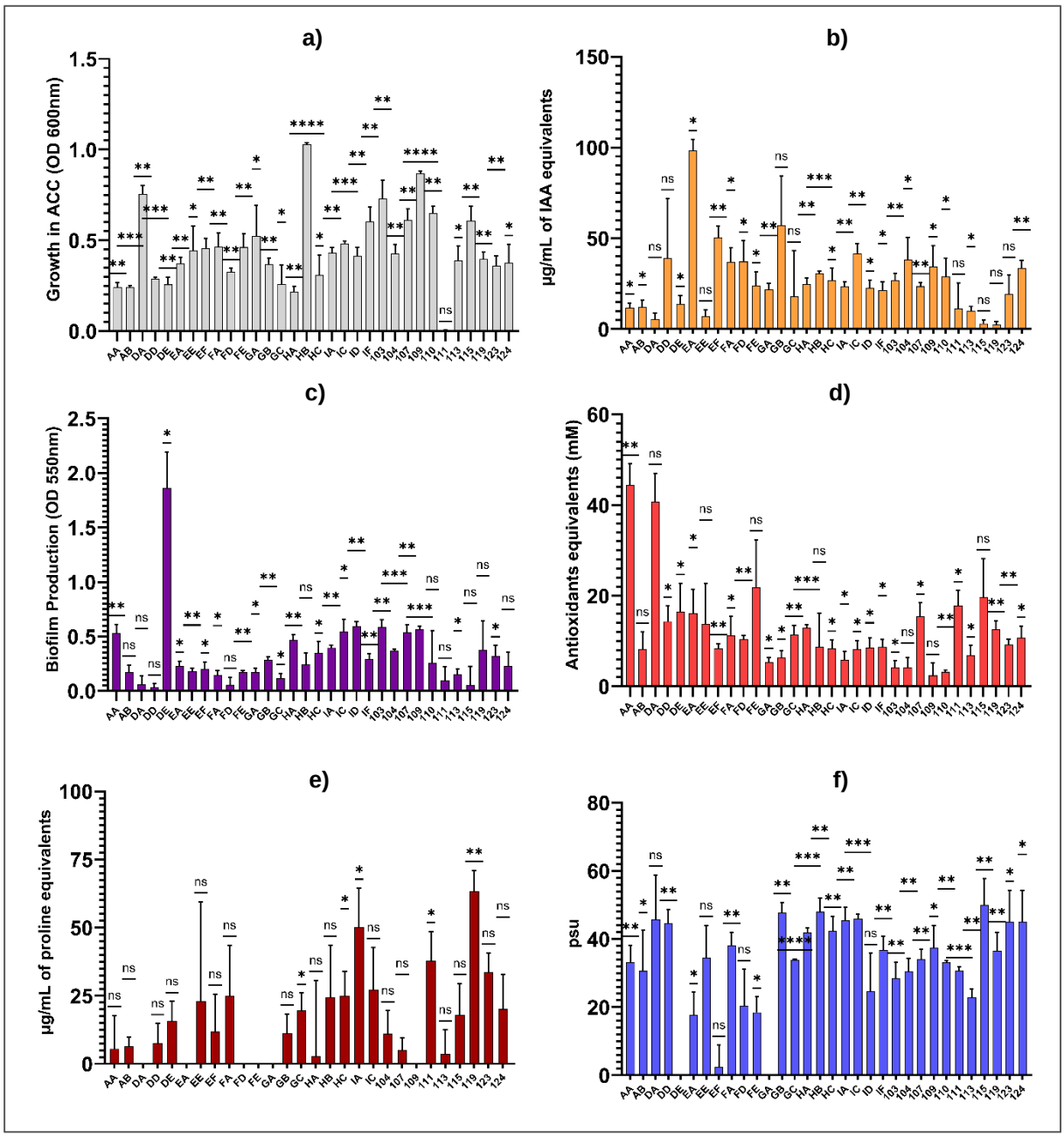

Figure 7.1 – Bacterial characterization under high salinity levels. The column graphs represent the performance at a 2 M of NaCl concentration of each candidate strain. Strains were characterized for **a)** their growth in ACC medium (in OD at 600 nm) **b)** auxins production (in IAA equivalents) **c)** biofilm production (in OD at 550 nm) **d)** antioxidants equivalents production (in mM) **e)** proline equivalents secretion and **f)** siderophores production (in psu). The species name for every label used on the strains are listed in Table 7.1. The data sets (n = 3) were analyzed using a Student's t-test. Asterisks indicate statistically significant differences at the following levels: * for $p < 0.05$, ** for $p < 0.01$, *** for $p < 0.001$, and **** for $p < 0.0001$. 'ns' denotes no statistical difference compared to the control (y = 0). Error bars indicate standard deviation.

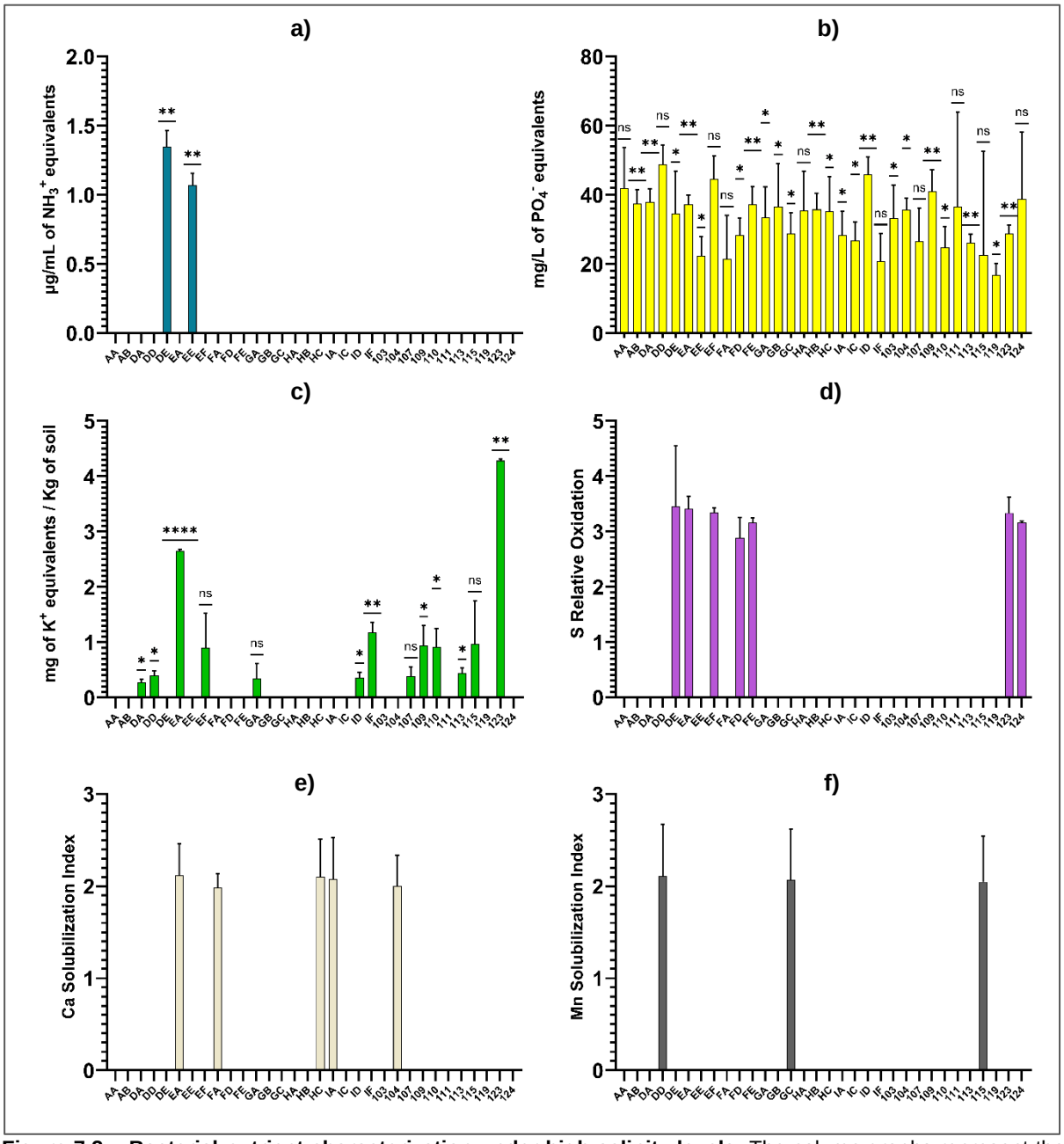

Figure 7.2 – Bacterial nutrient characterization under high salinity levels. The column graphs represent the performance at a 2 M of NaCl concentration of each candidate strain in the nutrient disposability tests. Strains were characterized for **a)** nitrogen fixation (NH_3^+ equivalents) **b)** phosphate solubilization (in PO_4^{3-} equivalents) **c)** potassium solubilization (in K^+ equivalents) **d)** sulfur oxidation (in relative activity) **e)** calcium solubilization (in solubilization index. SI) and **f)** manganese solubilization (in SI). The species name for every label used on the strains are listed in Table 7.1. The data sets (n = 3) were analyzed using a Student's t-test. Asterisks indicate statistically significant differences at the following levels: * for $p < 0.05$, ** for $p < 0.01$, *** for $p < 0.001$, and **** for $p < 0.0001$. 'ns' denotes no statistical difference compared to the control (y = 0). Error bars indicate standard deviation.

7.3 Metabolites Production by Halophile Bacteria

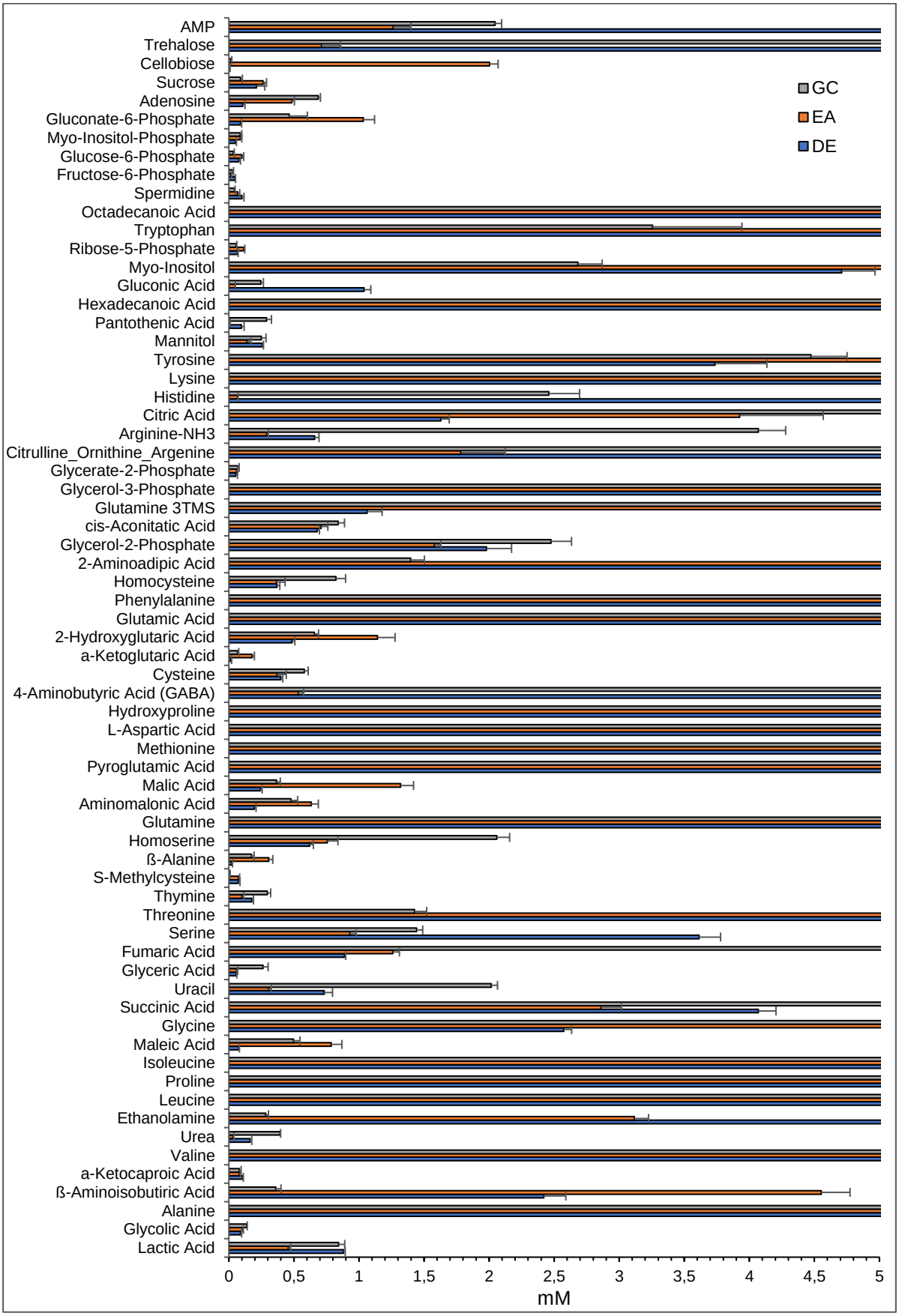
AMP
Trehalose
Cellobiose
Sucrose
Adenosine
Gluconate-6-Phosphate
Myo-Inositol-Phosphate
Glucose-6-Phosphate
Fructose-6-Phosphate
Spermidine
Octadecanoic Acid
Tryptophan
Ribose-5-Phosphate
Myo-Inositol
Gluconic Acid
Hexadecanoic Acid
Pantothenic Acid
Mannitol
Tyrosine
Lysine
Histidine
Citric Acid
Arginine-NH3
Citrulline_Ornithine_Argenine
Glycerate-2-Phosphate
Glycerol-3-Phosphate
Glutamine 3TMS
cis-Aconitatic Acid
Glycerol-2-Phosphate
2-Aminoadipic Acid
Homocysteine
Phenylalanine
Glutamic Acid
2-Hydroxyglutaric Acid
a-Ketoglutaric Acid
Cysteine
4-Aminobutyric Acid (GABA)
Hydroxyproline
L-Aspartic Acid
Methionine
Pyroglutamic Acid
Malic Acid
Aminomalonic Acid
Glutamine
Homoserine
ß-Alanine
S-Methylcysteine
Thymine
Threonine
Serine
Fumaric Acid
Glyceric Acid
Uracil
Succinic Acid
Glycine
Maleic Acid
Isoleucine
Proline
Leucine
Ethanolamine
Urea
Valine
a-Ketocaproic Acid
ß-Aminoisobutiric Acid
Alanine
Glycolic Acid
Lactic Acid
GC
EA
DE
0
0,5
1
1,5
2
2,5
3
3,5
4
4,5
5
mM

Figure 7.3 – Low concentration bacterial metabolites. The bar graph illustrates an ampliation of Figure 3.25 ranging from 0 to 5 mM in the X-axis. The blue bar is referent to the strain *Vreelandella* sp. DE, the orange bar to the strain *I. loihiensis* EA and the grey bar to the strain *V. salarius* GC. Error bars indicate standard deviation.

8

PRODUCTIONS DERIVED FROM THIS WORK

- 2 Journal articles:
  - "Isolation and Characterization of Culturable Osmotolerant Microbiota in Hypersaline and Hypergypsic Soils as New Treatment for Osmotic Stress in Plants" – https://doi.org/10.3390/soilsystems7040086
  - "Comparing native and non-native seed-isolated strains for drought resilience in maize (*Zea mays* L.)" – https://doi.org/10.1016/j.stress.2024.100462
- 1 Conference paper:
  - "Enhancing Maize (Zea mays) Resilience to Drought Stress Through Seed-Associated Microbiota" – https://doi.org/10.5281/zenodo.10684144
- 1 Oral communication:
  - "From salt flats to farmlands: Introducing new halophile bacteria-based biotreatments for enhancing crop resilience amidst rising salinity in Ribatejo (Portugal)" – Agenda (website-files.com)
- 3 Conference posters:
  - "New biotreatments against saline rising on Ribatejo (Portugal) farmlands using Iberian Peninsula salt flats-isolated, halophile strains" – Abstracts.pdf (sefin40.com)
  - "Understanding the positive impact of halotolerant bacteria isolated from hypersaline soils to enhance osmotic tolerance in Medicago plants" – https://doi.org/10.5281/zenodo.10497906
  - "Isolation and characterization of culturable halotolerant microbiota in hypersaline and hypergypsic soils as new treatment for osmotic stress in plants" – https://doi.org/10.5281/zenodo.8164619